2011

From DNA to Protein: a study of genomic instability candidate genes during zebrafish development

Kristine Griffett
University of South Florida, kristinegriffett@gmail.com

From DNA to Protein: A Study of Genomic Instability Candidate Genes During Zebrafish Development

by

Kristine Griffett

A dissertation submitted in partial fulfillment
of the requirements for the degree of
Doctor of Philosophy
Department of Cell Biology, Microbiology and Molecular Biology
College of Arts and Sciences
University of South Florida

Co-Major Professor: Richard S. Pollenz, Ph.D.
Co-Major Professor: Meera Nanjundan, Ph.D.
Patrick Bradshaw, Ph.D.
Brant Burkhardt, Ph.D.
Jessica L. Moore, Ph.D.

Date of Approval:
September 30, 2011

Keywords: *Danio rerio*, embryogenesis, morpholino
synbl, *mdm1*, RNA rescue, mosaic eye

DEDICATION

To my supportive family, thank you for enduring my long learning journey with patience, understanding and love. I would like to specifically dedicate this dissertation to the memory of my grandmother, Anna D'Alessio, my parents, Ralph and Laura D'Alessio, my sister, Danielle D'Alessio, and my husband, Josh Griffett. These family members have always been wonderful supporters of my educational endeavors, and I wish to honor and thank them.

ACKNOWLEDGEMENTS

This work could not have been completed without the mentorship and guidance of my original mentor, Dr. Jessica Moore, and my committee members, Dr. Richard Pollenz, Dr. Meera Nanjundan, Dr. Patrick Bradshaw and Dr. Brant Burkhardt. I would also like to acknowledge Dr. James Garey and Dr. Lindsey Shaw for their support and advice during the last few years of my studies. Transgenic *synbl* fish (hi2039aTg/+) were obtained from the Zebrafish International Resource Center, which is supported by grant P40 RR012546 from the NIH-NCRR. This work was also partially funded by the NIH 5R03HD056152-02 grant (Jessica Moore) and the University of South Florida Helen M. and Fred L. Tharpe Fellowship (Kristine Griffett). Sequence alignments and vector diagrams were made with the Geneious v5.4 software available from Biomatters Ltd. at www.geneious.com.

TABLE OF CONTENTS

LIST OF TABLES

LIST OF FIGURES

LIST OF ABBREVIATIONS

PCR – Polymerase Chain Reaction

MO – Morpholino Oligonucleotide

hpf – hours post fertilization

hpi – hours post injection

dpf – days post fertilization

EMS – Ethyl Methanesulfonate

ENU – Ethyl-Nitrosurea

RPE – Retinal Pigmented Epithelium

gin – Genomic Instability

LOH – Loss of Heterozygosity

WT(AB) – wildtype strain AB

ZIRC – Zebrafish International Resource Center

NCBI – National Center for Biotechnology Information

RT-PCR – Reverse Transcription Polymerase Chain Reaction

DIG – Digoxigenin

AP – Alkaline Phosphatase

CSPD – chemiluminescent substrate 3-(4-methoxyspiro {1,2-dioxetane-3,2'-(5'-chloro)tricyclo [3.3.1.1^{3,7}]decan}-4-yl)phenyl phosphate

PTU – 1-phenyl-2-thiourea

MBT – Mid-Blastula Transition

CNS – Central Nervous System

Tg-*synbl* – Transgenic zebrafish for *synbl* gene

NIH – National Institutes of Health

BLAST – Basic Local Alignment Search Tool

RIPA – Radio-Immunoprecipitation Assay

SDS-PAGE – Sodium Dodecyl Sulfate Polyacrylamide Gel Electrophoresis

VEGA – Vertebrate Genome Annotation Database

TnT – Transcription and Translation

NBT-BCIP – Nitro blue Tetrazolium Chloride 5-Bromo-4-Chloro-3-Indolyl Phosphate

IP - Immunoprecipitation

ABSTRACT

The zebrafish, *Danio rerio*, is a type of freshwater minnow often used to model human diseases including cancer, anxiety and aging diseases. The overall biology of zebrafish is strikingly similar to that of humans, allowing these fish to be used for drug discovery and toxicology studies for preclinical trials. In this study, zebrafish embryos were used to identify and characterize several candidate genes within two known regions of genomic instability on chromosome 18 and chromosome 4. This fish that were used in this study had been previously classified as genomic instability (*gin*) mutants due to increased incidence of somatic mutation during the early stages of embryogenesis, that can be detected with the mosaic eye assay at 48-72 hpf. Using published genome and mapping data, several candidate genes for two of the *gin* mutations were identified and studied during early zebrafish development.

The *gin* mutations are heritable, ENU-induced, and have both maternal and zygotic effects during zebrafish development. The first aim of this project was to study the normal gene characteristics of the *gin-10* candidate genes, *synbl, rfx4,* and *sir2* that are located on chromosome 18. Semi-quantitative RT-PCR, whole-mount *in situ* hybridization, and gene knockdown (using morpholino oligonucleotides) techniques were utilized in both wildtype and transgenic (Tg-*synbl*) zebrafish lines to gain an understanding of the function of each of these

genes during zebrafish embryogenesis. Additionally, the *synbl* paralog, *ric8a,* was also explored, as it has been implicated in the control of asymmetric cell division in *C. elegans*. Single gene knockdowns were performed for each candidate in the *golden* heterozygous (pigment mutant) zebrafish background to test for genomic instability activity. Genomic instability activity was not observed, however the results showed that these genes are expressed throughout zebrafish embryogenesis, and are necessary for the proper development of the central nervous system, notochord and tail, as well as metabolic functions in the early embryo. Moreover, the transgenic line used for the paralog studies of *synbl* and *ric8a* was incorrectly genotyped. Using PCR analysis and sequencing, it was found that the viral insert for the Tg-*synbl* fish was disrupting the *cry1b* gene on an adjacent contig.

The second aim focused on the *gin-12* region on chromosome 4, where the *mdm1* gene is located. Originally cloned from a transformed mouse cell line with *mdm2*, the function of the *mdm1* gene in these cells or during development had not yet been identified. To allow the Mdm1 protein to be evaluated, custom antibodies targeting Mdm1 were produced and the detection of Mdm1 optimized in zebrafish embryos. This would allow us to then determine whether Mdm1 was a possible regulator of the p53-Mdm2/Mdm4 pathway. Additionally, the *mdm1* gene was studied *in situ* and *in vivo* to determine the normal gene expression patterns and developmental role in the embryonic zebrafish. Moreover, this gene was also studied in the *golden* heterozygous zebrafish line to assess whether it had a role in modulating genomic instability activity using the mosaic eye assay.

Collectively, morpholino oligonucleotides, RNA rescue, whole-mount antibody staining, and overexpression studies suggest that the *mdm1* gene is involved in the development of the eye and portions of the central nervous system, but did not appear to be the *gin-12* mutant.

While the genes in this study did not appear to have genomic instability activity in the embryonic zebrafish based on the mosaic eye assay in the *golden* heterozygotes, normal developmental gene expression patterns were identified for *synbl, ric8a, rfx4, sir2*, and *mdm1* in wildtype zebrafish embryos. Additional information was gained by the reverse genetic studies using gene knockdowns, which identified the functional roles of these genes at various stages of embryogenesis. Notably, it was determined that the *mdm1* gene may be involved in retinal degenerative diseases based on our studies and recently published data. Future research of the Mdm1 protein should identify protein interactions and the specific role during eye development and retinal diseases.

CHAPTER ONE

INTRODUCTION

Zebrafish as a Model System

Zebrafish (*Danio rerio)*, are a species of small minnow native to the freshwater streams of Northern and Central India. Zebrafish belong to the cyprinid family of teleost fish, which includes several other popular model organisms such as medaka, pufferfish and the three-spined stickleback. These organisms are often used in genetic and behavioral studies. Over the last several decades, the zebrafish has gained popularity as a model organism in a variety of backgrounds including genetics and developmental biology (Eisen 1996; Dooley and Zon 2000; Grunwald and Eisen 2002).

More recently, zebrafish have become a widely used model system for studying human diseases, drug-targeting studies, toxicity screening, sleep and anxiety studies, neurodegenerative and aggression disorders (Eisen 1996; Gerlai *et al.* 2000; Hendricks *et al.* 2000; Grunwald and Eisen 2002; Gerlai 2003; Bilotta *et al.* 2004; Kari *et al.* 2007; Feitsma and Cuppen 2008; Guo 2008; Ingham 2009; Norton and Bally-Cuif 2010). Researchers have been using zebrafish to study behavioral, anxiety, sleep and learning disorders because the regulatory processes that underlie behavior in zebrafish and mammals is highly conserved. The zebrafish has also become extremely common in cancer research, drug

discovery and aging disease studies because of the similarity of tissue histology between fish and humans (Amatruda *et al.* 2002; Gerhard 2003; Rubinstein 2003; Zon and Peterson 2005). Using zebrafish gives researchers the advantage of directly testing a mutation in a whole animal background rather than a single cell. Additionally, using zebrafish in chemical screens allows researchers to understand the toxicity and targets of potential therapeutics before clinical trials are performed. The techniques developed over the last 30 years for zebrafish researchers have made all this possible.

The basic genetics and molecular biology methods can easily be applied in zebrafish research including PCR, cloning, gene-mapping, *in situ* hybridization and mutagenesis. Histological methods have also been important in zebrafish research since it is relatively easy to prepare paraffin sections of adult and embryonic fish, resin mounts and sections, and even cell-specific staining in the sections. Initial RNAi approaches in zebrafish were not very promising; however, the development of microinjection techniques have allowed reverse genetics or gene knockdown studies to be carried out using morpholino oligonucleotides (MOs) (Nasevicius and Ekker 2000; Ekker and Larson 2001; Grunwald and Eisen 2002; Ingham 2009). MOs are synthetic molecules, usually 25 bases in length, which bind complementary sequences of RNA by standard base pairing. Structurally MOs are very similar to DNA since MOs have standard bases; the difference is that in MOs, the bases are bound to a morpholine ring instead of deoxyribose rings and are linked through phosphorodiamidate groups instead of phosphates (Robu *et al.* 2007; Moulton 2007).

The importance of the MO chemistry is that unlike typical RNAi methods, MOs do not degrade their target RNA molecules but rather act by steric blocking, reducing the interaction of the target RNA with other molecules. The reduction in gene expression using this technique is only effective for the first 4-5 days of development, but allows for direct targeting of developmental genes (as reviewed by Gerhard 2003). Microinjections have also aided in transplantation and cell-labeling studies and development of transgenic zebrafish systems. Although other methods of introducing foreign DNA into zebrafish have been used including electroporation of fertilized eggs, particle gun bombardment, liposome-mediated gene transfer and sperm-mediated gene transfer, the highest survival rate and method of choice continues to be microinjection (Lele and Krone 1996).

Teleost Evolution: Despite having more than 300 million years separating the last common ancestor of fish and humans, the overall biology between the two are strikingly similar (Postlethwait *et al.* 1999; Gerhard 2003). As a vertebrate, zebrafish possess many anatomical and functional features that are similar to humans (as reviewed by Gerhard 2003). Analysis of the zebrafish genome, particularly focusing on Hox gene clusters, suggests that during the course of vertebrate evolution, the zebrafish and human lineages have shared two rounds of whole genome duplication prior to a third teleost-specific duplication event (Postlethwait *et al.* 1994; Postlethwait *et al.* 1999; Postlethwait *et al.* 1998). As a result of the genome duplication events, zebrafish often have

two functional homologs of the mammalian gene equivalent in which the function of the ancestral gene is now divided between two genes. For this reason, each zebrafish homolog has a more restricted function, often appearing as a divergence of spatial and temporal gene expression (Carroll, Grenier and Weatherbee 2000). Unfortunately, gene isolation and analysis in zebrafish tends to be more difficult because of the genome duplication, but in many cases the presence of two orthologs of a mammalian gene provides an advantage for developmental genetic analysis by providing the opportunity to investigate gene functions that may otherwise be obscured by other functions of those same genes in mammalian models (Postlethwait *et al.* 1998; Postlethwait *et al.* 1999, Carroll, Grenier and Weatherbee 2000).

Aside from the duplication event in teleosts, when compared to the human genome sequence, the zebrafish genome demonstrates conservation of functional domains, developmental pathways, syntenic genes, cell cycle and tumor suppressor genes, allowing the zebrafish to be an ideal model organism for the identification of genes and pathways involved in human diseases (Shin and Fishman 2002; Rubinstein 2003; Lieschke and Currie 2007). Additionally the general features of zebrafish during development through adulthood and its basic anatomy enable it to be a useful model in other areas of research as well.

Zebrafish Development, Life Cycle, and Physical Characteristics: Fertilization and development of zebrafish occurs externally and the optical clarity allows for easy manipulation of individual cells or embryos for cell-fate

determination or cell-labeling studies (Gerhard 2003; Eisen and Smith 2008). This also enables researchers to identify mutants based on phenotypes, specific behaviors or lethality simply under a microscope. This has led to the genetic identification of several developmental disorders and increased the usage of cell signaling assays originally developed for use with *Xenopus* larvae. Other useful advantages at the early stages of zebrafish development are that the developmental process occurs relatively synchronously among large clutches of eggs.

Zebrafish embryogenesis is a relatively rapid process. During the first 24 hours of development, zebrafish embryos are completely transparent making them easy to visualize and identify the development of organs and limbs (Figure 1.1A) (Eisen 1996; Grunwald and Eisen 2002). Pigmentation can be seen by 48 hours post fertilization (hpf), which helps with genetic screens exploiting pigment mutants such as *golden* and *albino*. By this time, zebrafish embryos display the vertebrate-specific body plan and most organs are fully developed (Figure 1.1B). At 72-hpf, most larvae will hatch from their chorions and swim freely (Figure 1.1C). At approximately six months of age the fish are sexually mature and ready to breed. The adult fish reach a size of 3-4 centimeters in length; females are often slightly larger than the males (Kimmel *et al.* 1995; Grunwald and Eisen 2002; Volff 2005). Adult zebrafish have a silver body with seven to nine bluish-black horizontal stripes that are present from dorsal to caudal fins. Male zebrafish also have a gold hue between the stripes.

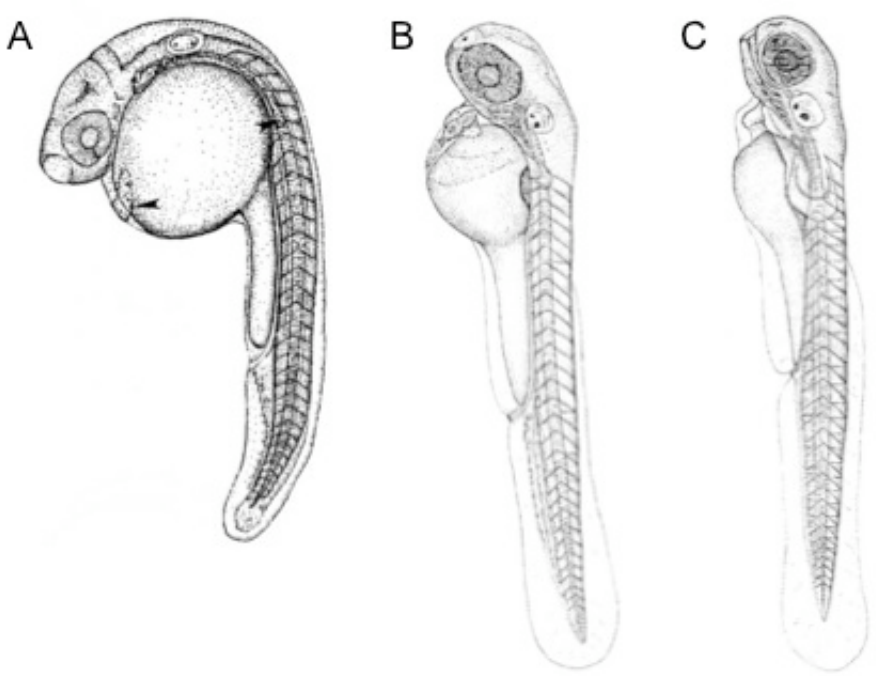

Figure 1.1: Images of wildtype zebrafish embryos (A) prim-6 or approximately 25-hpf (B) long-pec or 48-hpf (C) protruding mouth or 72-hpf (Adapted from Kimmel *et al.* 2005).

The breeding and aquaculture of zebrafish is relatively easy. Breeding pairs are set up in the afternoon before the fish are fed. Depending on the purpose of the breeding, stocks, collection or injections, the breeding tank set up has various options. When breeding for stocks, several males and females (group breeding) may be placed in the breeding tank and left overnight until the following day. This allows for a heartier stock by having multiple males fertilize eggs from various females. Another option that is particularly useful for identifying carriers of certain genes and other mutant studies is having a single male and a single female in a breeding tank. In other cases when embryos need to be of specific ages for and experiment, a divider is used to separate the male

and female fish. The dividers are then pulled at specific times the following morning and eggs are collected within a few minutes of deposition.

Streisinger and the Age of Zebrafish Genetics

George Streisinger was a molecular biologist who worked on transcription and protein synthesis in the T4 phage (Tsugita *et al.* 1968). Although he was quite established in this field, he wanted to find a vertebrate model that could be used to continue his studies. According to several published articles, Streisinger had a fondness for tropical fish and attempted to use several different species from pet stores in his lab prior to settling on zebrafish (Eisen 1996; Grunwald and Eisen 2002). In the early 1980s, breakthrough research was done when Streisinger and associates applied mutational analysis to study embryonic development, establishing a method to activate the development of zebrafish without genomic contribution from sperm, giving rise to haploid embryos. Streisinger reasoned that the zebrafish could be used in carcinogenicity and toxicology testing of chemical and environmental agents, and could serve as a model to establish quantitative dose-response relationships of carcinogenic exposures *in vivo* (Streisinger 1984; Walker and Streisinger 1983). In order to test for carcinogenicity, Streisinger developed a rapid genotoxicity test based on the current experiments using mice that exploited the zebrafish pigment mutation, *golden*. The *golden* heterozygous zebrafish were exposed to various mutagens, including gamma rays, ethyl methanesulfonate (EMS) and ethyl-nitrosourea (ENU) during the early stages of embryogenesis. These exposures

resulted in the appearance of mosaic patches of *golden* and wildtype pigmentation in the retinal-pigmented epithelium (RPE) at 48- to 72-hpf; this result suggested that the mutagens effectively targeted the early blastula cells and caused genotoxic effects (Streisinger 1984). Additionally, it was concluded that the *golden* cell patches arose from mutation, somatic crossing over, or loss of the chromosome containing the *golden* locus (Streisinger 1984). Later, it was found that exposure to EMS causes a large portion of chromosome breaks and induces a higher percentage of mosaics than ENU, which causes point mutations. These findings allowed for direct comparison of mutation frequency and tumor development, thereby increasing the significance of using zebrafish in these types of studies (Streisinger 1984; Currie 1996; Grunwald and Streisinger 1992). Streisinger's lab also laid the foundation for such techniques as the ability to breed zebrafish by *in vitro* fertilization and generate fully homozygous diploid embryos using UV-inactivated sperm. Before his death in 1984, George Streisinger showed that zebrafish could be used in classical forward genetic screens, mutation-based genetic analysis (*golden*) and gynogenetic assays. Thus, this body of work revolutionized the use of the zebrafish model system for studying development (embryology) and genetics.

Genomic Instability Mutants in Zebrafish

Genomic instability refers to a wide range of genetic alterations from point mutations to chromosomal anomalies leading to the disruption of the integrity of an organism's genetic material. The causes of genomic instability also vary from

replication errors, loss of repair mechanisms, improper chromosome segregation and cell cycle checkpoint errors. It is now known that genomic instability is a major contributor of diseases including cancer (Amatruda *et al.* 2002; Beckman and Loeb 2005).

The ability to perform genetic screens in zebrafish using the mosaic eye assay developed by Streisinger allows for the detection of mutant genes that lead to increased frequencies of somatic mutations and a cancer predisposition. Zebrafish *genomic instability* (*gin*) mutations can be induced by exposure to the point mutagen ethyl-nitro-urea (ENU) and quickly detected by the mosaic eye assay, which uses the *golden* locus on chromosome 18 to measure the somatic loss of gene function (Moore *et al.* 2006). Normally at 48-hpf, wildtype and *golden* heterozygous zebrafish embryos exhibit black pigmentation in the retinal-pigmented epithelium (RPE) of the eye and the melanophores (Figure 1.2). Embryos that are homozygous for the *golden* gene have a much lighter golden-brown pigmentation; these variations can be easily distinguished under a dissecting microscope. In order to detect the somatic mutation or *gin* phenotype, *golden* heterozygous embryos are screened for patches of lightly pigmented RPE cells; these patches indicate the loss-of-function of the wildtype allele in the cells and therefore verify the mosaic.

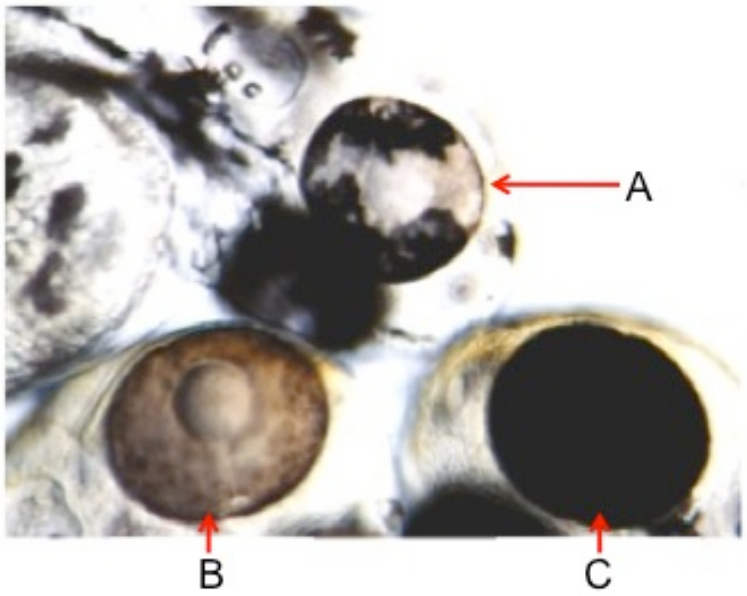

Figure 1.2: Eye pigmentation in the zebrafish embryo. Three different 72-hpf zebrafish embryos are shown above. (A) The embryo at the top of the photo with the *gin/gin; gol*/+ genotype displays the classic multiple patch mosaic eye phenotype, due to the loss of function of the wildtype *golden* allele in the lighter patches of cells. (B) The *gol/gol* (*golden* homozygous) embryo (lower left) has the characteristic light golden-brown eye color known to this pigment mutant. (C) A dark black color is visible in the +/+ (wildtype) or *gol*/+ (*golden* heterozygous) embryo in the lower right portion of the photo. Photo adapted from Moore *et al.* 2006.

Twelve *gin* mutant lines were generated by ENU mutagenesis followed by half-tetrad mapping that involved producing gynogenetic embryos from a cross by activating eggs with irradiated sperm and applying pressure to inhibit the second meiotic division (Moore *et al.* 2006). The goal of this mutant screen was to identify new genes that may be important in maintaining genomic stability. The mutants show a strong linkage to a centromeric marker on the same chromosome independent of its map position. Genetic experiments with the *gin* mutants indicated that they exhibited both maternal and zygotic gene expression in the developing zebrafish embryo (Moore *et al.* 2006). These zebrafish experiments proved to be the first direct genetic screen in a vertebrate for

somatic mutations based on a locus-specific assay (Moore, Gestl and Cheng 2004; Moore *et al.* 2006).

Consistent with the role of these genes in genomic instability, tumors spontaneously arose in adult carriers of the 12 *gin* mutations. However, carriers of the *gin-10* mutation showed a strong phenotype and became the focus of a survey to determine the frequency and variety of cancer in these fish. Although all of the *gin* carriers displayed a predisposition to malignant peripheral nerve sheath tumors, *gin-10* carriers also had approximately a 10-fold increase in the incidence in tumor formation when compared to wild type fish, and often had an earlier appearance of tumors as well. PCR-based LOH analysis was performed for several tumor samples, many were from *gin-10* fish, and the loss of a parental allele for a marker within the *gin-10* region had been lost from the tumor tissue itself, while it was still apparent in the normal tissue samples from the same fish. Additional analysis on the *gin-10* region in zebrafish tumors suggested that recombination or a regional deletion was the cause of LOH (Moore *et al.* 2006).

Potential Candidate Genes for *gin-10* Mutations

As a first step in identifying the *gin*-mutant genes, chromosome assignments were made for the 12 *gin* mutants based on preliminary mapping experiments. Most of the *gin*-mutants were confirmed using adjacent markers. Three of the mutants, *gin-5, -9,* and *-10* were all mapped to chromosome 18 where the *golden* locus is also found.

The *gin-10* mutant on chromosome 18 was mapped between bases 14,738,066 and 15,810,769 (Figure 1.3). Using this mapping data and the recent Sanger database information, a list of potential *gin-10* candidate genes was made. An overview of this region is shown in Figure 1.3. Several of these *gin-10* candidates were explored as part of this dissertation project and are the focus of Chapter Two. Although the focus for the *gin-10* candidates was specifically on *mapk12, rfx4, sir2,* and *synbl*, several other genes within the region were also cloned and analyzed by RT-PCR. The rationale for the role of these genes in genomic instability is discussed below.

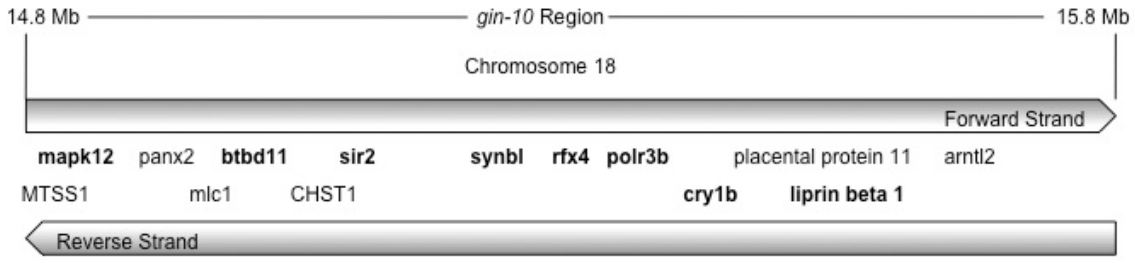

Figure 1.3: Overview of the zebrafish chromosome 18 region were *gin-10* was initially mapped in previous studies. Although there are several additional genes within this region (based on the Ensemble zv8 database), this diagram shows the key genes (bold) identified with potential for genomic instability activity.

Mapk12: The evolutionary conserved mitogen activated protein kinase (MapK) family is involved in diverse cellular processes including growth, proliferation, differentiation, survival, inflammatory response and development. Using sequential phosphorylation events, MapKs can transmit signals from the cells' environment to the nucleus and elicit an appropriate cellular response. These phosphorylation events occur on conserved domain (Thr-XXX-Tyr), which

leads to the activation and localization of the protein. There are three major subclasses of the MapK family: the extracellular signal related kinases (ERK), c-jun amino-terminal kinases (JNK), and the p38 MapKs. The middle amino acid residue of the dual-phosphorylation domain determines these subclasses; generally ERKs have a TEY motif, JNKs have a TPY motif and the p38 MapKs have a TGY motif (Krens *et al.* 2006).

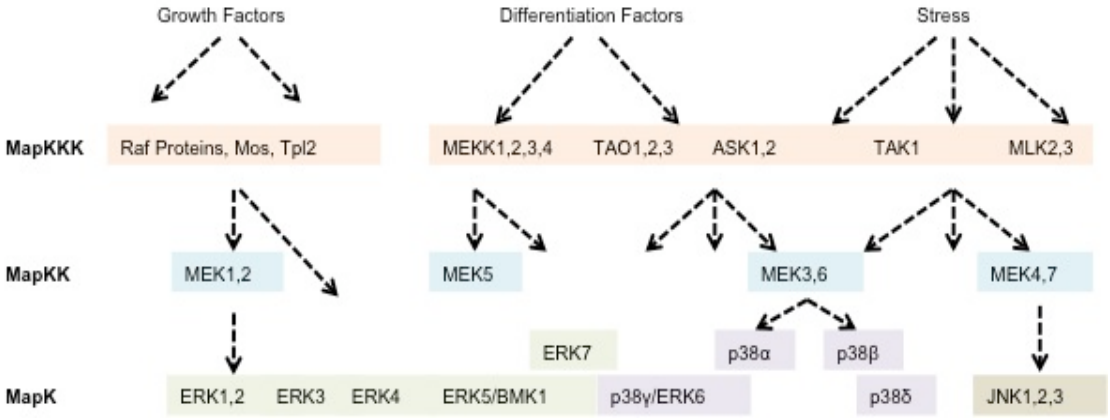

Figure 1.4: Schematic of the MapK family pathways showing initiating factors and the cascade of downstream targets (Adapted from Krens *et al.* 2006).

Several members of the MAPK family have been studied intensely because of their association with a number of diseases such as cancers, autoimmune diseases, and developmental abnormalities. For example, the Ras-MAPK (Erk1/2) pathway has been observed as one of the most oncogenic pathways in a variety of cancers, leading to uncontrollable cell proliferation by activating c-myc, c-jun, elk-1, and other transcription factors that promote DNA synthesis and cell growth. For this reason, ERK pathways are often targets for anti-cancer therapeutics and research (Tang *et al.* 2005).

This family has also been shown to be important during vertebrate development by regulating mesoderm induction and neuronal differentiation. Examples of this have been documented in the human prostatic PC12 cell line where a transient activation of the ERK pathway by EGF leads to proliferation whereas a sustained activation of this pathway in response to nerve growth factor causes differentiation (Krens *et al.* 2006). Activation by T- or B-cell receptors can also cause cell differentiation into platelet precursors.

p38γ (Mapk12) protein has been shown to be highly expressed in several human malignant cell lines, which may indicate a potential role in tumorigenesis (Tang *et al.* 2005). Several studies have revealed that the ERK/MAPK pathway activation is sufficient in transforming NIH 3T3 cells; furthermore Ras transformation is also dependant on the JNK pathway (Tang *et al.* 2005). Activation of p38 MAPKs is thought to inhibit Ras-induced cell proliferation in NIH 3T3 cells, suppress Ras transformation and induce K-Ras-dependent cell death in human colon cancers (Tang *et al.* 2005). Recent studies based on the p38 family of MAPKs have shown that K-Ras is an activator of p38γ; it has the ability to increase the expression of p38γ without phosphorylation. Consequently, this study also provided evidence that increased expression of p38γ was a requirement for K-Ras transformation by a new mechanism involving a complex with other ERK proteins (Tang *et al.* 2005).

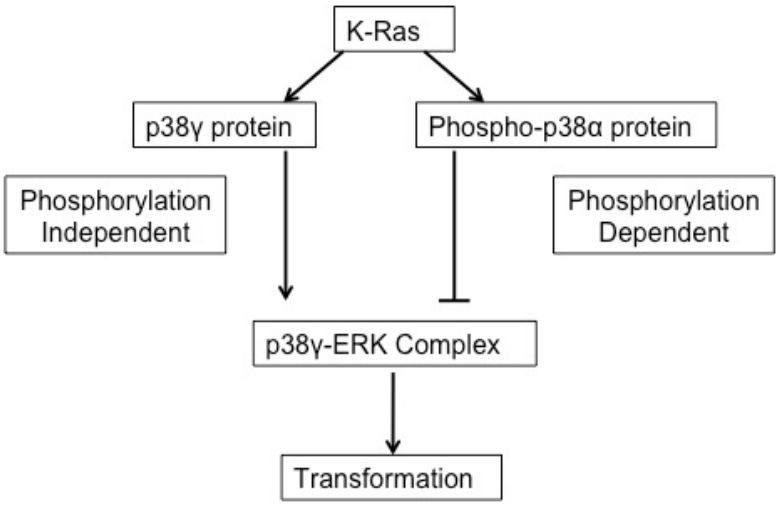

Figure 1.5: The proposed model showing the requirement of p38γ for K-Ras transformation and the inhibitory response from p38α (Adapted from Tang *et al* 2005).

Additionally, JNK and p38 MAPKs have been shown to modulate cellular responses to a variety of extracellular signals such as mitogens, inflammatory cytokines and UV irradiation; often these MAPKs are involved in promoting programmed cell death when activated (Krens *et al.* 2006). Interestingly, UV irradiation specifically activates the p38 MAPK pathway in many organisms, although it appears that each isoform is independent or has distinct biological roles (Wang *et al.* 2000; Krens *et al.* 2006). Studies have shown that all p38 isoforms can activate the transcription factor-activating factor 2 (ATF2) *in vitro*, and are involved in cell cycle arrest at particular cell cycle checkpoints. Wang *et al.* (2000) demonstrated that MKK6 and all p38 isoforms are activated by γ irradiation. Activation of this pathway is ATM-dependent and sufficient to arrest cells in G_2 following irradiation; additionally, the inhibition of MKK6 and or specifically p38γ disrupts this checkpoint (Wang *et al.* 2000).

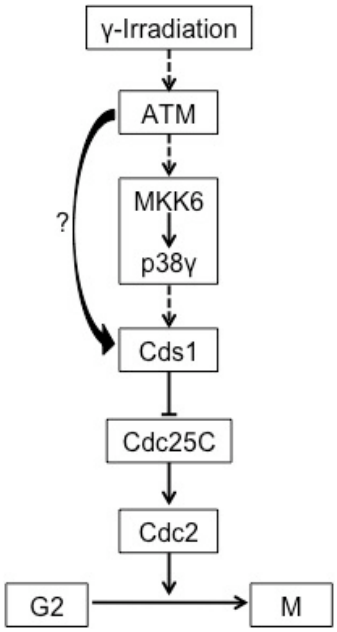

Figure 1.6: The MKK6-p38γ pathway is involved in the G2-M DNA damage checkpoint (Adapted from Wang *et al.* 2000).

The *mapk12* gene was initially found by screening human cDNA using a rat *erk-3* gene. Interestingly, *mapk12* was isolated from a human skeletal muscle cDNA library and was later confirmed to be identical to *sapk3*. From that finding it appeared that *mapk12* functioned in the differentiation of myoblasts. In *Xenopus*, MAPK12 or p38γ has been shown to phosphorylate Cdc25C and is important for G2/M progression of oocytes (Perdiguero *et al.* 2003). Additionally, data from Wang *et al.* (2000) supports the model of an important interplay between p38γ and the G_2 cell cycle checkpoint control.

Rfx4: Regulatory factor X (RFX) proteins are evolutionarily conserved transcription factors among *S. cerevisiae*, *S. pombe*, *C. elegans*, zebrafish, mouse and humans, that possess a winged helix DNA binding motif (Morotomi-

Yano *et al.* 2002). These proteins appear to function in a variety of unrelated systems including regulation of mitotic cell cycle in yeast, mammalian immune response, brain development and brain-specific diseases and testes development in mammals (Emery *et al.* 1996; Mach *et al.* 1996; Morotomi-Yano *et al.* 2002; Zhang, Zeldin and Blackshear 2007).

RFX1, RFX2, and RFX3 were first identified in human and mouse and classified as a family based on the 76-amino acid DNA-binding domain; RFX4 was found later fused to the estrogen receptor in two aberrant cDNA clones from human breast tumor tissue while other RFX proteins have just been recently identified (Emery *et al.* 1996; Matsushita *et al.* 2005). Several alternative splice variants of RFX4 have been reported in the testis and brain and may function during both morphogenesis and disease formation (Blackshear *et al.* 2003; Matsushita *et al.* 2005). More recently, Matsushita *et al.* (2005) have shown that there are several human isoforms of RFX4 and they are often overexpressed in gliomas but are not detectable in other cancers including liver, colon and stomach. The function of *rfx4* in zebrafish development and disease has yet to be explored.

Rpc2/Polr3b: RNA polymerase III (Pol III) is a 17-subunit complex that is responsible for the transcription of various small non-coding and nuclear RNAs in eukaryotes (Yee *et al.* 2007). One of the largest subunits, Rpc2, is highly homologous to its Pol I and Pol II counterparts, and the gene happens to lie within the *gin-10* region in zebrafish. Previous studies analyzing the structure of

Pol III as well as yeast two-hybrid and biochemical investigations have identified its unique functions including high processivity, efficient transcription termination and recycling, RNA 3' cleavage activity, and interaction with diverse promoters to specific individual subunits (Yee *et al.* 2007). Additionally, mutational analysis in yeast have shown that intact Pol III is essential for cell growth; reduced Pol III function are broad including disruption of protein synthesis, incomplete ribosome biogenesis, mRNA splicing defects and defects in membrane targeting for newly translated proteins. Studies in human cell lines have also implicated the roles of known oncogenes and tumor suppressors, including c-myc and Rb, in controlling the interactions of transcription factors that bring the Pol III complex to the promoters of its target genes (White 2005; Yee *et al.* 2007). Deregulated Pol III activity has been shown to be a common feature of tumorigenic cells in culture; however, there is little evidence that it is elevated Pol III activity. Determining the role of *rpc2* in zebrafish tumors will increase the understanding of human cancer.

Sir2: Sirtuins (sir2) are NAD-dependent deacetylases that are found in a variety of organisms from bacteria to humans. They were originally found in yeast and have been shown to act in transcriptional repression, recombination, cellular division, microtubule organization, cellular responses to DNA damage and aging (Buck, Gallo and Smith 2004; North and Verdin 2004). The sirtuin family has a unique catalytic domain characterized by its requirement for NAD as a cofactor (Blander and Guarente 2004; North and Verdin 2004). One of the main functions of this protein family is the regulation of transcriptional repression

through binding a multiprotein complex. Sequence-specific DNA binding proteins mediate the initial recruitment of sirtuin protein complexes to telomeres and other loci for transcriptional repression (North and Verdin 2004).

There are several types of sirtuins found in yeast, mammals, and zebrafish. Sirt1 has been implicated in the repair of DNA damage by negatively regulating the p53 pathway; it has been shown to deacetylate p53, which is initially acetylated at two lysine residues in response to DNA damage in order to activate it (Sakaguchi *et al.* 1998; North and Verdin 2004). The human Sirt2 protein has been shown to localize in the cytoplasm and is involved in the regulation of the microtubule network by deacetylating lysines of α-tubulin. Recent studies have also shown that Sirt2 is upregulated prior to mitosis and is potentially involved in cell-cycle regulation (Blander and Guarente 2004; North and Verdin 2004). Additionally, recent proteomics research has provided a role for Sirt2 in cancer pathogenesis since the gene is located in a region of frequent chromosomal deletions in human gliomas, indicating that Sirt2 may act as a tumor suppressor (North and Verdin 2004). Mammalian Sirt3 has been shown to localize in the mitochondrial matrix mediated by an amphipathic α-helix at its amino terminus (Buck, Gallo and Smith 2004; North and Verdin 2004). Several studies have shown that *in vitro*, Sirt3 has robust histone deacetylation activity; since it appears to be localized in the mitochondria, the relevance of its HDAC activity is still not understood (North and Verdin 2004). Recent research has also shown that sirtuins may play a considerable role in the genetic control of aging and related diseases. Additionally, the mammalian Sirt4, Sirt5, Sirt6 and Sirt7

also display some histone deacetylation properties; however, that research is still underway.

Synbl & Ric8a: Asymmetric cell division plays an important role during embryogenesis by producing daughter cells with distinct differentiation pathways (Cowenbergs, Spilker and Gotta 2004). Members of the RIC-8 or synembryn family proteins are known to be key regulators of asymmetric cell division in invertebrate and vertebrate embryogenesis. Appropriate centrosome positioning and movement determines the alignment of the mitotic spindle and is an essential feature of development since it determines the cleavage plane during cytokinesis (Miller and Rand 2000; Miller *et al.* 2000). Many studies have been modeled in *C. elegans* showing the importance of accurate spindle orientations for an asymmetric first cell division. The movement and positioning of centrosomes also mediates nuclear migration in a variety of cells and organisms (Miller *et al.* 2000). The machinery that regulates these movements during development are still not fully understood; however recent studies in *C. elegans* and *Drosophila* are beginning to identify the mechanisms involved.

The *ric-8* gene was first identified in a screen of *C. elegans* mutants that were resistant to inhibitors of cholinesterase and defective in vesicle priming (Miller *et al.* 2000; Miller and Rand 2000; Cowenbergs, Spilker and Gotta 2004). Subsequently *ric-8* has been identified as a required cytoplasmic protein for G-protein signaling in the *C. elegans* nervous system and more recently as an important part of the machinery that regulates the mitotic spindle, nuclear

migration and other centrosome-mediated events during early embryogenesis (Miller *et al.* 2000; Miller 2000). RIC-8 proteins are G-protein positive regulators, which exhibit G-protein coupled receptor-independent guanine nucleotide exchange activity for Gα subunits. These proteins act downstream of partitioning-defective (PAR) proteins, which contributes to spindle and centrosome anchoring events (Wilkie and Kinch 2005).

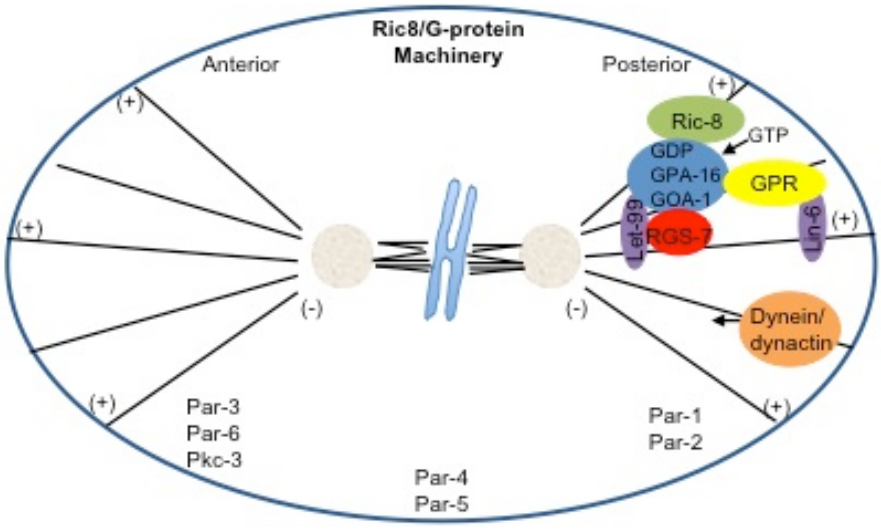

Figure 1.7: Schematic of the Ric8 mediated asymmetric cell division in *C. elegans* zygotes (Adapted from Wilkie & Kinch 2005).

Other studies in *C. elegans*, *Drosophila* and in mammals have also shown that Ric-8 proteins are required for signaling during synaptic transmission and thus seem to also be involved in receptor-dependent signaling (Hampoelz *et al.* 2005). Ric-8 mutants have been created in *C. elegans*, *Drosophila,* and in zebrafish; all homozygous *ric-8* mutants are lethal but studies have shown in all three models that they can be rescued by injection of a transgene that covers the *ric-8* genomic locus (Hampoelz *et al.* 2005). In addition to the role in

development, dysregulation of asymmetric cell division has recently been shown to play an important role in cancer.

In Xenopus, mouse and other mammals, there are two *ric-8* homologs: *ric-8A* (*synembryn-a*) and *ric-8B* (*synembryn-b*), while there is only one *ric8* gene in *C. elegans* that gives rise to two proteins by alternative splicing. The zebrafish *synembryn-like* gene (*synbl*) is a *ric-8b* homolog and is located on chromosome 18 within the interval thought to contain the gene responsible for the ENU-induced *gin-10* genomic instability mutation. The zebrafish *ric-8a* gene is located on chromosome 25 and appears to have at least three protein-coding transcripts. The role of these different *ric-8* transcripts during zebrafish development is not clear.

Mdm1 as a *gin-12* Candidate Gene

Similar to *gin-10*, the ENU-induced genomic instability mutation, *gin-12*, has been shown to cause embryonic somatic mutations in *golden* heterozygous zebrafish; this mutant was mapped to an interval on chromosome 4 in zebrafish in previous studies (Cheng and Moore 1997; Moore, Gestle and Cheng 2004; Moore *et al.* 2006). Several genes within the *gin-12* region may potentially display genomic instability activity including *mdm1*, which was originally cloned from 3T3DM cells along with *mdm2* and *mdm3*.

The well-studied Mdm2 protein has been shown to cause acentric chromatin bodies or double minutes (DMs) and mediate the immortalization and transformation of rat embryo fibroblasts when overexpressed in cooperation with

Ras (Freedman, Wu and Levine 1999). Additionally, Mdm2 has been shown to negatively regulate the p53 tumor suppressor and is classified as an oncogene. Since *mdm1* was originally identified on DMs with *mdm2*, it is possible that it also functions as an oncogene in the p53 pathway, giving rise to genomic instability (Snyder *et al.* 1988).

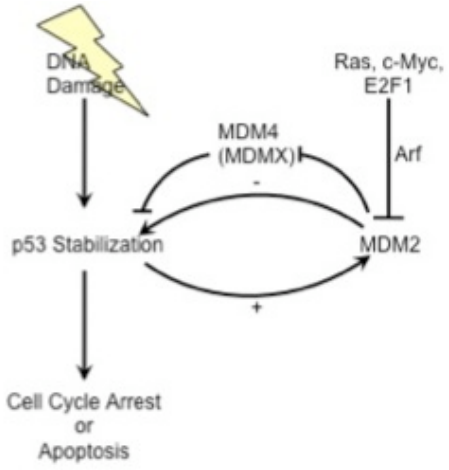

Figure 1.8: Diagram of the autoregulation of p53, Mdm2 and Mdm4 following DNA damage and/or mitogenic signals in the cell.

Unlike Mdm2, the structure and functional domains of the Mdm1 protein have yet to be studied. Using the ExPasy Proteomics server (www.expasy.org), phosphorylation, glycosylation, and myristoylation sites were predicted the known zebrafish Mdm1 peptides (Figure 1.9, Appendix C). Interestingly, two potential sumoylation (SUMO) sites were also predicted, which may play and important role in the cellular localization and stability of the Mdm1 protein. While it does not appear that Mdm1 shares the same functional domains as the Mdm2 protein

based on the bioinformatics predictions, it remains an interesting candidate for the *gin* studies.

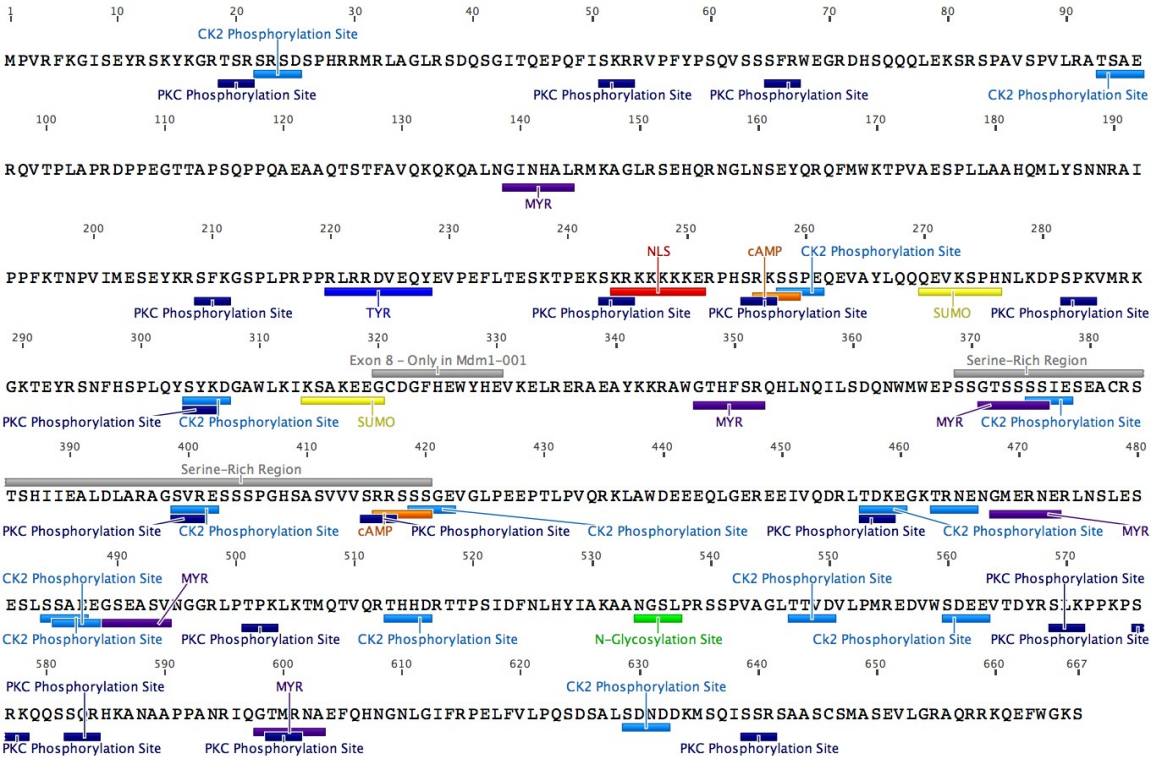

Figure 1.9: Predicted functional sites of the zebrafish Mdm1-001 (long) peptide. The ExPasy Bioinformatics resource portal predicted several Protein Kinase C (PKC) phosphorylation sites, Casein Kinase II (CK2) phosphorylation sites, five *N*-myristoylation (MYR) sites, two cAMP/cGMP dependent protein kinase (cAMP) phosphorylation sites, one Tyrosine Kinase (TYR) phosphorylation site, and one *N*-glycosylation site. Additionally, two SUMO sites were predicted in the Mdm1 peptide sequence, along with a potential Nuclear Localization Signal (NLS) and a 52- amino acid serine-rich region. A larger version of this image can be found in Appendix C.

Not much is known about *mdm1* in human, mouse, or zebrafish; however there have been studies suggesting that it is involved in retinal degenerative diseases including *arrd2* in mouse (Chang *et al.* 2008). A nonsense mutation in the *mdm1* gene appears to cause a late-onset RPE atrophy and hypopigmentation, similar to human AMD, in the affected mice; the complete absence of *mdm1* in mice leads to severe retinal degeneration. Further

investigation of the *mdm1* gene in zebrafish as a model to knockdown and overexpress this gene will allow for a better understanding of its function during development and whether it has any genomic instability activity.

Summary and Specific Aims

Several zebrafish mutations have been found that display increased frequencies of somatic mutations during embryonic development and cause an increase in tumor formation during adulthood. These genomic instability mutants (*gin*) are heritable, ENU-induced mutations that have been shown previously to act both maternally and zygotically in the zebrafish embryo (Moore *et al.* 2006). The focus of this dissertation project was to study candidate genes for the *gin-10* and *gin-12* genomic instability mutations.

There are three Specific Aims for this project.

1. Explore and study potential *gin-10* candidate genes and determine whether these candidates have the potential for genomic instability activity by knocking each down in *golden* heterozygous embryos.
2. Distinguish the differences in gene expression and developmental function of the paralogs *synbl* and *ric8a*, both of which have been shown to regulate asymmetric cell division in the development of *C. elegans*.
3. Characterize the *gin-12* candidate gene *mdm1* in early zebrafish development using transcript expression analysis and morpholino

knockdown technology, as well as analyzing potential protein-protein interactions.

Chapter Two focuses on *gin-10* candidate genes and Specific Aims 1 & 2. The goal of Specific Aim 1 is to explore the potential candidate genes within the *gin-10* region on chromosome 18 in zebrafish embryos and determine which of the candidate genes may contribute to genomic instability during development. The initial prediction was that only 1-2 genes within the *gin-10* region would model genomic instability activity and lead to future research in the characterization of its function during development and cancer. Specific Aim 2 is based on a candidate gene found within the *gin-10* region, *synembryn-like* (*synbl*), which has been shown to regulate asymmetric cell division in *C. elegans*. A homolog was found on chromosome 25, *ric8a*, which recent studies have shown that it is often abnormally regulated in certain cancer types. The purpose of this aim is to characterize the functions of these two homologs in zebrafish by exploring developmental expression patterns and through the use of transgenic zebrafish models.

Chapters Three and Four explore Specific Aim 3, which is a study of the *gin-12* candidate gene *mdm1*. It was initially thought that the *mdm1* gene might play a role in the p53 tumor suppressor pathway by either regulating p53 directly or as part of an overall regulatory component. Based on the amino acid sequence of Mdm1 and it's homology to Mdm2 and Mdm4 (known p53 regulators), it appeared that Mdm1 did not contain the p53 binding sequences and most likely did not directly bind to the p53 protein. Thus, studies were

designed to determine whether *mdm1* functioned in the p53 pathway or displayed genomic instability activity in the zebrafish embryo.

CHAPTER TWO

AN INVESTIGATION OF THE ZEBRAFISH *GIN-10* CANDIDATE GENES

Rationale and Experimental Design

An ethyl-nitrosurea (ENU) mutagenesis experiment led to the discovery of twelve genomic instability (*gin)* mutants with the phenotype of increased frequencies of embryonic somatic mutations (Moore *et al.* 2006). The *gin-10* mutant line showed noticeably increased frequencies of tumor development and somatic loss of heterozygosity (LOH) based on PCR assays; thus the goal of these studies was to identify the gene or genes involved in the *gin-10* line. In previous studies, half-tetrad analysis and SSR markers were used to approximate the *gin-10* region on the zebrafish chromosome 18 (Moore *et al.* 2006).

Table 2.1: Potential *gin-10* Candidate Genes on chromosome 18

Sanger Gene	Gene Information
si:dkey103i16.1	PTPRF interacting protein (liprin beta 1)
cry1b	cryptochrome 1b
rpc2/polr3b	RNA pol III subunit B
rfx4	regulatory factor X, 4
synbl	synembryn-like; resistance to inhibitors of cholinesterase B
si:dkey103i16.6	sir2 homolog
btbd11b	btb (POZ) domain containing 11b
mapk12 (ERK6 or p38γ)	mitogen-activated protein kinase 12a
cirh1a	cirrhosis, autosomal recessive 1a (cirhin)
rpb5	RNA pol II subunit 5

Since ENU causes point mutations that can be difficult to map, a candidate gene approach was used to identify the potential *gin-10* mutant genes. Initially, a list of genes within the *gin-10* region was created based on the SSR mapping data, most current Sanger Ensemble database (www.ensemble.org) and evaluated based on potential for genomic instability activity using the known orthology information from NCBI and Sanger databases. The 10 candidate genes identified are presented in Table 2.1

Since previous genetic studies suggested that the *gin* carrying mutants must be expressed both maternally and zygotically during development, the first step was to determine the candidate gene expression profiles during various stages of development by RT-PCR. The *synbl, mapk12, cry1b, rfx4*, and *sir2* candidate genes were fully cloned as cDNA from the wildtype (WT(AB)) strain of zebrafish for future sequence comparison to *gin-10* fish. Additionally, expression profiles of the *synbl, rfx4*, and *sir2* were explored using semi-quantitative RT-PCR and whole mount *in situ* hybridization in zebrafish embryos of various ages. To formally investigate the contribution to genomic instability of *synbl, ric8a, rfx4*, and *sir2*, the genes were knocked down in zebrafish embryos using morpholino oligonucleotides (MOs) in both WT(AB) and *golden* heterozygous fish. The use of MOs in the zebrafish embryo provides information about the biological function of *synbl, ric8a, rfx4*, and *sir2*. Lastly, *synbl* heterozygous transgenic zebrafish were obtained from the Zebrafish International Resource Center (ZIRC), in order to further explore the function of this candidate and the paralog, *ric8a*, in a background other than WT(AB).

Cloning and Sequencing Candidate Gene Fragments from WT(AB) Embryos

The initial phase in these studies was to determine whether the candidate genes were expressed both maternally and zygotically in WT(AB) embryos. To do this, zebrafish embryos were collected at various stages of development and euthanized in order to isolate total RNA. Several pairs of primers were made to amplify cDNA from each candidate gene (Table 2.1). The primers were designed specifically to amplify a region of the transcript that spans more than one exon in the genomic DNA; this allowed for the successful amplification from the RNA without any trace of genomic DNA contamination.

Candidate gene fragments were amplified using 4-hpf and 24-hpf embryo RNA and ligated into the pCR4 vector (Invitrogen) for sequencing. The pCR4 vector was used primarily because it allowed for a greater percentage of positive clones since it contains the TA cloning feature and has a fast ligation time. Additionally the sequencing promoters are much closer to the PCR insert, allowing for better sequencing results (Figure 2.1).

Creating a Bank of cDNA Clones from WT(AB) Stocks: It had been suggested that cDNA libraries of wild type zebrafish genes be created for this project to provide a stable and consistent source of cDNA. Therefore, this project began by preparing cDNA stocks from 24-, 48-, 72-hpf, and 7-dpf WT(AB) embryos using two different commercial kits: Invitrogen's Superscript III First Strand Synthesis kit and New England BioLab's Protoscript II kit. Unfortunately,

several of the candidate genes showed poor amplification from the cDNA stocks or had numerous, non-specific amplification on the gel photos (Figure 2.2). These results were seen using both cDNA kits with multiple primer sets for several candidate genes; however a preliminary direct RT-PCR experiment gave robust clean amplification of specific candidate gene fragments of interest (Figure 2.3 and Appendix 1). Thus, RT-PCR became the method of choice for cloning the *gin-10* candidate genes.

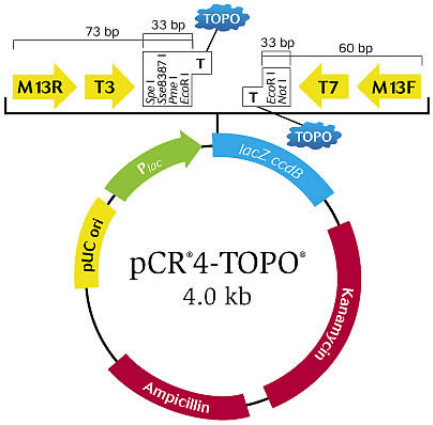

Figure 2.1: pCR4-TOPO cloning vector (Invitrogen) used to clone fragments of candidate *gin-10* genes for sequencing and later probe making for other experiments.

RT-PCR and Cloning: WT(AB) embryos were collected from breeding tanks and brought over to the lab in system water, transferred to a glass dish and sorted into petri dishes in groups of 100 embryos or less. Embryos were allowed to develop under normal conditions in a 27^{o}C incubator until the desired developmental age was reached, when they were collected into microfuge tubes in groups of 50 and total RNA was isolated using the Trizol method (Invitrogen). RT-PCR reactions for each candidate gene were performed several times for each primer pair initially to determine whether the gene was expressed both

maternally (4-hpf RNA) and zygotically (after 8-hpf). All reactions were run on the appropriate concentration agarose gel and photographed.

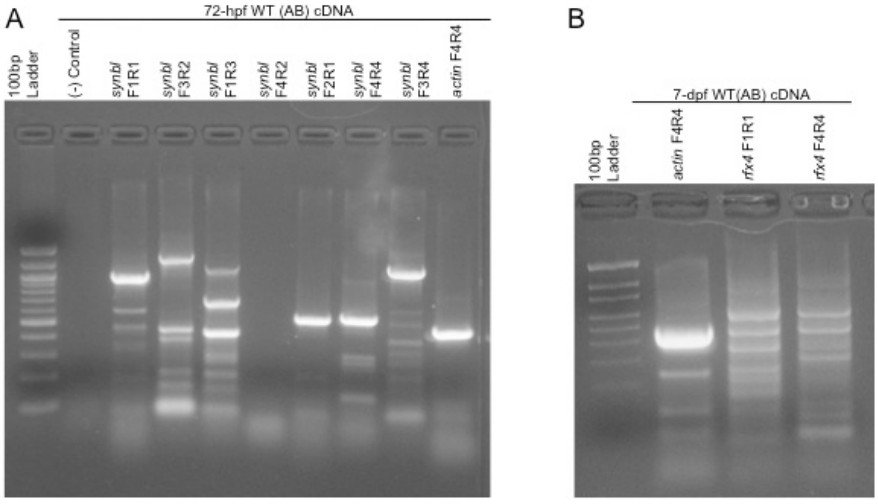

Figure 2.2: PCR performed using the Invitrogen Superscript III First Strand Synthesis kit and several sets of *synbl* and *rfx4* primer sets. (A) Most of the primer sets shown here amplified multiple fragments when using the cDNA stocks, except for *synbl* F2R1. These same primer sets amplified single, robust bands with direct RT-PCR. Additionally, *synbl* F4R2 did not amplify with this method. (B) Primers for the *rfx4* gene were also used to amplify fragments from cDNA, and gave rise to multiple fragments appearing on the gel. *Actin* is shown as a positive control in both gel photos.

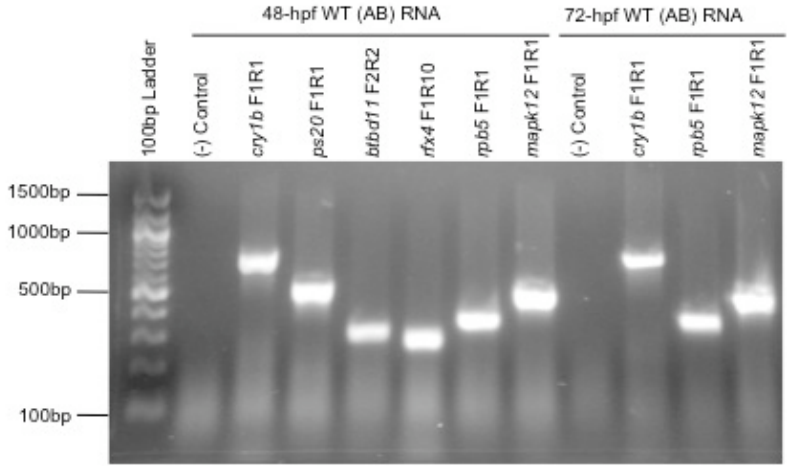

Figure 2.3: RT-PCR results of several *gin-10* candidate genes at 48- and 72-hpf.

Candidate gene fragments were amplified from WT(AB) RNA at various ages to determine if the genes were expressed both maternally and zygotically in the embryos. Figure 2.3 demonstrates the zygotic expression of several candidate genes, *cry1b, ps20, btbd11, rfx4, rpb5,* and *mapk12*; this is a representative experiment with complete RT-PCR data for all of the *gin-10* candidates shown in Table 2.2. The initial objective was to narrow down the *gin-10* candidate list by removing genes that were not expressed both maternally and zygotically. However, it appears that all of the candidates screened had both maternal and zygotic expression. Before pursuing these candidate genes further, it was important to search Sanger and NCBI databases for information regarding the function and orthology of the current list of zebrafish *gin-10* candidate genes. By doing so, several of the genes were immediately removed from the list based on orthologous information in human and mouse studies. For example, although *cry1b* is close to one of the *gin-10* markers on chromosome 18 in zebrafish, database, and publication searches revealed that it is involved in circadian rhythms with *CLOCK* genes and has been regularly studied without inference to genomic instability activity. Other genes that were removed from the candidate list included *cirh1a, rpb5,* and *ps20*. Full developmental expression profiles were obtained for the rest of the candidate genes, including *rpc2/polr3b*, which was also eventually removed from the candidate list since recent publications determined that it functioned mainly in the development of the digestive system and also did not appear to have genomic instability activity (Yee

et al 2007). Table 2.2 shows complete results for RT-PCR data, based upon individual experiments that can be found in Appendix A.

Table 2.2: Summary of RT-PCR Maternal and Zygotic Expression Results from the *gin-10* Candidate Genes on Chromosome 18 in Zebrafish.

Gene/Fragment		4-hpf	8-hpf	12-hpf	18-hpf	24-hpf	36-hpf	48-hpf	72-hpf	7-dpf
	F1R1	+				+			+	+
btbd11	F2R2	+				+		+	+	+
	F1R1	+				+		+	+	
cirh1a	F2R2	+				+		+	+	
	F1R1	+				+		+	+	
	F2R2	+				+				
cry1b	F3R3	+				+				
	F1R1	+				+		+	+	
mapk12	F2R2	+				+				
	F1R1 (long)	+				+		+	+	+
ps20	F3R3 (short)	+				+			+	+
	F1R10	+				+		+	+	
	F5R9	+				+			+	
	F5R13	+				+			+	
	F6R9	+				+			+	
	F5R5								+	
	F7R6								+	
rfx4	F1R1									+
	F4R4									+
	F1R1	+				+		+	+	
rpb5	F2R2	+				+				
	F1R5	+	+	+	+	+	+	+	+	+
	F3R1							+		
	F4R6							+		
	F5R7							+		
rpc2	F3R2					+			+	
	F2R3			+	+	+	+	+	+	+
	F1R1	+				+		+	+	
	F2R2	+				+		+	+	
sir2	F3R3	+				+		+	+	
	F1R1			+		+		+	+	+
	F6R3							+	+	
	F3R2			+		+		+	+	+
	F1R5 (genomic 5'UTR)								+	
	F2R1	+	+	+	+	+	+	+	+	+
	F3R4			+					+	
	F4R2			+						
synbl	F4R4			+					+	
	F1R3								+	

Due to the apparent involvement in asymmetric cell division during development of *C. elegans*, the focus of the *gin-10* candidates shifted towards the *synbl* gene and its homolog *ric8a* on chromosome 25. The goal was to continue investigating the candidates that remained on the list including *sir2* and *rfx4*, but to concentrate particularly on the function of *synbl* and *ric8a* since asymmetric cell division is a known characteristic of many cancer types (Aguilera and Gomez-Gonzalez 2008).

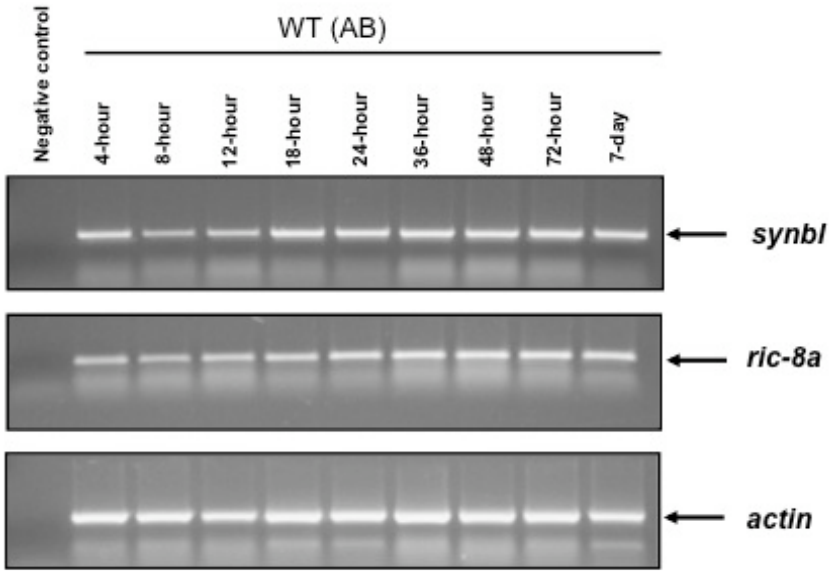

Figure 2.4: Developmental profile of embryonic gene expression of *synbl, ric8a* and *actin* in WT(AB) zebrafish.

A developmental RT-PCR profile was performed using WT(AB) RNA and primers for *synbl* and *ric8a*; *actin* is shown as a positive control. As seen in Figure 2.4, both *synbl* and *ric8a* appear to be expressed throughout zebrafish embryonic development through larval stage day 7. From this data, it appears that maternal expression of *synbl* is slightly more robust than its homolog, *ric8a*.

Noticeably, *synbl* expression decreases from Mid-Blastula Transition (MBT) through 12-hpf, then remains robust and constant through 7-dpf. Expression of *ric8a* appears relatively low in comparison through approximately 18-hpf, then increases slightly at 24-hpf and remains constant through 7-dpf. It is important to note that although *actin* was used as a positive control, its expression does vary slightly during development.

Normal Expression of Candidates in Developing Zebrafish Embryos

Semi-Quantitative RT-PCR: In order to further explore the developmental profiles of the *gin-10* candidate genes, a more quantitative approach was pursued. All of the candidates initially tested by RT-PCR showed consistent levels of both maternal and zygotic gene expression (Table 2.2, Figure 2.4). Rather than using qPCR, which is very expensive and unavailable in the laboratory, it was suggested that the expression of candidate gene transcripts was assessed by the semi-quantitative RT-PCR technique (Marone *et al.* 2001; Livingston *personal communication*). This method uses a low-cycle RT-PCR in combination with a partial Southern blotting procedure, allowing for better visualization of the quantity of a transcript than standard PCR (Marone *et al.* 2001). For these experiments, DIG-labeled DNA probes for the candidate genes were used on developmental blots and detected with CSPD substrate (Roche).

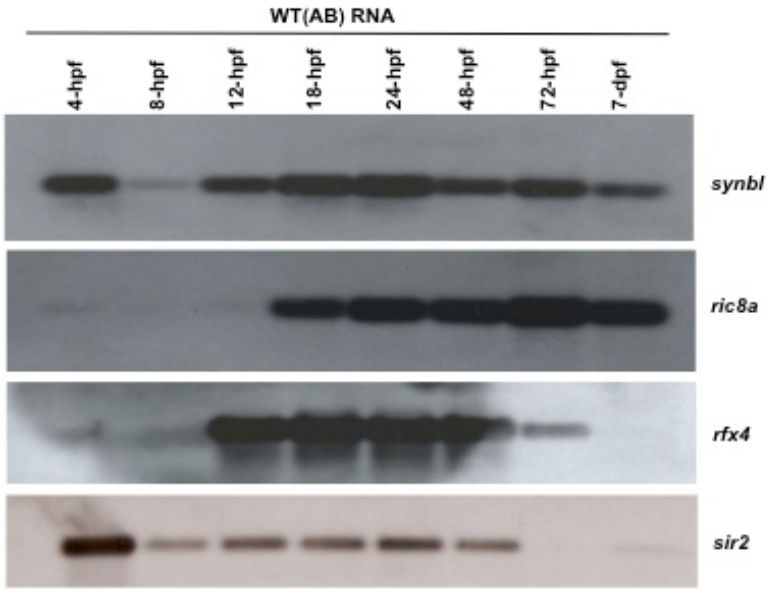

Figure 2.5: Semi-quantitative RT-PCR Developmental Profile of several *gin-10* candidate genes, *synbl, rfx4* and *sir2*. *ric8a* is not a *gin-10* candidate; however it is a paralog of *synbl* making it an important gene to study and determine what expression and functional differences occur between the two.

Previous examination of the gene expression of these particular *gin-10* candidates resulted in all of the candidates displaying both maternal and zygotic gene expression (Figure 2.4). In contrast, Figure 2.5 shows a very distinct difference in the gene expression patterns of *synbl, ric8a, rfx4,* and *sir2*. Particularly, there appears to be an apparent differential expression pattern between paralogs *synbl* and *ric8a*. As demonstrated earlier, *synbl* has a strong maternal expression that decreases around MBT, then steadily increases through 24-hpf. This data suggests that *synbl* expression is slightly decreased at 48-hpf, peaks at 72-hpf then continues to decrease through larval stage (day 7). Interestingly, *ric8a* displays very low expression through 18-hpf, where it begins to increase until its expression peaks at 72-hpf, then decreases by 7-dpf. Since these results initially appeared very different from the original RT-PCR experiments, the semi-quantitative experiments were repeated several times for

verification. By using a more sensitive application of RT-PCR, a variation in gene expression between these homologs was finally identified.

Similarly, *rfx4* and *sir2* exhibited robust bands when amplified by the standard 35-cycle RT-PCR experiments at various ages. The semi-quantitative data suggests that *rfx4* has very little maternal expression while the zygotic expression peaks by 12-hpf and remains at a constant level through 48-hpf. By 7-dpf, expression of *rfx4* in WT(AB) is completely absent. Maternal expression of *sir2* appears to be very robust in comparison with original RT-PCR and some of the other candidate genes, and then gradually decreases at MBT. From 12- to 24-hpf, there is a gradual increase in the expression level of the *sir2* transcript; by 48-hpf the transcript level appears to decrease again until it is hardly detectable from 72-hpf through 7-dpf.

Whole-mount in situ Hybridization: This technique was used to investigate the temporal and spatial expression of specific candidate gene transcripts at various ages during development. WT(AB) embryos treated with 1-phenyl-2-thiourea (PTU) to stop pigment formation and *golden* embryos were utilized for these experiments. Several DIG-labeled RNA probes were made from the candidate clone library using the Ambion MaxiScriptT3/T7 kit.

It is important to note that many ages of zebrafish embryos were used for the *in situ* hybridization experiments. Due to the complexity of this procedure, many of the embryos disintegrated during the various washing steps (See

Chapter Six for detailed methods). The results shown here are representative examples of the data gathered.

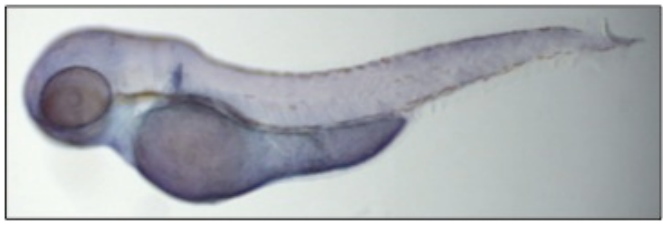

Figure 2.6: Whole-mount *in situ* hybridization of a 48-hpf WT(AB) zebrafish embryo using an DIG-labeled *actin* RNA probe. Both sense and antisense probes were made for each gene tested; *actin* was used as a positive control since it results in the staining of the entire embryo when using the antisense RNA probe. Other controls (not shown here) were (1) batches of embryos that were not subject to an RNA probe but were blocked and stained, and (2) embryos that were not subject to an RNA probe or Anti-DIG antibody but were stained. Controls were used to verify that non-specific staining by BM Purple (Roche) would not occur in the experimental embryos.

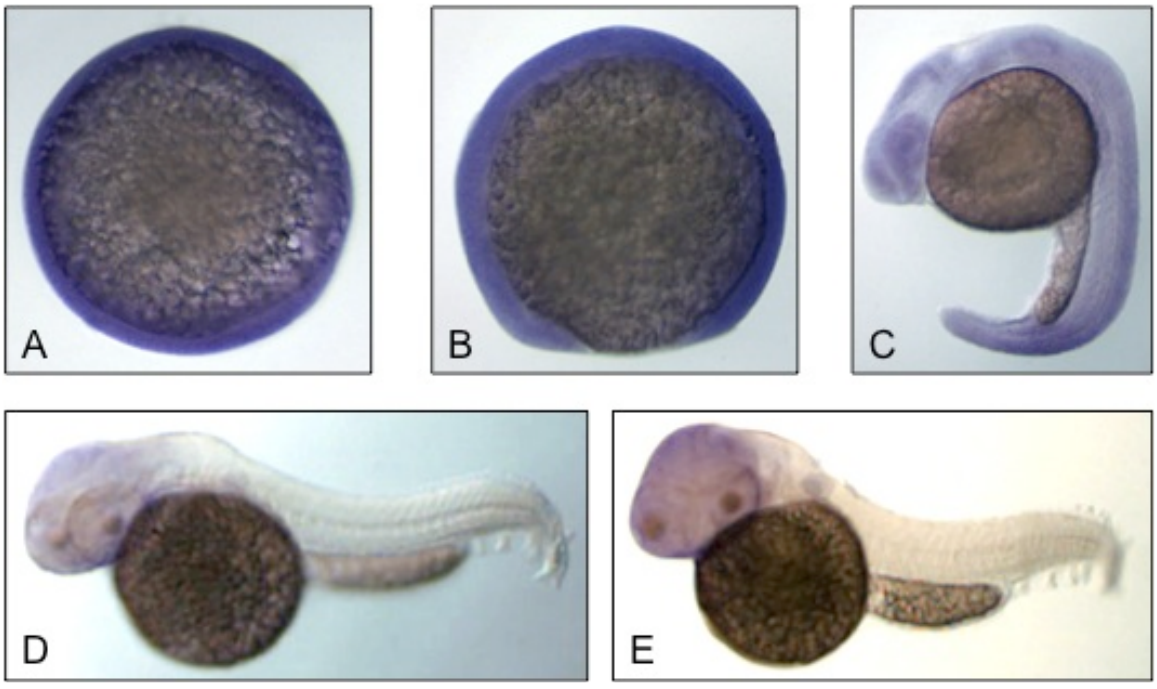

Figure 2.7: Whole-mount *in situ* hybridization of WT(AB) embryos using a DIG-labeled *synbl* RNA probe (A) 8-hpf (B) 12-hpf (C) 24-hpf (D) 48-hpf (E) 72-hpf. It is important to note that embryos were treated with PTU to prevent the development of pigment after 24-hpf.

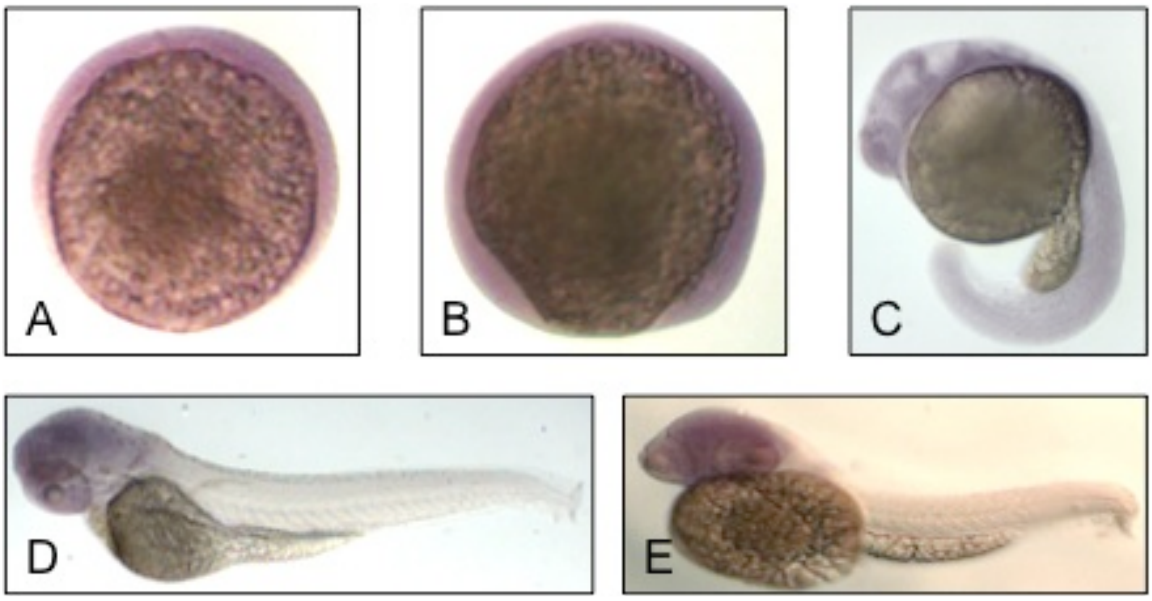

Figure 2.8: Whole-mount *in situ* hybridization of WT(AB) embryos using a DIG-labeled *ric8a* RNA probe (A) 8-hpf (B) 12-hpf (C) 24-hpf (D) 48-hpf (E) 72-hpf. It is important to note that embryos were treated with PTU to prevent the development of pigment after 24-hpf.

The expression pattern of *synbl* in developing zebrafish embryos is shown in Figure 2.7. These results suggest that the *synbl* gene is ubiquitously expressed in the early embryo through approximately 24-hpf, then expression becomes restricted to the brain as seen in the 48- and 72-hpf embryos. Figure 2.8 shows the *in situ* results for *ric8a* in WT(AB) embryos. Although there appears to be some staining in 8- and 12-hpf embryos, the staining is muted and not robust, and may be contributed to background staining. The deep purple stain is apparent in the 24-hpf embryo, and like the *synbl* homolog, appears to be ubiquitous at this time point, with some more concentrated staining in the hindbrain and cerebellum. Likewise, between 48- and 72-hpf, staining for *ric8a* appears to become restricted to the brain.

Based on teleost evolution, it was anticipated that the *ric8* homologs, *synbl* and *ric8a*, would diverge in their expression and function as a result of gene duplication events. Thus, the differential expression patterns during zebrafish development were expected. The data suggests that the temporal expression of *synbl* and *ric8a* are significantly different, as it appears that *ric8a* is transcribed well after MBT. Interestingly, both genes appear to be initially expressed ubiquitously throughout the embryo, and then becoming restricted to the brain based on *in situ* data. It is possible that both genes function cooperatively during development within the central nervous system (CNS). In order to further the understanding of these two homologs, it became necessary to identify specific gene function during early development by knocking down each gene with Morpholino Oligonucleotides (MOs).

Consequently, *rfx4* and *sir2* were still priority candidates on the *gin-10* list. The functions of these two genes in zebrafish development were still unknown. Therefore it was important to investigate these genes further using MOs into a WT(AB) background for functional analysis and *golden* heterozygotes for genomic instability analysis.

Testing Candidate Genes for Genomic Instability

In the mosaic eye assay used to identify *gin* mutations, mosaicism at the golden locus was seen in *gin/gin* homozygotes (Streisinger 1984; Moore *et al.* 2006). Candidate genes were therefore knocked down in *golden* heterozygous embryos to determine if they would also cause mosaic eye pigmentation. The

preferred method of gene knockdown in zebrafish embryos is to inject the antisense oligonucleotides known as morpholinos (MOs). MOs have become the standard gene knockdown tool in embryonic animal systems. MOs are not degraded by nucleases in animals, serum, or cells since cellular proteins do not recognize the structure (backbone). Furthermore, injections of MOs do not activate Toll-like receptors or activate innate immune responses, or modify the methylation of DNA. Therefore, the effects of MOs during embryogenesis can be seen up to several days following the injection.

Morpholino Design: Morpholinos have a higher binding affinity than equivalent DNA-based antisense oligos, which allows them to target a specific gene more effectively. Part of the reason for the success of MOs is because they act by steric blocking as opposed to an RNase H-mediated mRNA degradation mechanism. In eukaryotes, pre-mRNA is transcribed from the DNA in the nucleus, introns are spliced out, and then mature mRNA is exported into the cytoplasm where translation of the peptide product occurs (Figure 2.10A). MOs can be made to modify or block the splicing process, or block translation depending on the sequence of the oligo.

The most common MOs used are those that block translation by binding to the 5'UTR of mRNA (just upstream of the AUG), which allows the MO to interfere with the progression of the ribosomal initiation complex from the 5' cap to the start codon (Figure 2.10B). By preventing translation initiation, the MO effectively

knocks down gene expression; this allows for the function of the gene during development to be identified.

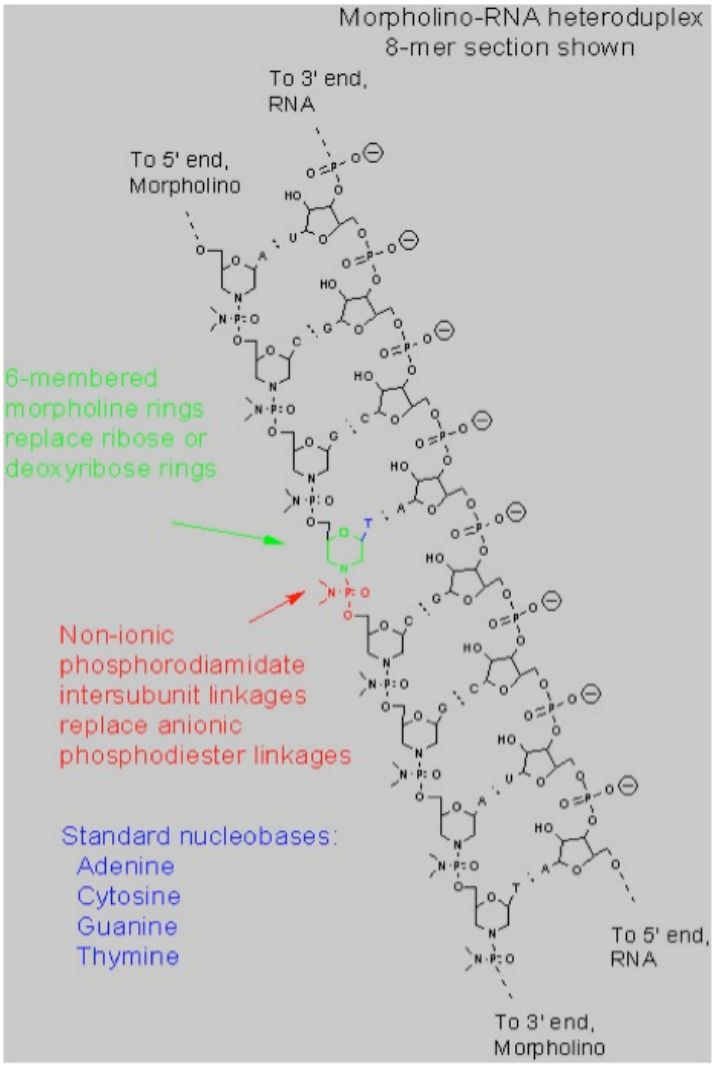

Figure 2.9: Structure of a Morpholino Oligonucleotide shown in heteroduplex with RNA. Morpholinos are synthetic molecules, approximately 25 bases in length that bind to complementary RNA sequences by standard base pairing. Although morpholinos contain the standard nucleic acid bases (adenine, cytosine, guanine and thymine), they are structurally different from DNA or RNA since the bases are bound to morpholine rings rather than deoxyribose or ribose rings. Additionally, phosphorodiamidate groups rather than phosphates link the morpholine rings, which eliminates ionization; when injected into cells or whole embryos, morpholinos are uncharged molecules (Adapted from Moulton 2007).

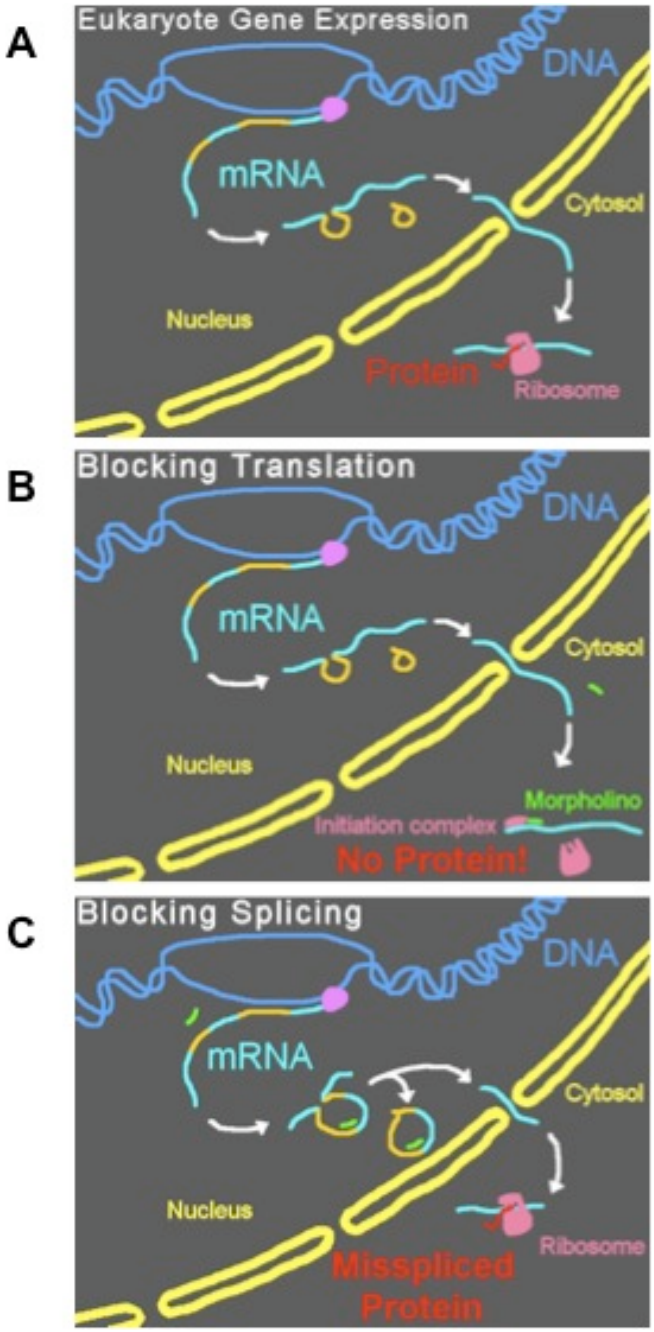

Figure 2.10: Schematic showing normal gene expression in eukaryotes and types of morpholino targeting. (A) Normal gene expression where mRNA is transcribed and processed in the nucleus and exported into the cytosol to be translated by ribosomes into protein precursors. (B) Translation-blocking morpholinos work in the cytosol and target the 5'cap and start codon of the processed mRNA, which blocks the binding of the translation initiation complex. (C) Splice-blocking morpholinos target the pre-mRNA in the nucleus and prevent the formation of the splice lariat or blocks the binding of splice complexes to splice sites. In some cases, these mRNAs are translated into mis-spliced proteins (shown above) or occasionally be degraded (Adapted from Moulton 2007).

Additionally, MOs can be used to hinder the pre-mRNA processing steps by preventing snRNP complexes from binding to target sequences, by blocking the nucleophilic adenine and preventing the formation of the splice lariat, or by interfering with the binding of splice regulatory proteins (Figure 2.10C) (Summerton and Weller 1997; Moulton 2007). While splice-blocking MOs can be efficient in knocking down gene expression, several other effects can occur including modified splicing, intron inclusions, and activation of cryptic splice sites. However, assaying for splice blocking MOs can be conveniently done by RT-PCR and visualized by agarose gel electrophoresis.

Use of the p53 ATG Morpholino: The downside to using MOs in developing embryos is that the MO can produce non-specific or off-target effects. It has been shown that up to 18% of MOs appear to have non-targeted phenotypes in the central nervous system (CNS) and somite tissues of zebrafish embryos; this is due to the activation of p53-mediated apoptosis (Robu *et al.* 2007). These non-target effects can be suppressed by co-injection of the standard p53 MO along with the experimental MO (Robu *et al.* 2007).

Optimization of Injection Experiments using the golden Morpholino: Knockdown experiments began by injecting *golden* heterozygous embryos (between 1-8 cell stage) with various concentrations of the golden morpholino reconstituted in Danieau buffer with 0.1% phenol red dye. The lethality of the injections and the concentration needed to knockdown the single wildtype

pigment allele was determined, then used as a baseline in the following injections into WT(AB) embryos to produce the golden phenotype. Additionally, *golden* heterozygous and WT(AB) embryos were also injected with Danieau buffer and 0.1% phenol red dye in order to determine if any effects occurred. These embryos were raised in the nursery and bred, showing that there were no negative effects of the buffer solution on lethality or fertility of the fish. The data obtained from these initial experiments was used to standardize the concentrations used in future morpholino injection experiments and also served as a positive control since it clearly demonstrated that the morpholino was effectively getting into the cytosol of the zebrafish embryonic cells.

Experimental Morpholino Injections: Zebrafish embryos were injected with MOs specific to the target candidate genes and screened for mosaic eyes at 48-72 hpi. Based on the genetic evidence that *gin-10* has maternal activity, translation-blocking MOs were initially used for knockdown experiments in an effort to knockout and/or significantly reduce maternal transcripts within the embryo prior to MBT. The goal of the morpholino injections was to further evaluate the *gin-10* candidate genes and potentially narrow down the list to one or two genes, Effects of the morpholinos on the *golden* heterozygous embryos were verified by injections into WT(AB) embryos.

Table 2.3: Morpholino oligonucleotide sequences against specific *gin-10* candidate genes.

Target Gene	Morpholino Type	Sequence	Purpose
golden	Translation Blocker	5'-GCTGGAGAAACACGTCTGTCCTCAT-3'	Positive Control
p53	Translation Blocker	5'-GCGCCATTGCTTTGCAAGAATTTG-3'	Standard
rfx4	Translation Blocker	5'-GCTCTTCCAGCAGCCCACAATGCAT-3'	Experimental
sir2	Translation Blocker	5'-CTCTGCTCAACCTCGCCTTGCTCAT-3'	Experimental
synbl	Translation Blocker	5'-CACTCAAACTCATCTCTGAATGATG-3'	Experimental
	Splice Blocker	5'-ACTGTCACTCTCACCTTAT-3'	Experimental
ric8a	Translation Blocker	5'-TTAAGTCCATTTTCATCGCTGTTCC-3'	Experimental

Morpholinos were designed and ordered from Gene Tools, LLC.

Both WT(AB) and *golden* heterozygous embryos were injected with various concentrations of morpholinos that were custom designed to target specific *gin-10* candidate genes (Table 2.2). Initially, embryo survival following morpholino injections was very low (at 24-hpi) due to neural death and necrosis. After completing the optimization of *golden* morpholino injections and co-injecting embryos with the *p53* morpholino, embryo survival increased while neural death and necrosis was visibly less noticeable, which allowed for the mutant phenotype to be screened. Controls for each injection session included setting aside approximately 50-100 not-injected embryos to verify normal development within the clutch, and injections of the *p53* morpholino into embryos as well as dye-only injections to verify that the phenol red solution that the morpholino was diluted did not cause any change to normal embryonic development.

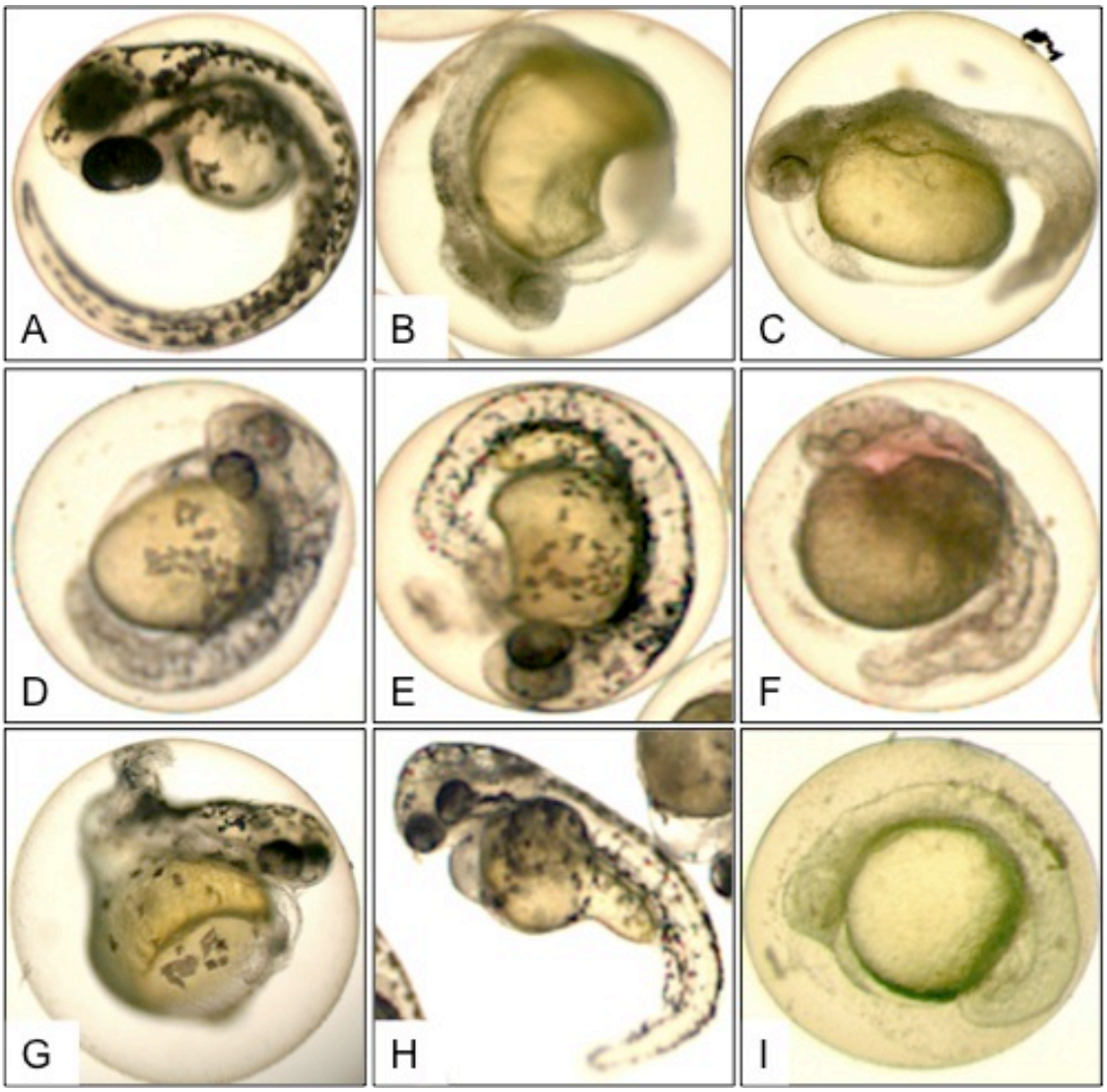

Figure 2.11: Representative results of Morpholino Injections into WT(AB) and *golden* heterozygous zebrafish embryos. (A) 48-hpf WT(AB) not injected control embryo (B) 48-hpf *golden* heterozygous embryo injected with *sir2/p53* morpholino (C) 48-hpf WT(AB) embryo injected with the *sir2/p53* morpholino (D) 48-hpf *golden* heterozygous embryo injected with *rfx4/p53* morpholino (E) 48-hpf WT(AB) embryo injected with *rfx4/p53* morpholino (F) 24-hpf *golden* heterozygous embryo injected with *rfx4/p53* morpholino (G) 48-hpf WT(AB) embryo injected with *ric8a/p53* morpholino (H) 48-hpf WT(AB) embryo injected with *synbl(splice)/p53* morpholino (I) 48-hpf WT(AB) embryo injected with *ric8a/synbl(splice)/p53* morpholino.

Wildtype embryos injected with *sir2/p53* morpholinos displayed a decrease in metabolic processes, delayed growth, severe pericardial edema and a 90-100% lethality rate by 48-hpi (Figure 2.11B-C). The same phenotypes were

seen when injected into *golden* heterozygous embryos. Since lethality was an issue at 48-hpi, it was not possible to use the mosaic eye assay to test for genomic instability by observing the RPE. Therefore, a lower dosage was used in *golden* heterozygous embryos, which enabled the use of the mosaic eye assay, as well as having embryos with less severe metabolic defects, although the defects were still observable. By doing so, the survival of the injected embryos was increased to approximately 4-dpi. Unfortunately, no mosaics were found in the zebrafish embryos injected with the *sir2* morpholino.

Based on the cloning and morpholino experiments, it appears that the *sirtuin* gene within the *gin-10* region of zebrafish may be most closely related to the human *sirt3* gene. In humans, SIRT3 is a soluble protein located within the mitochondrial matrix, and has been implicated in regulating metabolic processes including adaptive thermogenesis based on overexpression and fasting studies in mammalian cells (Blander and Guarente 2004; North and Verdin 2004). Although there are a few studies that suggest SIRT3 is also found within the nucleus and has some histone deacetylase properties, it is much more likely, based on the well-known published data and morpholino knockdown results in zebrafish, that the zebrafish *gin-10* candidate, *sir2*, is involved specifically in metabolic regulation and not genomic instability activity (Buck, Gallo and Smith 2004).

Embryos injected with the *rfx4/p53* morpholinos exhibited delayed growth through 24-hpi and some CNS abnormalities. Interestingly, these embryos either had very long, curly tails or short, stubby tails (Figure 2.11D-F). No mosaics

were observed in any of the *rfx4* morpholino injected embryos, suggesting that this gene is not involved in the genomic instability activity seen in the *gin-10* mutants.

The *synbl* gene was the first *gin-10* candidate on the priority list due to the known involvement in asymmetric cell division in *C. elegans* development (Wilkie and Kinch 2005). Since there is a paralog on chromosome 25, it was important to determine whether the knockdown of either of these genes causes mosaic eyes, and whether they appear to function similarly in the developing zebrafish embryo. Morpholinos were designed to target both *synbl* and *ric8a,* and were used separately and in combination in WT(AB) and *golden* heterozygous embryos.

Embryos injected with *ric8a/p53* morpholinos appeared to have defects in tail development, which may have been caused by non-specific off target effects of the morpholino. More importantly, there was noticeable defects in the brain, which most likely led to the observed cerebral edema in injected embryos 24-hpi and older (Figure 2.11G). Embryos injected with either the *synbl/p53* (Translation-blocking) morpholino or *synbl splice/p53* (splice-blocking) morpholino had severe developmental delay through 24-hpi, but interestingly also had similar defects in brain and CNS development that resulted in embryos with abnormally developed heads as compared to WT(AB) not-injected embryos (Figure 2.11H). None of these morpholinos, when injected into *golden* heterozygous embryos, resulted in mosaic eyes. When injected in combination (*ric8a/synbl/p53*), embryo survival past 48-hpi significantly decreased while the

brain and head development still appeared to be considerably underdeveloped (Figure 2.11I). This data suggests that *synbl* and *ric8a* work cooperatively during zebrafish embryonic development.

Several publications have suggested that *synbl* mutants and knockdowns have tiny, round, smooth melanophores that migrate abnormally during development, which was the expected phenotype of the *synbl* morpholino injections into WT(AB) embryos (Nagayoshi *et al.* 2008, Amsterdam *et al.* 2004). After many injection sessions using various concentrations of *synbl* and *ric8a* morpholinos, this expected phenotype was never observed. Rather, the morphants were typically small and underdeveloped, with abnormal brain development while the melanophores appeared to migrate properly with the wildtype rough-edge appearance. The *synbl* MOs used for these experiments were custom designed based on the VEGA annotated sequence information and appeared to be different than those used in the published methods from Nagayoshi *et al.* 2008. Additionally, the 5' UTR and portions of exon 1 were difficult to clone and were eventually cloned using genomic DNA from WT(AB) embryos (Appendix A); morpholinos were designed using both the sequencing information that was gained as a result of the cloning and the published VEGA sequence. The differences in the phenotype of the injected embryos may have been due to the effectiveness of the *synbl* MOs to appropriately target the *synbl* transcripts. In order to determine the role of *synbl* and its paralog *ric8a*, transgenic zebrafish were utilized.

Table 2.4: Summary of Morpholino Results for the *gin-10* Candidate Gene Knockdowns

Morpholino	# Injected Embryos	% Survival at 48-hpi	% Embryos displaying Abnormal Phenotype
Golden (Control)	407	33.2	45.9
Rfx4	350	66.9	61.5
Rfx4 + p53	1137	80.1	75.4
Sir2 + p53	406	73.6	82.9
Synbl (ATG)	2422	83.4	85.2
Synbl (Splice)	325	60.9	61.1
Synbl (Splice) + p53	558	82.8	76.6
Ric8a	1649	66.8	89.7
Ric8a + p53	1080	80.9	90.6
Ric8a + Synbl (Splice) + p53	1235	78.1	93.6

Transgenic *synembryn-like* (Tg-synbl) Zebrafish from ZIRC

The Zebrafish International Resource Center (ZIRC) in Oregon listed transgenic zebrafish embryos that were heterozygous for *synbl* (Tg-*synbl*), which were purchased in order to evaluate the effects of the *ric8a* and *synbl* morpholino knockdowns in a background other than wildtype and *golden* heterozygous. Since homozygous mutants are lethal within a few hours after fertilization, morpholino injections into the heterozygotes should provide better insight to the function of each gene during development. The purchased fish were placed in the nursery area in 10L tanks until they reached breeding age. Only two males survived, therefore they were outcrossed with WT(AB) females in order to maintain the stock.

Morpholino Injections into Tg-synbl Fish: The two male Tg-*synbl* fish were bred to various Tg-*synbl* females for the morpholino injection experiments; this

self-cross should have resulted in wildtype and Tg-*synbl* heterozygous embryos since the homozygous mutants are lethal. Immediately, it was recognized that the 25% lethality by 24-hpf from these crosses did not occur, which was interesting and unexpected. Morpholino injections using the *synbl* splice-blocker, the *ric8a* morpholino and a combination of both were used in the resultant Tg-*synbl* self-cross embryos. The results obtained appeared to be consistent with the data from prior injections into WT(AB) and *golden* heterozygous embryos (Figure 2.12).

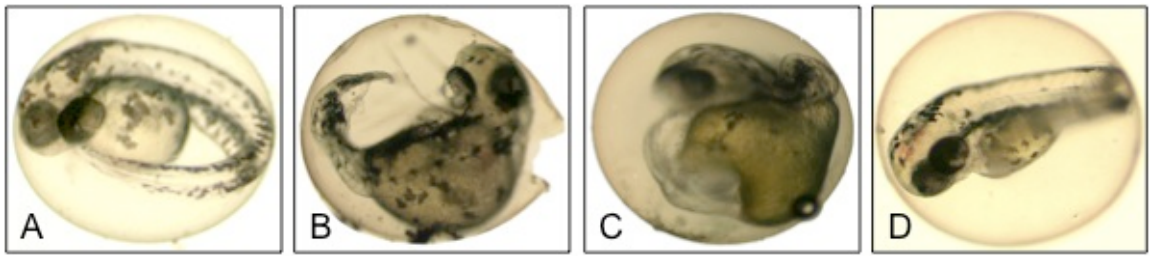

Figure 2.12: Morpholino injections into the embryo progeny of the transgenic fish self-cross breeding purchased from ZIRC. (A) Control, not injected 48-hpf embryo (B) 48-hpf embryo injected with *synbl(splice)/p53* morpholino (C) 48-hpf embryo injected with ric8a/*synbl(splice)/p53* morpholino (D) 48-hpf embryo injected with *ric8a/p53* morpholino.

PCR Analysis of the Transgenic Insert: Based on the self-cross and morpholino results in the Tg-*synbl* fish, ZIRC was contacted for the genotyping protocol for this particular transgenic line. Primer sequences were obtained from ZIRC and ordered from IDT (primers were called Tg-*synbl* F1 and Tg-*synbl* R1). Genomic DNA was prepared from fin clippings of all the existing ZIRC fish and several of the young fish from a self-cross mating (not-injected embryos that were tanked in the nursery system). According to ZIRC, the primers were created in such a way that one primer anneals to the viral sequence and the

other anneals to the flanking genomic region, resulting in a 238bp band on an agarose gel (Figure 2.13A).

As seen in Figure 2.13B, the PCR results suggest that approximately 40% of the fish from ZIRC had the transgenic insert, revealing that the initial cross was Tg-*synbl*/+ x WT(AB); based on the original ZIRC information, it was thought that all of the purchased fish contained the transgenic insertion (Figure 2.14).

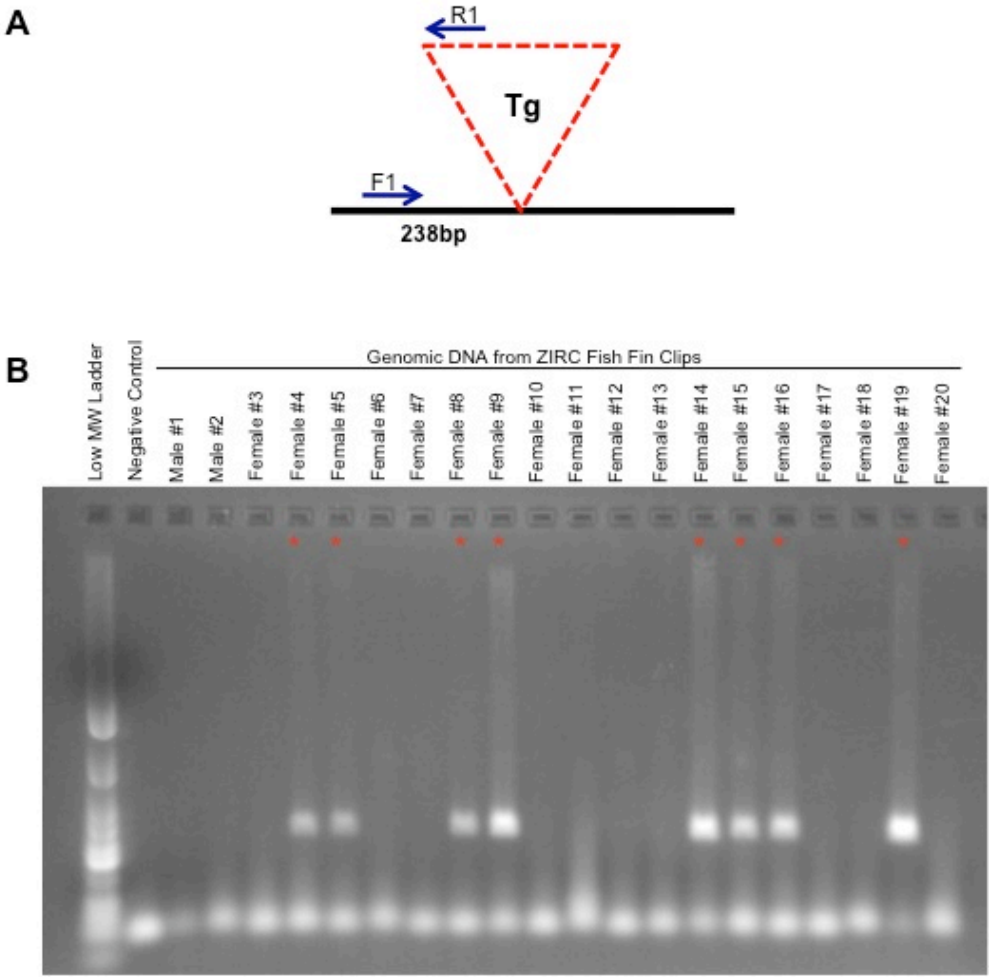

Figure 2.13: Identifying the Transgenic ZIRC fish (A) Schematic showing the transgenic viral insert (red dotted line) within the gene (black line) at an intron-exon boundary. Primers designed to specifically genotype the Tg-*synbl* fish obtained from ZIRC (blue arrows) will result in a PCR band of 238bp on an agarose gel. (B) PCR results from the genotyping assay of the 20 transgenic fish received from ZIRC. These results suggest that approximately 40% of the fish carried the transgenic insert, while the rest are wildtype.

More importantly, neither of the males carried the transgenic insert and the initial outcross to WT(AB) simply produced wildtype fish; the embryos resulting from self-crosses that were also genotyped did not carry the transgenic insert either. Preservation of the transgenic line was important, so those females carrying the transgenic insert were out crossed to robust looking WT(AB) males.

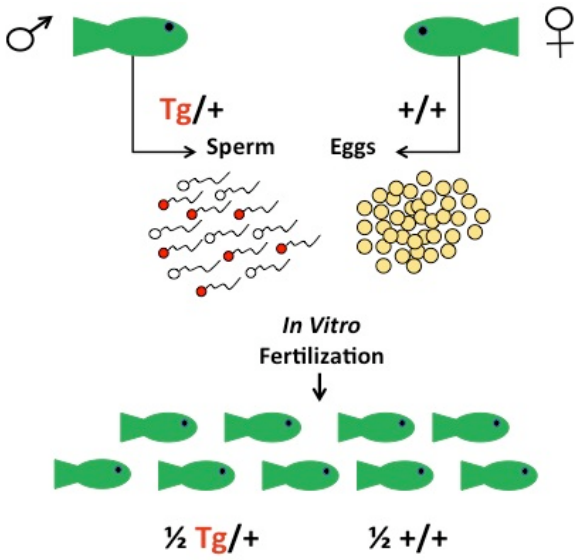

Figure 2.14: *In vitro* fertilization was performed at ZIRC using frozen sperm from a Tg-*synbl* heterozygous male to fertilize a WT(AB) female. This resulted in half of the F1 progeny to be heterozygous for the transgenic insert while half of the progeny was fully WT(AB).

Verification of the Transgenic Insertion Point: Since the results from the morpholino injections did not vary from prior injection experiments, the PCR product from the transgenic analysis was cloned into the pCR4 vector (Invitrogen) and sent out to Macrogen Inc (S. Korea) for sequencing. Using the NIH BLAST program, the sequencing results revealed that the transgenic insert was on chromosome 18 but not actually interfering with the *synbl* gene; the

results suggested that the insert was actually in the second intron of the *cry1b* gene, a former *gin-10* candidate gene on the adjacent contig to the *synbl* gene (Figure 2.15).

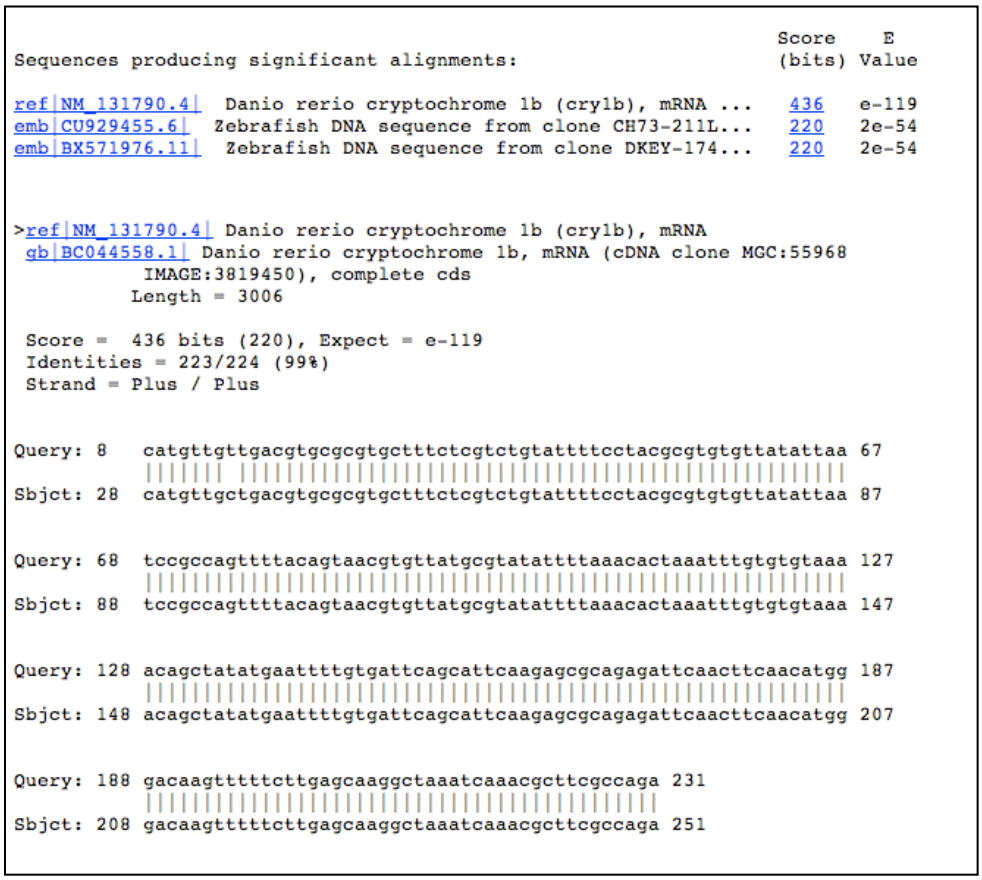

```
                                                                  Score    E
Sequences producing significant alignments:                       (bits) Value

ref|NM_131790.4|  Danio rerio cryptochrome 1b (cry1b), mRNA ...    436   e-119
emb|CU929455.6|  Zebrafish DNA sequence from clone CH73-211L...    220   2e-54
emb|BX571976.11|  Zebrafish DNA sequence from clone DKEY-174...    220   2e-54


>ref|NM_131790.4| Danio rerio cryptochrome 1b (cry1b), mRNA
 gb|BC044558.1| Danio rerio cryptochrome 1b, mRNA (cDNA clone MGC:55968
           IMAGE:3819450), complete cds
          Length = 3006

 Score =  436 bits (220), Expect = e-119
 Identities = 223/224 (99%)
 Strand = Plus / Plus


Query: 8   catgttgttgacgtgcgcgtgctttctcgtctgtattttcctacgcgtgtgttatattaa 67
           ||||||| ||||||||||||||||||||||||||||||||||||||||||||||||||||
Sbjct: 28  catgttgctgacgtgcgcgtgctttctcgtctgtattttcctacgcgtgtgttatattaa 87


Query: 68  tccgccagttttacagtaacgtgttatgcgtatattttaaacactaaatttgtgtgtaaa 127
           ||||||||||||||||||||||||||||||||||||||||||||||||||||||||||||
Sbjct: 88  tccgccagttttacagtaacgtgttatgcgtatattttaaacactaaatttgtgtgtaaa 147


Query: 128 acagctatatgaattttgtgattcagcattcaagagcgcagagattcaacttcaacatgg 187
           ||||||||||||||||||||||||||||||||||||||||||||||||||||||||||||
Sbjct: 148 acagctatatgaattttgtgattcagcattcaagagcgcagagattcaacttcaacatgg 207


Query: 188 gacaagtttttcttgagcaaggctaaatcaaacgcttcgccaga 231
           |||||||||||||||||||||||||||||||||||||||||||
Sbjct: 208 gacaagtttttcttgagcaaggctaaatcaaacgcttcgccaga 251
```

Figure 2.15: Representative results from BLAST analysis of the cloned viral insert and flanking genomic region of the PCR genotyped ZIRC fish. These results suggest that the insert is actually within the *cry1b* gene on an adjacent contig to the *synbl* gene.

The full viral sequence was obtained from ZIRC and new primers were designed to amplify the ends of the insert and *synbl* genomic sequence. Primers were also designed for *cry1b* genomic sequence based on the cloning and sequencing results. Genomic PCR of the viral primers in combination with the *synbl* primers never yielded a band on the agarose gels; only one combination of

the viral primer with a *cry1b* primer yielded a band (Table 2.3). The resultant PCR product was also cloned and sequenced for verification; the results still implied that the viral insert was in the second intron of the *cry1b* gene.

Table 2.5: Results of the Genomic PCR using Primers to Identify the Location of the Transgenic Insert in WT(AB) and Confirmed Transgenic Fish.

Primer Pair	Results		
	WT(AB)	Male #1	Confirmed Transgenic Female
F1/R1	-	-	+
F1/R5	-	-	-
F1/F3	-	-	-
F1/R3	-	-	-
F1/R5	-	-	+
F1/R1	-	-	-
F11/R1	-	-	-
F3/R1	-	-	-
F5/R1	-	-	-
R3/R1	-	-	-
F1/R5	+	+	+
F3/R3	+	+	+
Viral Primers Synbl Primers Cry1b Primers			

This was an unfortunate finding in that it did not allow for an expanded insight into the functional differences between the *synbl* paralogs, other than they do not appear to function within the *cry1b* gene network (based on the morpholino injections into the transgenic embryos in comparison with the injections into WT(AB) and *golden* heterozygous embryos).

Summary of Experimental Results:

- Candidate genes were analyzed for maternal and zygotic activity in WT(AB) zebrafish embryos by RT-PCR. Since the entire set of candidate genes initially listed within the *gin-10* region showed both maternal and zygotic

expression, the candidate gene list was narrowed down based on the known orthology information on the Sanger and NCBI databases. This left *synbl, rfx4,* and *sir2* as the main candidates on the *gin-10* list.

- The *ric8a* gene is a paralog of *synbl* located on chromosome 25. This gene was being studied simultaneously with the *gin-10* work, in order to determine if there were any differences in expression and function of the homologs during early zebrafish development.
- Expression analysis of the four genes (*synbl, ric8a, rfx4,* and *sir2*) was performed using the semi-quantitative RT-PCR protocol and whole-mount *in situ* hybridization. It was interesting to find that *synbl* and *ric8a* did appear to have some divergence in the temporal expression, whereas *synbl* is expressed throughout early development and *ric8a* appears to show activity after 12-hpf. Additionally, both genes appear to be expressed specifically in the brain and CNS after 24-hpf.
- Morpholino oligonucleotides were used to knockdown individual candidate gene expression in both WT(AB) embryos and *golden* heterozygous embryos in order to determine whether genomic instability activity occurs by using the mosaic eye assay. Unfortunately, none of the morpholino knockdowns led to mosaic eyes in the *golden* heterozygous embryos, although some general information on the function of the candidate genes was determined.
- Transgenic fish were obtained to further study the *synbl* homologs. Since the injection phenotypes did not vary from the previous experiments and the

self-crosses did not lead to a 25% dead-loss of homozygous mutants, the integrity of the transgenic insert was questioned. By PCR and cloning analysis, it was concluded that the insert was only in approximately 40% of the fish purchased, and the insert was actually affecting the *cry1b* gene rather than the *synbl* gene.

- The conclusions and implications of these results are discussed in Chapter Five.

CHAPTER THREE

METHODS FOR ANALYZING MDM1 PROTEIN EXPRESSION IN ZEBRAFISH EMBRYOS

Rationale and Experimental Design

The most interesting gene within the *gin-12* candidate region on the zebrafish chromosome 4 was *mdm1*. This gene was originally cloned from a transformed murine cell line, and found to be overexpressed in these cells along with the known oncogene *mdm2* (Snyder *et al.* 1988). The aim was to determine whether the Mdm1 protein is involved in the regulation of the tumor suppressor p53 following DNA damage, or interact with other proteins in that pathway. In order to explore this hypothesis, it was necessary to first establish protein expression analysis of Mdm1 and other p53 regulators in zebrafish embryos.

Protein expression analysis and general proteomics experiments are not common in the current realm of zebrafish research. Therefore, the availability of antibodies reactive in zebrafish is limited. In order to perform western blots and possible protein-protein interaction studies, custom anti-Mdm1 antibodies were produced for these experiments. The custom anti-Mdm1 antibodies were assayed for specificity and quality before more detailed analysis was carried out. This chapter describes the experiments designed to optimize protein detection in

zebrafish. These experiments utilize custom and commercially available antibodies to assess the expression of Mdm1, Mdm2, Mdm4 and p53 protein in zebrafish as well as *in vitro* transcription and translation (TNT) expression of Mdm1, Mdm2, Mdm4 and p53 protein that are used as controls in these and future experiments.

Optimization of Western Blotting Techniques in Zebrafish Embryos

Preparing Embryo Lysate for Western Blot Analysis: As a first step towards analyzing protein expression in zebrafish, it was necessary to optimize the preparation of good quality embryo protein lysates There are very few published protocols for lysate preparation from zebrafish, since protein work is relatively rare in this model organism. An issue with generating protein lysates from embryos is that the chorion must be removed before the lysate can be produced. Zebrafish embryonic chorions can be removed either manually or dissolved with a brief pronase treatment. For these experiments, manual dechorionation was used to prevent exposure of the embryo lysate to proteinases. It was important that after dechorionation that the yolk also be removed from the embryos because it contains an abundance of protein that could impact the sensitivity of antibody detection of the target proteins. Initial experiments utilized two syringes with 25-G needles for the removal of the yolk from the embryo. While observing the embryo under a dissecting microscope, it was held with one syringe while the other was used to peel the yolk away from the body. Although this technique worked well for removing the yolk, it was time-

consuming and often led to embryo damage and poor lysate quality. Therefore the process was changed to a technique utilizing a two-buffer system (Link, Shevchenko and Heisenberg 2006) that proved to be optimal in removing the yolk without causing damage to the embryo itself. This technique involved washing embryos in a high salt deyolking buffer, which dissolved the yolks while shaking the embryos in a microfuge tube (See Chapter Six for full protocol).

After optimizing the deyolking step, it was essential to develop a successful protocol for preparing embryo lysates. Three different protocols were obtained and tested for quality and standardization of lysate preparation – Myers lab protocol, the Look lab protocol and the Zebrafish book protocol (Karlovich *et al.* 1993; Maslow *personal communication*; O'Shea and Westerfield 1993). The first two protocols exploited the use of RIPA buffer with various protease inhibitors (Roche). The resulting Ponceau staining of the lysate on a western blot showed clear protein bands, but was frequently light and inconsistent in clarity from one sample to the next (Appendix C). The Zebrafish book protocol, which utilized a Sample buffer containing SDS and β-ME along with sonication, appeared to result in the most consistent lysate samples from different embryo samples based on clarity upon transfer and intensity of the bands, when loading 5µl on an SDS-PAGE gel and staining the blot with Ponceau-S (See Chapter Six).

Standardizing the Western Blotting Technique: Before using any custom antibodies, commercially available antibodies for zebrafish Actin and p53 were

purchased and used to optimize the western blotting procedure. Actin was used because of its abundance and ubiquitous expression and p53 was used since this was potential interacting protein with Mdm1. During these studies, embryo lysates were resolved on 10% SDS-PAGE gels and blotted as detailed in Chapter Six. Blots were incubated in either anti-Actin or anti-p53 antibodies at 4^{o}C from one hour to overnight using concentrations recommended by the suppliers. Primary antibody detection was carried out with the CSPD chemiluminescent reagent. These experiments were repeated several times for consistency with each antibody. Representative results for the standardization experiments can be seen in Figure 3.1.

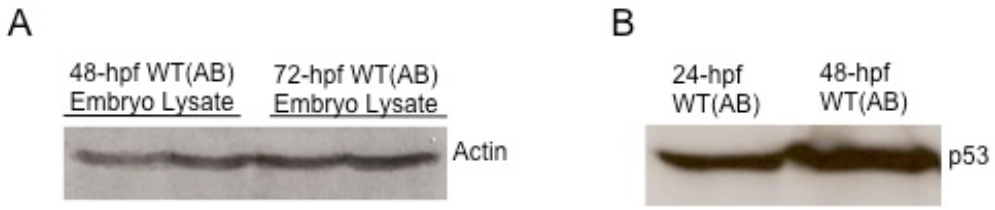

Figure 3.1: Western blots detecting β-Actin and p53 protein in WT(AB) zebrafish embryo lysate. (A) Two sets of lysate samples for 48-hpf embryos and 72-hpf embryos were run on a 10% SDS-PAGE gel. A polyclonal rabbit anti-Actin antibody was purchased from Cell Signaling Technology and used at a dilution of 1:1000, and detected with CSPD Chemiluminescence substrate on X-Ray film. The β-Actin protein appeared at a molecular weight of 45kDa. (B) 24-hpf and 48-hpf zebrafish embryo lysates were run on a 10% SDS-PAGE gel. A polyclonal rabbit anti-Zebrafish Anti-p53 antibody that exclusively reacts to the zebrafish C-terminal protein sequence was purchased from Anaspec and used at a dilution of 1:1000 for these experiments. An immunoreactive band at approximately 53kDa that corresponds to the p53 protein is visible in the embryo lysate.

Western Blots using Custom Mdm1 Antibodies: Custom Mdm1 antibodies were purchased from 21st Century Biochemicals to be used for these and future protein experiments. Two epitope sites were chosen in the Mdm1 peptide

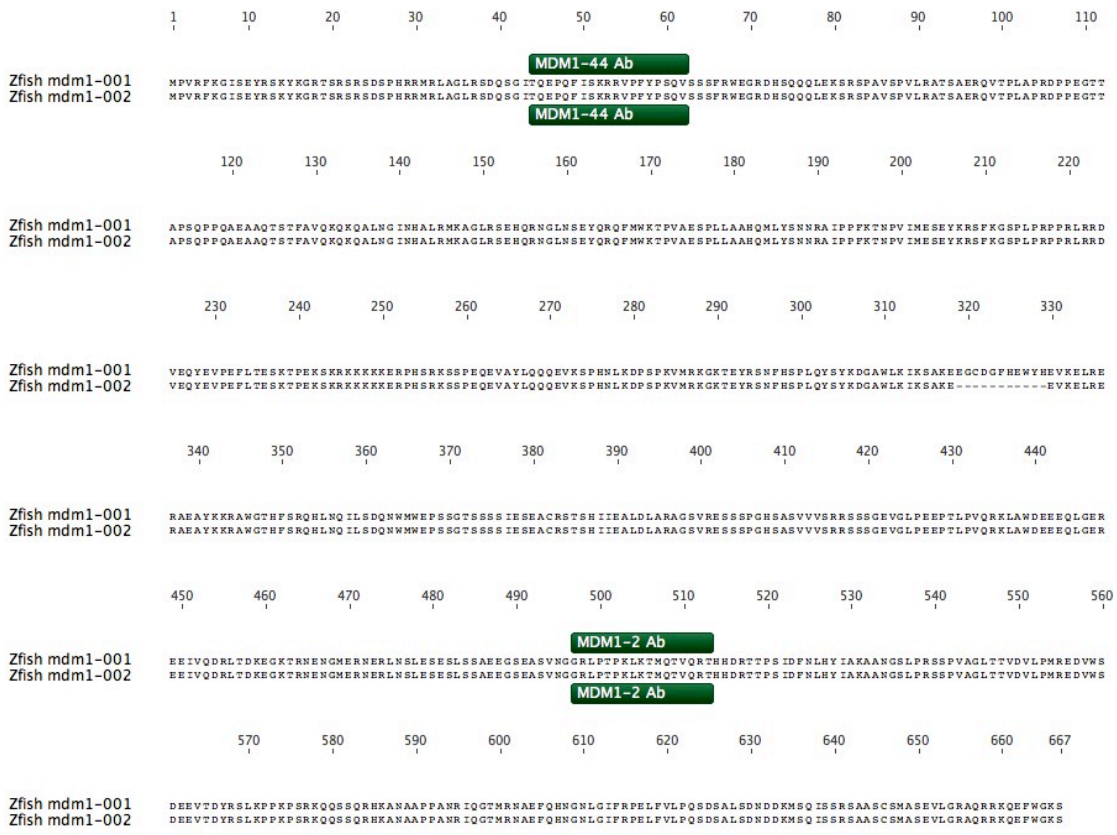

Figure 3.2: Epitope sites for the custom zebrafish anti-Mdm1 antibodies ordered from 21st Century Biochemicals. Both monoclonal antibodies, Mdm1-44 and Mdm1-2, were designed to be specific to the zebrafish Mdm1 protein with the ability to detect both known protein sequences based on the Sanger and VEGA database information. BLAST analysis and HPLC Mass Spectometry by the supplier verified sequences of the peptides. The finished products were supplied as affinity purified antibodies, which are extremely fragile and specific care was taken to ensure the stability of each sample.

sequence that would detect both known peptide sequences (Figure 3.2). After achieving consistent results with the western blots using the zebrafish anti-Actin and anti-p53 antibodies, the new custom zebrafish anti-Mdm1 antibodies were used at several dilutions on embryo lysate in order to obtain a consistent protocol when using these antibodies. Based on the peptide information for Mdm1 in the Sanger and VEGA databases, it was expected that the Mdm1 protein from zebrafish lysate would appear at approximately 74kDa on a western blot.

Interestingly, there was consistent detection of bands from various zebrafish lysates at approximately 55kDa. In order to determine if the custom antibodies were correctly detecting the Mdm1 protein, the zfMdm1 was produced using TNT so that it could be used as a control on the western blots.

In vitro Transcription and Translation of Mdm1, Mdm2, Mdm4 and p53

The full-coding sequences of *mdm1, mdm2, mdm4* and *p53* were amplified by RT-PCR from WT(AB) zebrafish embryos using several sets of primers for each gene. Upon successful amplification, the PCR products were gel purified and inserted into the pCR4 vector (Invitrogen), and sequenced to assess the integrity of the gene and determine the orientation (Figure 3.4A). This vector had been used previously to transcribe mRNA for *in situ* hybridization probes (Chapter Two), and therefore is a suitable vector for the *in vitro* transcription of inserted genes. The first TNT experiment utilized the Promega Coupled *in vitro* Transcription and Translation (TnT) kit to express the full-length *p53* clones in the pCR4. However, these experiments did not yield any protein product on Western blots stained with commercially available anti-p53 antibodies. These results were puzzling since the p53 clones had been sequenced to verify that they contained the full-length cDNA insert. To assess these results, full-length zebrafish *mdm2* clones in the pCR4 vector were also expressed using the Promega TNT system. These clones also failed to produce protein from the TnT reaction.

To troubleshoot these results, the sequencing data was revisited and it was noted that there was no Kozak sequence prior to the ATG transcription start sites in any of the clones (Figure 3.3). Therefore, the forward primers used to originally amplify the full-length sequence were resynthesized to incorporate the Kozak sequence prior to the ATG start site the four genes (Figure 3.4). The sequences were again amplified by RT-PCR from zebrafish embryo, cloned into the pCR4 vector and sequenced. This process produced several clones that contained the correct full-length insert with the Kozak sequence and were inserted in the T7 direction. These clones were used for TNT reactions. Unfortunately, the final products of these TnT reactions did not yield any protein on an SDS-PAGE gel.

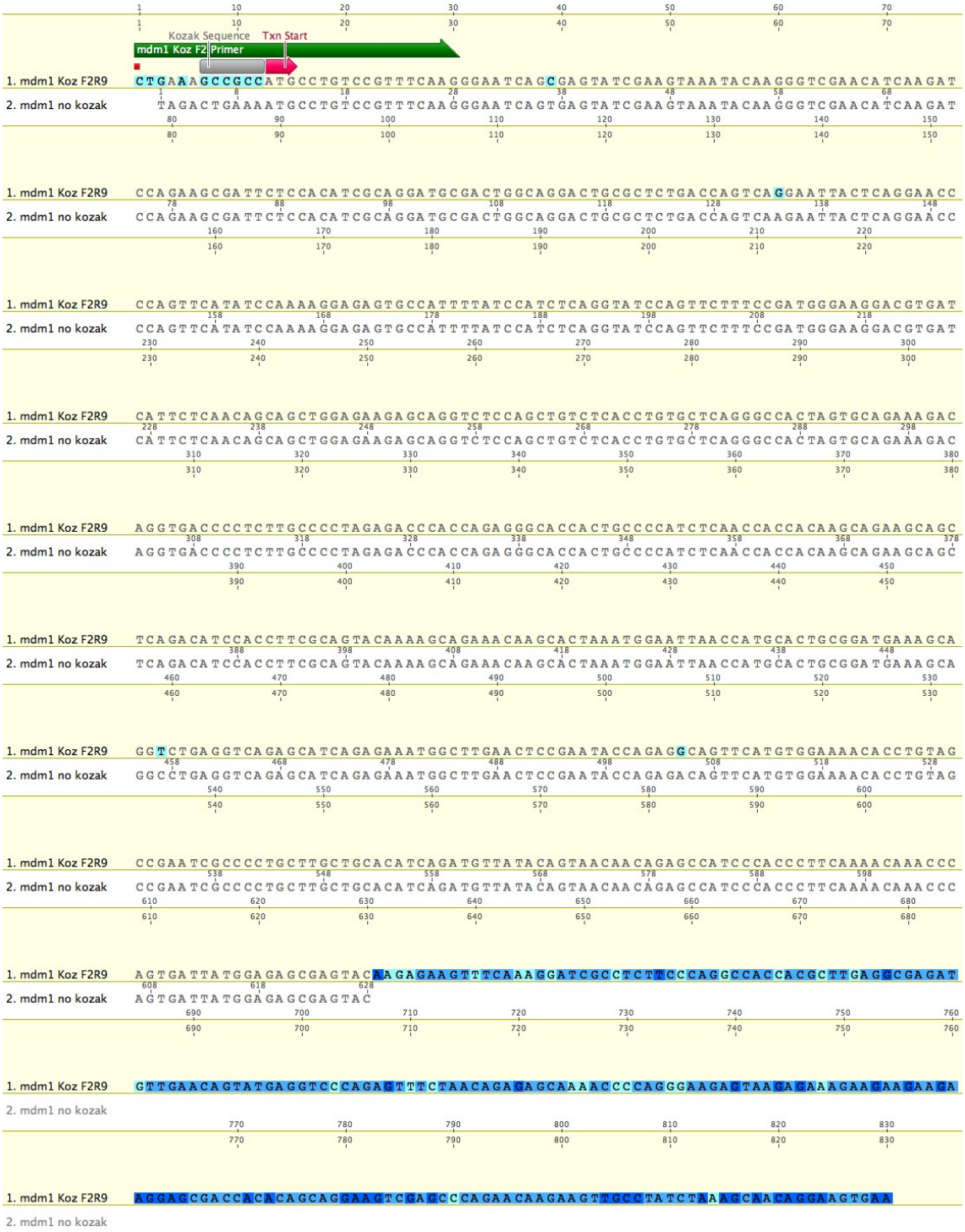

Figure 3.3: Sequence of the *mdm1* gene with the Kozak sequence cloned prior to the transcription start site and *mdm1* sequence cloned without the Kozak sequence. Shown here is the first 831 bases of the modified *mdm1* gene sequence in the pCR4 vector with the Primer, Kozak sequence, and Transcription start site annotated (Sequence 1) and the first 628 bases of the original cloned *mdm1* sequence (Sequence 2).

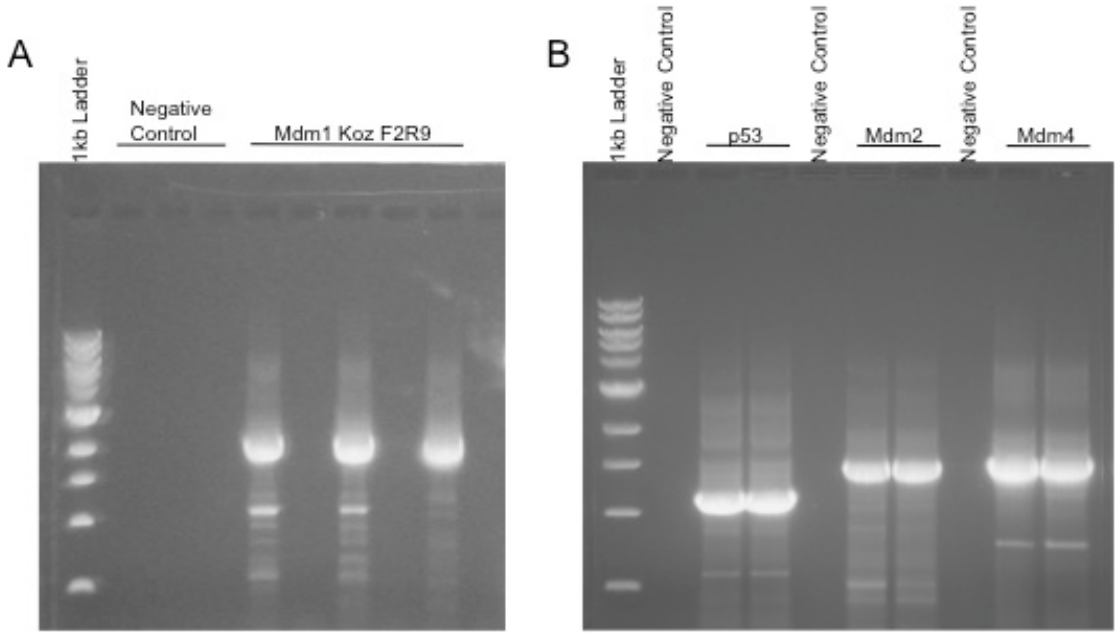

Figure 3.4: The addition of the Kozak sequence to *mdm1, mdm2, mdm4,* and *p53* zebrafish sequences. (A) WT(AB) Zebrafish embryo RNA was used to RT-PCR the *mdm1* sequence with a modified forward primer to include the Kozak sequence directly upstream of the ATG-Transcriptional Start site. The PCR products were run on an agarose gel, purified and cloned into the pCR4 vector. Three RT-PCR reactions were set up to test the annealing temperatures (58^{o}C, 60^{o}C, and 62^{o}C) for the new primer set. (B) Kozak cloning was performed for *p53, mdm2,* and *mdm4* in the same manner as shown for *mdm1*. Amplified gene sequences from zebrafish embryo RNA were cloned into the pCR4 vector and verified by sequencing.

Upon further discussion with the technical support at Promega, it was determined that the genes of interest should be subcloned into the Promega vector, pCMVTnT, which was made specifically for this TNT kit (Figure 3.5B). Full length *mdm1, mdm2, mdm4* and *p53* cDNA clones were excised from the pCR4 vector by an *EcoR1* digest and subcloned into the pCMVTnT vector using T4 DNA ligase (New England BioLabs). The new pCMVTnT clones were sequenced using both the T7 EEV promoter and internal primers to confirm that the full sequence was present and correctly oriented within the vector.

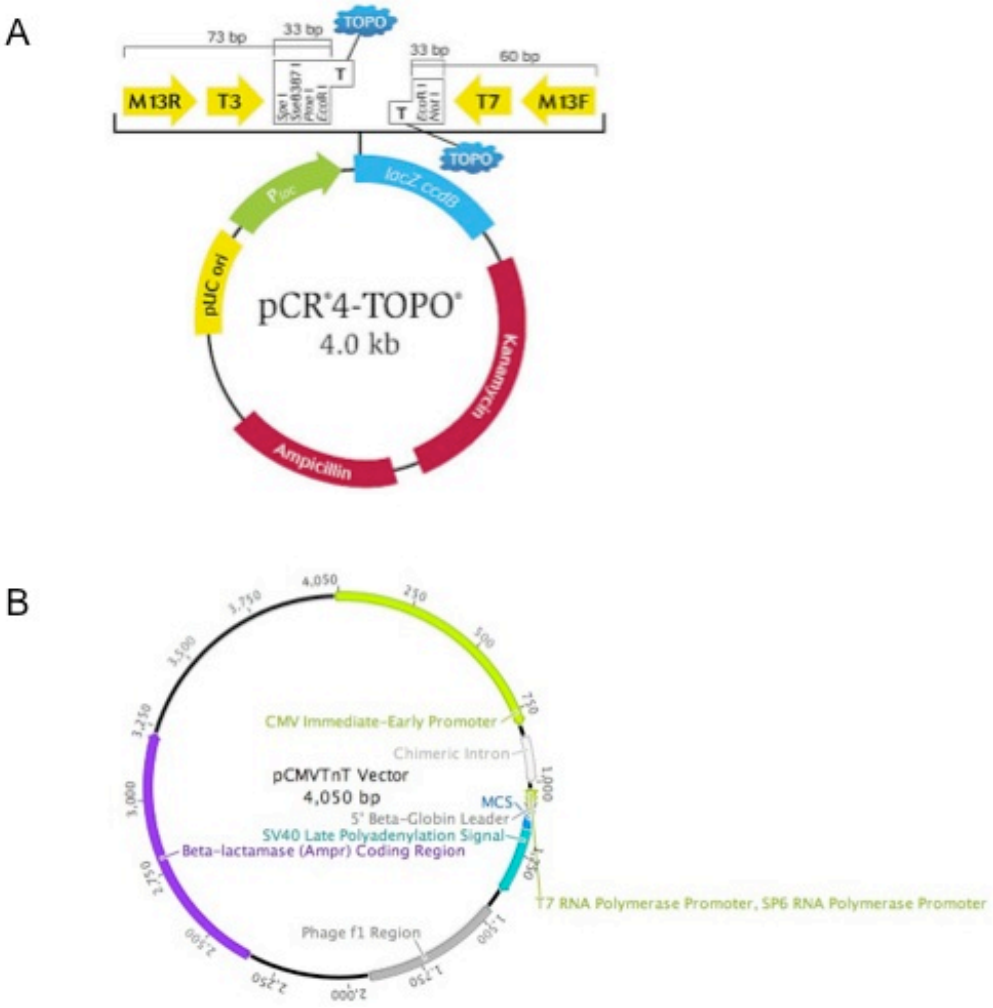

Figure 3.5: Cloning vectors used for *in vitro* Transcription and Translation experiments. (A) Invitrogen's pCR4 TOPO-TA cloning vector which was initially used for the TnT experiments but did not appear to function properly with the TnT kit (Promega). The clones in this vector were shuttled to the (B) Promega pCMVTnT vector, which was created by Promega to be used specifically with the TnT kit. This vector has a T7EEV promoter and 5'-β-Globin Leader directly upstream of the Multiple Cloning Site. It also includes an SV40 late polyadenylation signal, which ultimately allowed the TnT kit to work seamlessly with this vector. Figure B was created with the Geneious v5.4 software program.

The confirmed pCMVTnT clones of *mdm1*, *mdm2*, *mdm4,* and *p53* were used in conjunction with the Promega Coupled *in vitro* Transcription and Translation kit with the addition of biotinylated tRNA (lysine), so that all of the translated products could be detected on a single western blot using the Streptavidin-AP conjugated antibody (supplied in the Promega kit) and detected

with NBT-BCIP. As shown in Figure 3.6, protein did result from these reactions. Two *mdm1* clones in the pCMVTnT (Promega) vector were used for these TnT reactions along with a single *mdm2* and *mdm4* pCMVTnT (Promega) clone. As the results indicate, all of the reactions produced the expected size *in vitro* translated protein product. The Mdm2 translated protein appears to have the best expression with the colorimetric detection, which may be due to the number of biotinylated lysines incorporated during the translation process. Confirming that the TnT reaction worked correctly and produced the correct size protein was an important and necessary step. These TnT products were then used to test the custom Mdm1 antibodies and commercially available antibodies for Mdm2 and Mdm4 to correctly detect these proteins in zebrafish lysates.

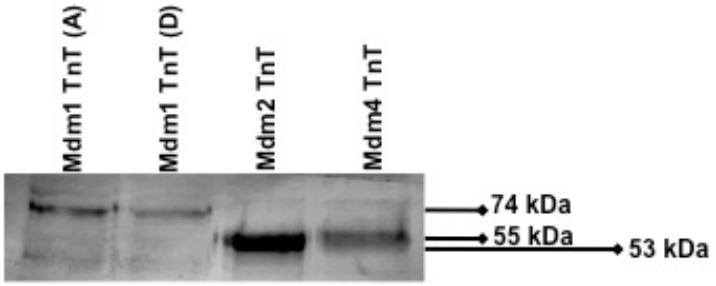

Figure 3.6: *In vitro* Transcription and Translation results using the Promega vector, pCMVTnT, coupled with the Promega TnT kit and biotin-labeled tRNA (lysine). Two *mdm1* (kozak) samples were used along with an *mdm2* (kozak) and *mdm4* (kozak) samples. The TnT reactions were performed according to the Promega protocol (Chapter Six) with added biotin-labeled tRNA (lysine). The TnT products were diluted 1:2 in 2X Sample buffer and run on a 10% SDS-PAGE gel and transferred to nitrocellulose paper. Using Streptavidin-AP primary antibody, the TnT products were colorimetrically detected with NBT-BCIP and shown above. Both Mdm1 products appear around 74 kDa, while the Mdm2 and Mdm4 TnT products appear at 53 kDa and 55 kDa respectively.

Using the *in vitro* Translated Mdm1 Product to Test the Custom Antibodies

Since the *in vitro* synthesized Mdm1 appeared to migrate at the expected molecular mass (Figure 3.6), it was used as a control on the embryo lysate

western blots to determine the specificity of the custom Mdm1 antibodies; the Promega TnT mastermix was also loaded on these gels as a control. Representative results shown in Figure 3.7. The data indicate that the Mdm1-44 and Mdm1-2 antibodies do not detect the synthesized protein product but rather detect proteins within the TnT mastermix. Furthermore, the custom Mdm1 antibodies do not appear to detect the appropriate size protein in embryo lysate (expected size of Mdm1 is approximately 74 kDa).

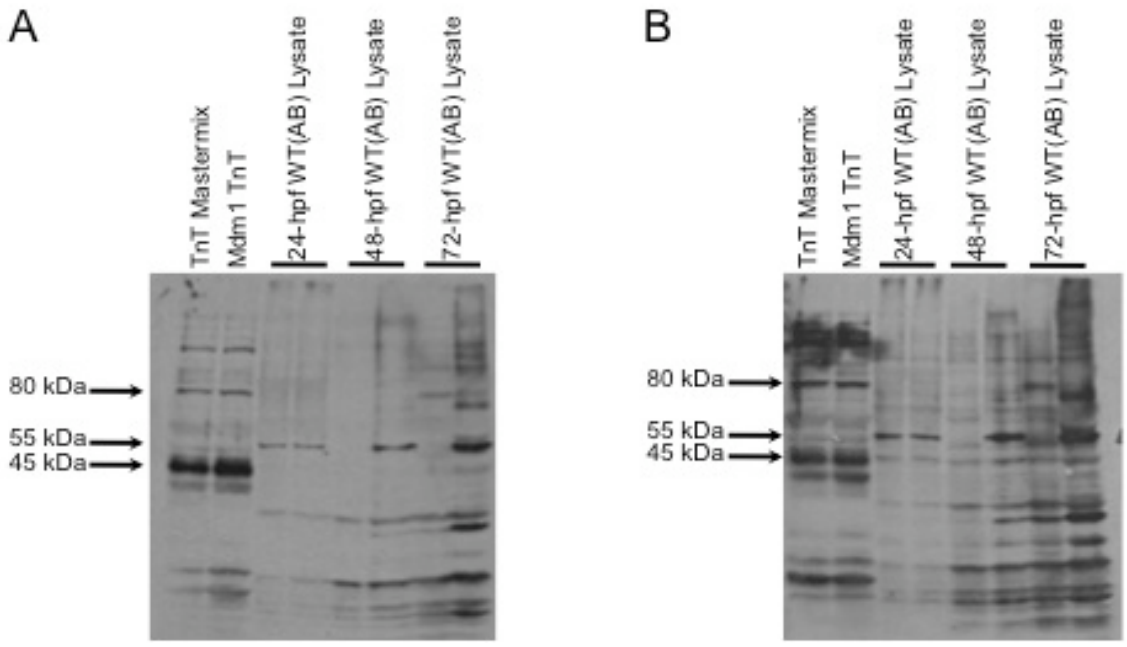

Figure 3.7: Testing the Custom Monoclonal Mdm1 Antibodies by Western Blots. Identical gels were loaded with TnT mastermix, verified Mdm1 TnT reaction product, and 24-72-hpf embryo lysates (in duplicate). (A) Gel blot incubated in the Mdm1-2 monoclonal antibody overnight and detected with CSPD. It is clear that this antibody is not detecting the synthesized protein product in the TnT lane, but is detecting a 55 kDa protein in the embryo lysate. (B) Gel blot incubated in the Mdm1-44 monoclonal antibody overnight and detected with CSPD. Similar results are seen here, where the custom antibody is not detecting the synthesized Mdm1 protein or the correct size protein in embryo lysate. These experiments were repeated several times for confirmation.

Since the Mdm1 antibodies did not appear to detect the Mdm1 protein in embryo lysate or the synthesized product from the TnT reaction, the sensitivity

and specificity of the reagent was in question. The custom antibodies were pooled together and used at a dilution of 1:500 (2.22 µg/µl) on a western blot containing the TnT product and zebrafish embryo lysate (Figure 3.8A). Again, 74 kDa proteins were not detected in the lanes containing embryo lysate, although protein was detected in the lysate around 55 kDa. Figure 3.8B shows two western blots that were loaded with TnT mastermix and synthesized Mdm1, Mdm2, and Mdm4. The first gel was incubated with custom Mdm1 antibody mixture (1:500 dilution) while the second gel was incubated in a 1:1000 dilution of the commercially available zebrafish anti-Mdm2 antibody (Anaspec). The results suggest that the custom Mdm1 antibodies are solely detecting the TnT mastermix (Figure 3.8B, Gel #1) whereas the anti-Mdm2 antibody also detects some of the TnT mastermix proteins but clearly detects the zebrafish Mdm2 synthesized protein at approximately 53 kDa (Figure 3.8B, Gel #2). Based on these results, it was apparent that using the custom Mdm1 antibodies for future experiments such as Co-IPs would not be possible, since they were not detecting endogenous or synthesized Mdm1 protein. In an attempt to identify proteins associated with Mdm1 in zebrafish, embryos injected with a tagged version of Mdm1 could be used for Co-IPs, which may provide further insight about interacting protein partners and regulatory pathways during zebrafish development.

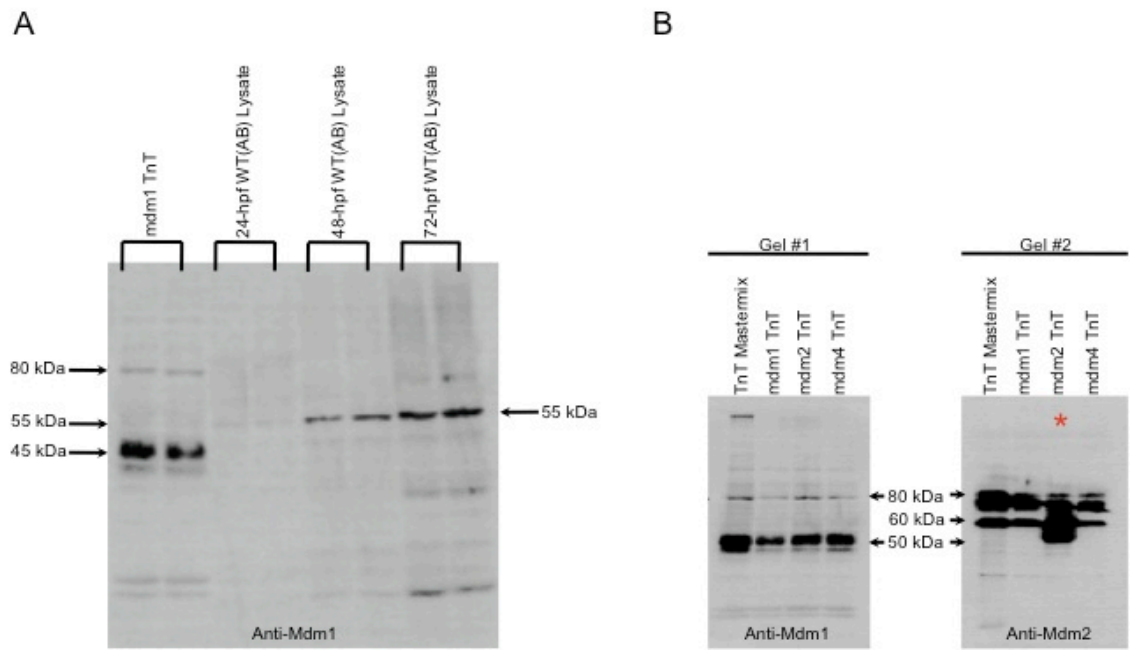

Figure 3.8: Analysis of the Specificity of the Custom Mdm1 Antibodies. (A) The Mdm1-44 and Mdm1-2 antibodies were both used to detect the Mdm1 *in vitro* translated protein and endogenous Mdm1 protein from zebrafish embryo lysates at several developmental time points. Each sample was loaded in duplicate to ensure quality of the results. The custom Mdm1 antibodies did not appear to detect the protein product in the TnT sample at 74-75 kDa, but did appear to detect a band at approximately 55 kDa in the lysate samples (24-hpf lysates have a very light band). (B) The *in vitro* transcribed products of Mdm1, Mdm2 and Mdm4 as well as TnT mastermix were run on two separate gels. The custom Mdm1 antibodies were used on Gel #1, which should have detected a 74-75 kDa band in the lane containing the Mdm1 TnT product. Rather, the same results were apparent in all four lanes suggesting that the custom Mdm1 antibodies do not detect the zebrafish Mdm1 protein. The anti-Mdm2 antibody supplied by Anaspec, was used on the Gel #2, which also showed some non-specific staining in the four sample lanes, but a clear band was present at approximately 53 kDa in the Mdm2 TnT lane, verifying that this antibody is detecting the correct protein.

FLAG and His-Tagging Mdm1

Based on the results from the custom Mdm1 antibody experiments, it was necessary to use another method to detect the Mdm1 protein from zebrafish embryos for possible protein-protein interaction studies. The FLAG peptide is a widely utilized tag that can be used for affinity chromatography for the isolation of protein complexes (Hopp, Gallis and Prickett 1988; Einhauer and Jungbaur 2001). In addition to the FLAG tag, polyhistidine or His-tags are another useful

tool that can be exploited and easily applied in protein purification and binding assays (Hochuli *et al.* 1988; Hengen 1995). Thus, experiments were designed to use tagged Mdm1 proteins that could be injected into embryos for subsequent purification to identify possible binding partners of Mdm1, and also potentially determine its functional and biological role in zebrafish. Since the Kozak sequence and some restriction sites had already been added to the 5'- end of the *mdm1* gene with custom primers, it was decided that the tags would be individually added to the 3'- end of the gene so that it would not interfere with the previously adapted sequence. The methodology used to add these tags is described below.

FLAG-Tagging mdm1 Clones in the pCR4 and pCMVTnT Vectors: The pCR4 vector (Invitrogen) was used as a shuttle vector for these experiments since it was known that the inserted gene sequences can be easily excised and ligated into the pCMVTnT vector once they were verified by sequencing. Figure 3.9 shows the two-step primer process to insert the FLAG tag at the 3'-sequence of the *mdm1* gene by PCR. Since the *mdm1* R9 primer was used in previous experiments to amplify the full-length coding sequence of *mdm1*, it was modified into two separate new primers that included a partial DNA sequence of the FLAG tag (Figure 3.9B) and the complete DNA sequence of the FLAG tag (Figure 3.9C), primers *mdm1* R12a and 12b respectively. The *mdm1* coding sequence was amplified by RT-PCR from embryo RNA using the *mdm1* Kozak F2 primer in combination with the *mdm1* FLAG R12a primer to add the first portion of the

FLAG tag to the *mdm1* gene sequence. The PCR product was run on an agarose gel for size verification (Figure 3.10A), purified, then ligated into the pCR4 vector and plated on ampicillin and carbenicillin plates in transformed in Top 10 cells (Invitrogen). Plasmid DNA was isolated from individual colonies and the second round of FLAG tagging was performed using this DNA and the corresponding *mdm1* primers (Figure 3.10B). Products from the second round of FLAG amplification were ligated into the pCR4 vector (shuttle vector for cloning), then excised out using an *EcoR1* restriction digest and subcloned into the pCMVTnT vector (Promega).

Figure 3.9: Experimental Design of the FLAG tag in the *mdm1* sequence. (A) Peptide and DNA sequence of the FLAG tag. A two-step PCR procedure was used to add portions of the tag to the 3' end of the *mdm1* coding sequence. (B) The first round of PCR inserts the 5'-GACGACGATAAG-3' just before the stop codon. This was done by modifying the R9 primer (new R12a primer) to add the FLAG tag bases. (C) The second round of PCR completed the FLAG tag by adding the 5'-GACTACAAGGAT-3' to the tag sequence already in the coding region. The new R12b primer was used for this.

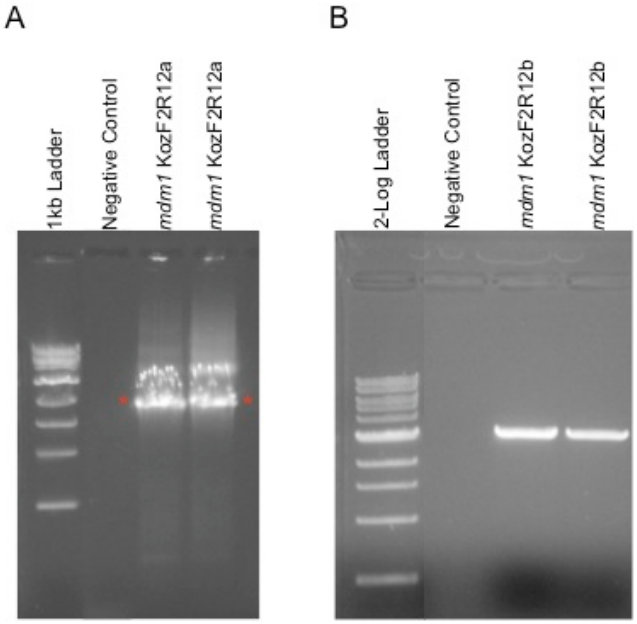

Figure 3.10: PCR Results of FLAG Tagging the *mdm1* Coding Sequence. (A) Round 1 PCR using the *mdm1* Kozak F2 primer with the FLAG Tag primer 12a. (B) Round 2 PCR results of adding the FLAG tag using the R12b primer. Asterisks denote the portion of the gel that was purified and ligated into the vector for cloning.

Analyzing the FLAG-Tag Clones in the pCMVTnT Vector: In order to determine if the FLAG tag was successfully added to the 3' end of the *mdm1* coding sequence, the pCMVTnT clones were subjected to digests using the *Hpy99I* restriction enzyme (New England BioLabs). Based on the vector sequence information, plasmids containing the FLAG tag would show four bands on an agarose gel since the enzyme cuts the vector itself in three locations, while also recognizing a restriction site in the FLAG tag itself. Using this method required very little time and effort, while quickly allowing for analysis of each clone generated by the PCR and ligation process. It is important to note that in

addition to these digests, a representative sample of the FLAG tag clones were also sent off for sequencing to verify the digest results. Not only would the restriction digests verify the insertion of the FLAG tag, it would also identify the direction of the *mdm1* insert within the pCMVTnT vector. Hundreds of clones were analyzed using the *Hpy99I* restriction enzyme and run on agarose gels. Representative results of these digests are shown in Figure 3.12. Based on the sequence map and the schematic of the pCMVTnT vector (Figure 3.11), if the FLAG tag was correctly inserted into the *mdm1* sequence, four bands were expected on the agarose gels, sizes corresponding to the orientation of the insert within the vector.

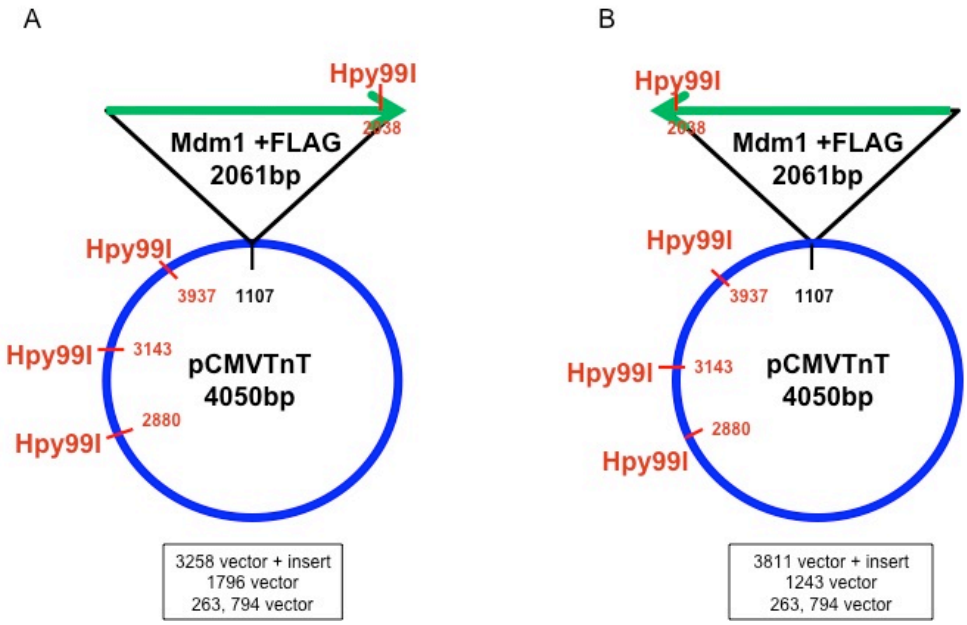

Figure 3.11: Restriction Analysis of the FLAG Tag Clones by *Hpy99I*. In addition to several *Hpy99I* restriction sites within the pCMVTnT vector, a recognition site was also within the FLAG tag, and used to identify clones containing the *mdm1*-FLAG insertion. (A) Shows the expected fragment sizes following the digest if the *mdm1*-FLAG sequence was inserted in direction 1. This was the desired result, since the insertion would be in the correct orientation for the TnT reaction. (B) Shows the expected fragment sizes following the digest if the *mdm1*-FLAG sequence were inserted in direction 2.

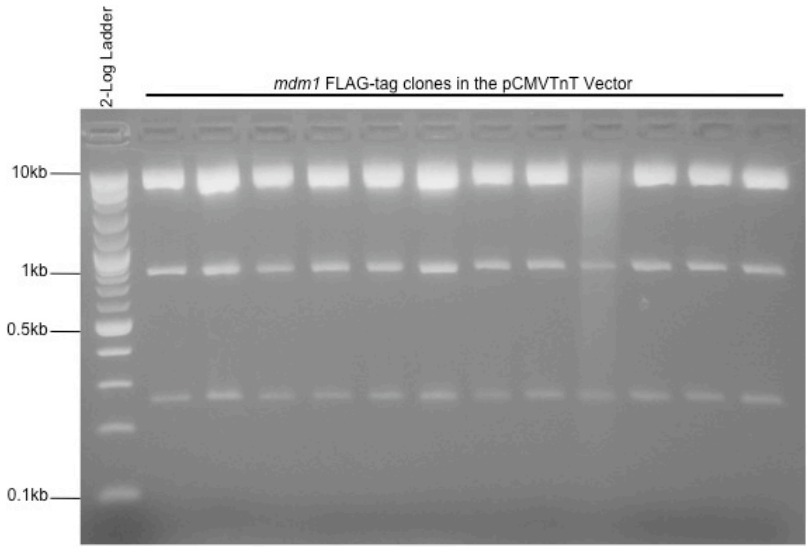

Figure 3.12: Results of the *Hpy99I* digests. All lanes contain three fragments following the restriction digests, suggesting that the FLAG tag was never successfully inserted into the *mdm1* coding sequence.

As shown in Figure 3.12, only three bands corresponding to the vector appeared on the gels following the restriction digests using the *Hpy99I* enzyme. To support these results, several of the clones were sent to Macrogen for sequencing confirmation of the FLAG tag; the *mdm1* insert was present without the FLAG tag in each of the clones analyzed. Based on this evidence, it was decided that the FLAG tag was too difficult to insert within the *mdm1* coding sequence, and therefore the efforts turned to using a 6X-His tag instead.

6X-His Tagging mdm1 Clones in the pCR4 Vector: Similar to the FLAG tagging efforts, the 6X-His tag sequence was added to the *mdm1* R9 primer, but as a single-step amplification. Because the addition of the His tag significantly increased the melting temperature of the primer, two different reverse primers (R13 and R14) containing the His tag, were designed to be used with the Kozak

F2 forward primer. Figure 3.13 shows the location of the His tag within the coding sequence of the *mdm1* gene.

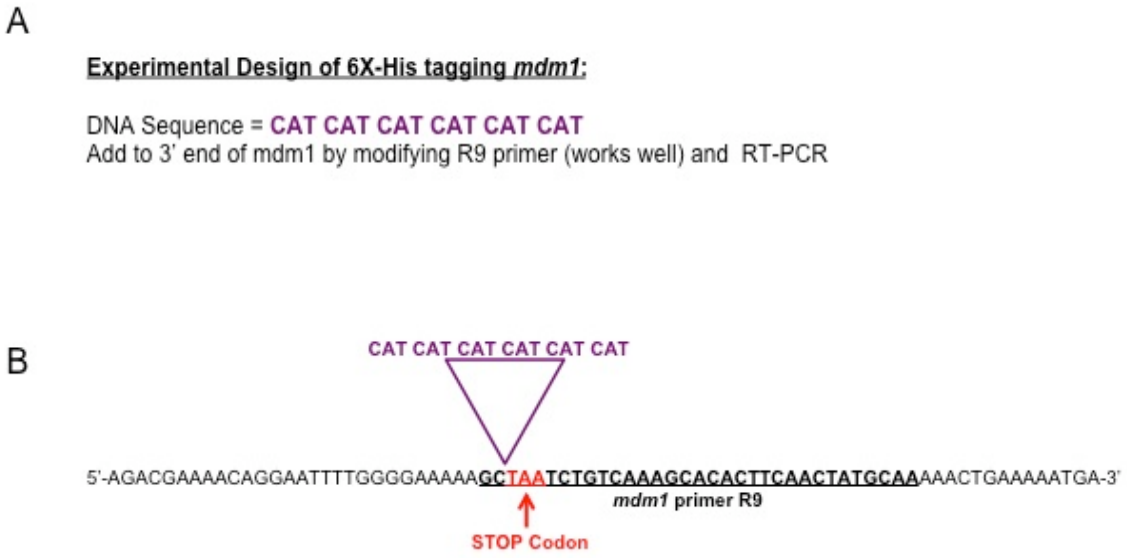

Figure 3.13: Schematic of adding the 6X-His Tag to the *mdm1* Coding Sequence. (A) DNA sequence of the 6X-His Tag, which was added to the R9 primer (new R13 and R14 primers). (B) Location of the tag, just before the STOP codon in the *mdm1* coding sequence.

Since the His tag was added in a single step by RT-PCR using zebrafish embryo RNA, the PCR products were run on an agarose gel, purified and ligated into the pCR4 vector (Figure 3.14). Due to the difficulties with the FLAG tagging effort, the products were analyzed within the pCR4 vector, rather than shuttling the gene inserts into the pCMVTnT vector (Figure 3.15). Similar to the restriction analysis of the FLAG tag, the 6X-His tag insertion was also analyzed within the pCR4 vector by restriction digests of hundreds of clones using the *Ase1* enzyme along with sequencing several samples of the clones (New England BioLabs). Based on the restriction site analysis of the vector and *mdm1*-His insert, and the orientation of the insert within the vector, upon digestion with *Ase1*, three bands

would appear on an agarose gel if the clones were positive for the 6X-His tag (Figure 3.15).

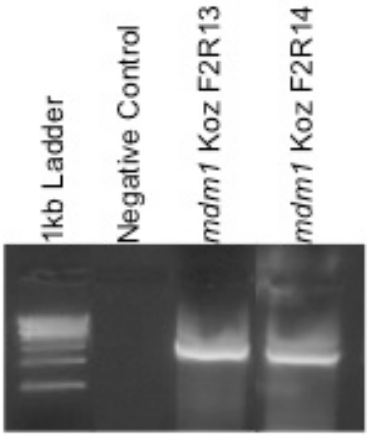

Figure 3.14: RT-PCR results of adding the 6X-His Tag to *mdm1*. Each of the fragments were gel purified and ligated into the pCR4 vector (Invitrogen) for cloning and analysis.

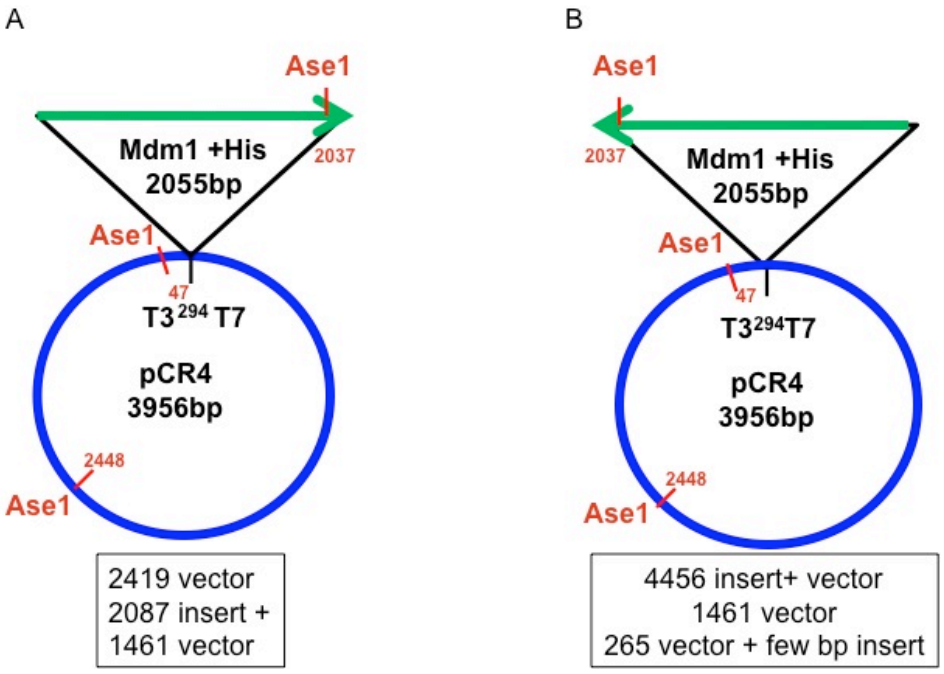

Figure 3.15: Schematic of the *Ase1* digests to confirm the insertion of the 6X-His tag in *mdm1*. Similar to the restriction analysis of the FLAG tags, the expected fragment sizes were dependent on the orientation of the insert within the vector. In this case, orientation was not important, as positive clones would be shuttled into the pCMVTnT vector for TnT reactions. (A) Shows the expected fragment sizes if the *mdm1*-His were inserted in the T3 direction. (B) Shows the expected fragment sizes if the *mdm1*-His were inserted in the T7 direction. Restriction site locations in the vector were based on the information provided by Invitrogen.

After restriction mapping hundreds of pCR4 clones, it was evident that none of the clones contained the 6X-His tag, since only two bands were apparent on all of the agarose gels following the restriction digests. Representative results of these digests are shown in Figure 3.16. Based on the restriction mapping and sequencing evidence, it was determined that none of the clones contained either the FLAG or His tag in the *mdm1* coding sequence, and thus could not be used for future experiments such as injections into embryos for Co-IPs.

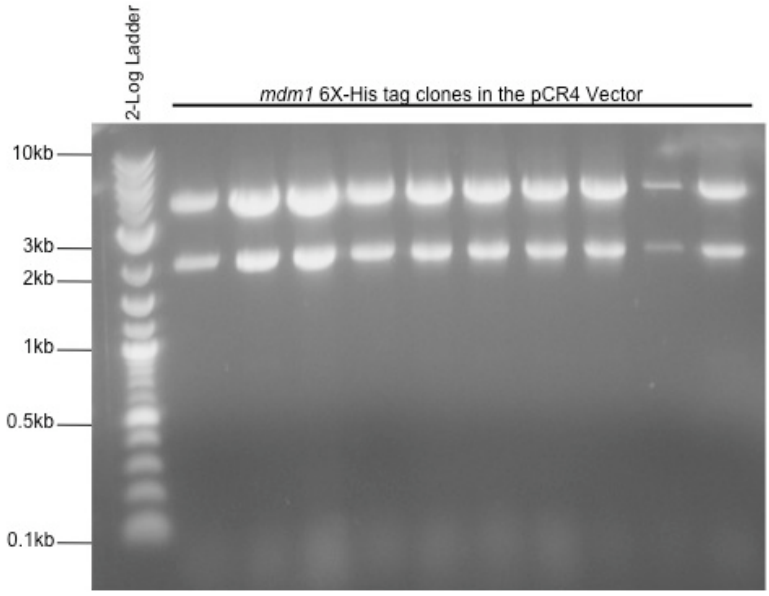

Figure 3.16: Restriction Analysis Results of the 6X-His tag *mdm1* Clones in the pCR4 Vector. All clones that were examined by *Ase1* restriction digests appeared to only have two fragments on the agarose gels, suggesting that the His tag was not added to the 3' *mdm1* coding sequence.

Summary of Experimental Results

- The *in vitro* Transcription and Translation requires delicate handling and specific vector qualities to synthesize proteins of interest. This can also be a powerful tool in determining the quality and specificity of commercially available and custom antibodies. In these studies, the synthesized proteins were used as a control to determine the ability of the custom Mdm1 zebrafish antibodies to detect the correct protein on a western blot. Without this control, the custom antibodies may have been inappropriately used in other protein experiments, such as Co-IPs, leading to costly results.
- The use of tags is not novel, especially in zebrafish research. It was, however, unfortunate that with all of the effort put forth, neither FLAG nor 6X-His tags were inserted into the coding sequence of the *mdm1* gene. The combination of restriction mapping and sequencing clearly identified *mdm1* clones without tags. A 5' tag was never attempted since the Kozak and in some cases, an *Xho1* site for cloning purposes were already added in this region.
- The *mdm1* gene remains an important focus in the lab. Based on the results of the westerns with the custom antibodies, and the inefficiency of Tag cloning, it was decided that the gene function and expression should be examined before looking at the protein expression.

CHAPTER FOUR

INVESTIGATING THE ROLE OF MDM1 IN ZEBRAFISH DEVELOPMENT

Experimental Design and Rationale

Similar to the *gin-10* candidate studies, the *gin-12* mutation was identified on zebrafish chromosome 4 by ENU mutagenesis studies and half-tetrad mapping (Moore *et al.* 2006). Within this region that maintains synteny with human chromosome 12, several genes were identified as candidate genes for *gin-12*, including *mdm1*. The aim of this chapter is to determine the expression patterns of the *mdm1* gene and identify its role in zebrafish development.

To formally investigate this candidate gene, the ability to study transcript expression within the embryo was explored by *in situ* hybridization techniques, as well as the ability to knockdown gene function by Morpholino oligonucleotides (MOs). Embryos injected with biotin-labeled *mdm1*-Ex2 MO were stained to identify the exact regions of the MO targets, leading to the identification of *mdm1* gene expression and developmental function in zebrafish embryos. The use of MOs to knockdown *mdm1* gene expression was verified by RNA rescue, as well as RT-PCR and *in vitro* protein studies. Additionally some of the knockdown experiments were designed to further explore the potential genomic instability activity of the *mdm1* gene (Figure 4.1).

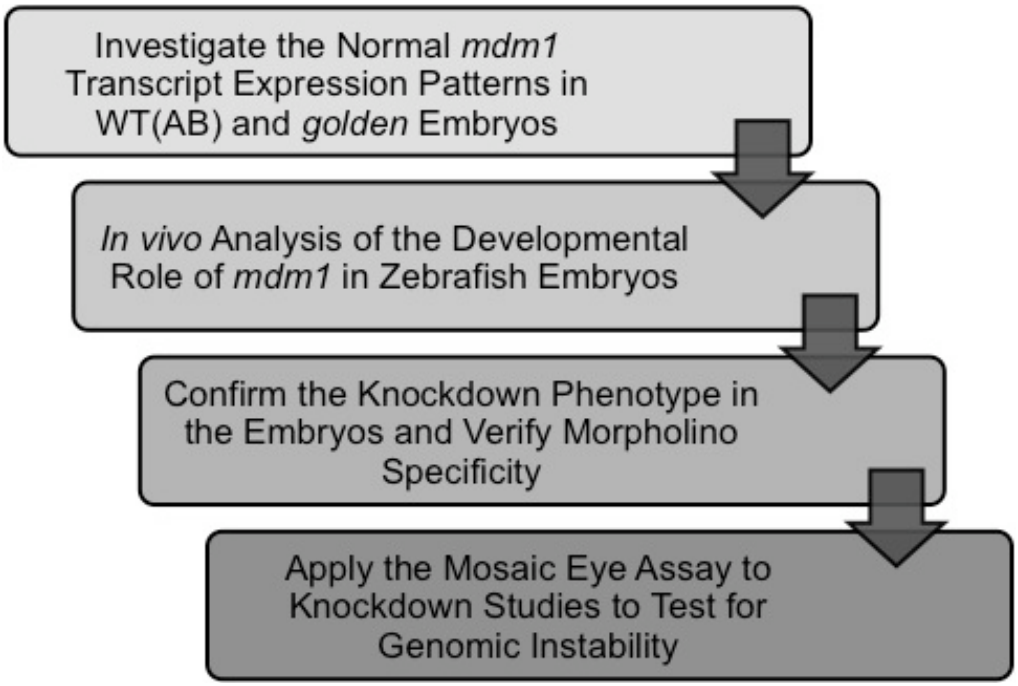

Figure 4.1: Schematic of the Experimental Design to Establish the Role of *mdm1* in Zebrafish Development.

Temporal and Spatial Expression Analysis of *mdm1* in Zebrafish Embryos

Background: In addition to the full-length cloning of *mdm1* that was described in Chapter Three, RT-PCR was also used to amplify several smaller fragments of this gene, which were cloned into the pCR4 vector. The amplified cDNA products were sequenced for confirmation and orientation within the plasmid, and kept in a library. These small *mdm1* gene clones were later used as templates for RNA and DNA probes in various experiments.

Developmental Expression Analysis of the mdm1 Gene: Preliminary RT-PCR amplification of *mdm1* had suggested that expression of *mdm1* transcripts was variable during zebrafish development (data not shown). In order to further

explore the temporal expression patterns of *mdm1*, semi-quantitative RT-PCR was performed. This method utilizes the low-cycle RT-PCR reaction from WT(AB) zebrafish RNA and a modified Southern blotting technique to detect expression of the *mdm1* cDNA with a DIG-labeled DNA probe (Figure 4.2).

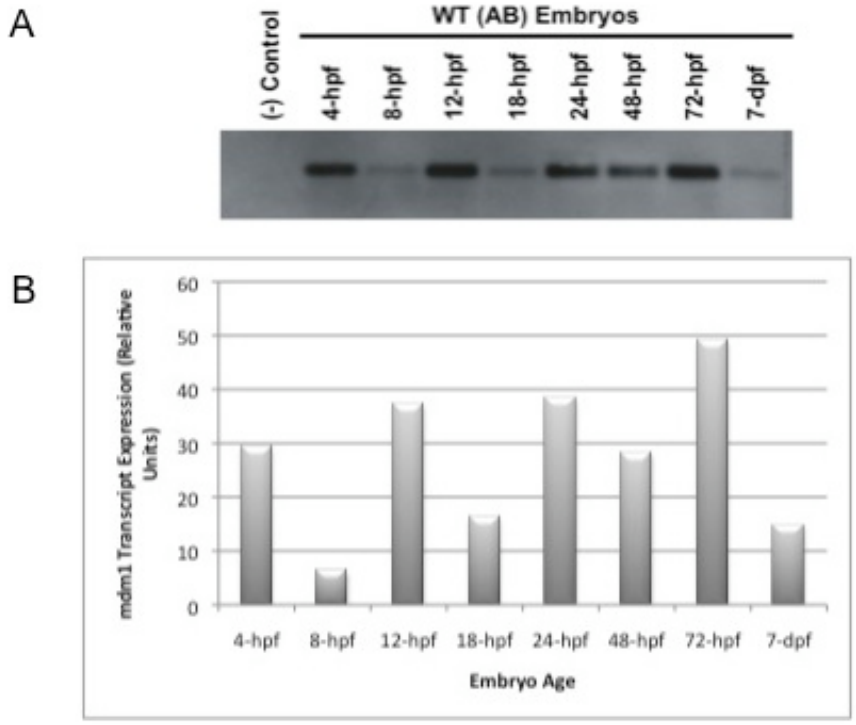

Figure 4.2: Results of the *mdm1* semi-quantitative expression analysis from developing zebrafish embryo RNA. (A) Blot results detected with CSPD following hybridization with an *mdm1* DIG-labeled DNA probe. Expression of the transcript appears to vary significantly from maternal expression (4-hpf) through larval stage (7-dpf). (B) ImageJ software (NIH) was used to graphically represent the blot data from this analysis. Units indicate detection above that seen in the negative control lane.

As shown in Figure 4.2, *mdm1* transcript levels appear to vary during zebrafish development. At 4-hpf, the maternal expression of *mdm1* was very robust suggesting that it plays a critical role in the earliest stages of embryogenesis. The apparent decrease in *mdm1* expression at 8-hpf occurs

shortly after the Mid-Blastula Transition (MBT), suggesting that the maternal transcript of this gene has been depleted and the zygotic gene is not yet active. The zygotic *mdm1* gene is activated after this transition, which is seen in the increased expression level at 12-hpf. This is also the time that the optic vesicle and Kupffer's vesicle develops in zebrafish embryos. Expression of this gene appears to decline around 18-hpf before increasing in quantity again by 24-hpf. At 72-hpf, *mdm1* was expressed at the highest level. 72-hpf is the period of the completion of rapid morphogenesis of the embryo into the early larval stage. By 7-dpf observed a low but consistent level of mdm1 gene expression observed in the larval zebrafish.

Since the temporal expression of *mdm1* was carried out through the semi-quantitative analysis of the cDNA, it was important to further investigate the expression of the *mdm1* gene by identifying specific tissue expression of *mdm1* mRNA in zebrafish embryos of different ages (spatial expression analysis). Although little is known about the *mdm1* gene in zebrafish or mammals, recent studies suggest that *mdm1* may be involved in the development of the retina and/or optic nerves and may also play a role in retinal degenerative diseases (Chang *et al.* 2008). To investigate the role of *mdm1* in these processes, experiments were carried out using WT(AB) embryos treated with phenylthiourea (PTU) to inhibit pigment formation, and *golden* embryos. Several DIG-labeled *mdm1* RNA probes were generated (approximately 600bp-1200bp) with the Ambion MaxiScript T3/T7 kit. As shown in Figure 4.3, the *mdm1* transcript is expressed ubiquitously around 12-hpf and appears to be concentrated near the

anterior portion of the embryo from 24-hpf through 72-hpf. In the 24-hpf embryo, staining appears to be the darkest in the diencephalic roof, near the epiphysis (midline, dorsal region of the diencephalon), the dorsal tectum, telencephalon, and within the otic primordium. By 48-hpf, there has been a rapid morphogenesis of the embryo, and it appears that the expression of the *mdm1* gene is prominent in the midbrain (dorsal region), the midbrain tegmentum (ventral region), and optic tectum. Staining appears to be consistent in the CNS at 72-hpf, when the embryo enters the larval stage. Each set of *in situ* hybridization experiments also included control embryos for no RNA probe (no hybridization), no RNA probe/no antibody, and no antibody. These control embryos remained translucent indicating that the staining observed in the experimental embryos was due to *mdm1* transcript targeting.

The combined results of these experiments indicate that the *mdm1* gene is expressed at different levels throughout the developmental process. Expression begins as a maternal transcript that is ubiquitously expressed throughout the early embryo followed by zygotic gene expression that is ultimately confined to the anterior portion of the embryo. Specifically, based on the location of the *mdm1* transcript it appears that *mdm1* may play a role in the development of the otic primordium, optic cup, and other components of the brain and CNS as shown in the figures above. Thus, it is important to confirm these analyses with experiments to study and identify the function of the *mdm1* gene *in vivo*.

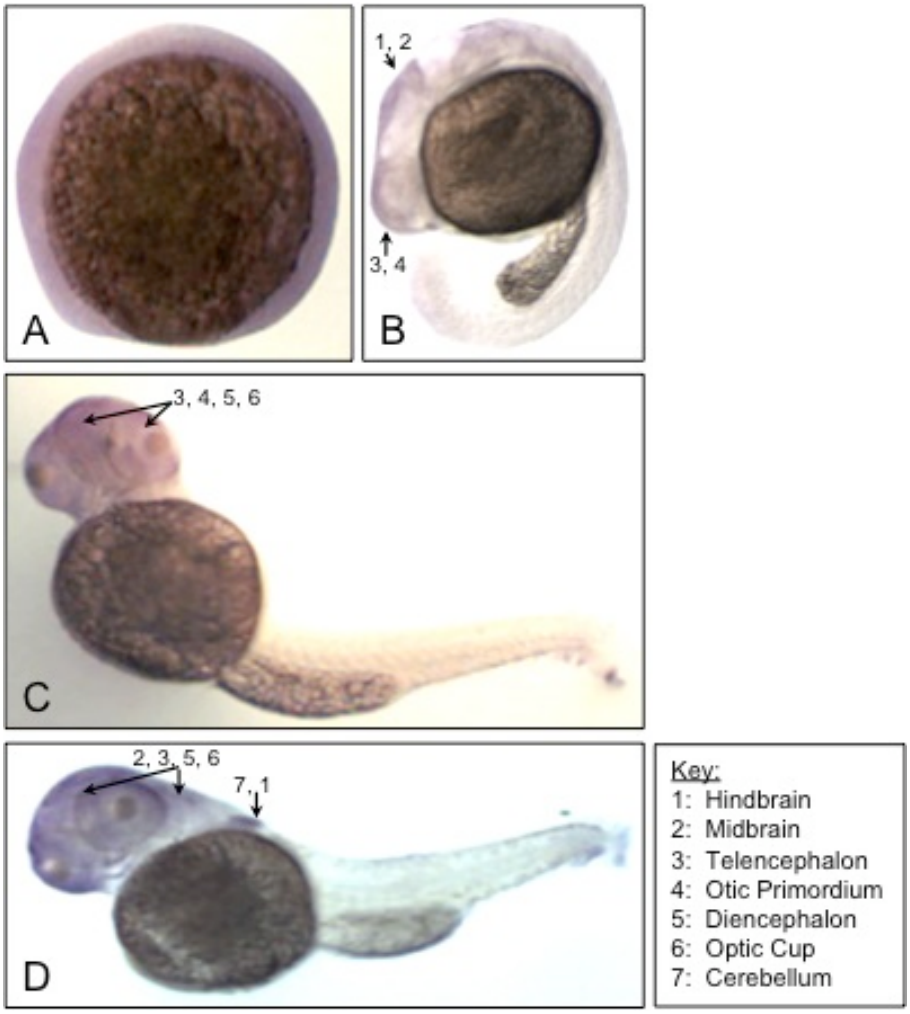

Figure 4.3: Results from the Whole-Mount *in situ* Hybridization Expression Analysis of *mdm1* Transcripts in Zebrafish Embryos. (A) Ubiquitous expression of *mdm1* in 12-hpf embryos (B) Expression appears to be localized in the CNS of 24-hpf embryos, including midbrain, hindbrain and otic primordium (C) Localization of *mdm1* transcripts in the anterior region of the zebrafish embryo continues at 48-hpf and also includes staining for *mdm1* in the optic cup and optic tectum (D) Robust staining for the *mdm1* transcripts remain in the CNS as well as within the eyes and cerebellum in 72-hpf embryos.

Using Morpholinos to Determine the Role of *mdm1* During Zebrafish Development

The use of synthetic antisense morpholino oligonucleotides (MOs) is the standard method for creating gene knockdowns in zebrafish, *Xenopus,* and other model systems. Successful binding of a morpholino to a gene of interest

requires identifying a region that is within 20 bp of the initiating AUG that allows the MO to effectively block translation of mature mRNA molecules *in vivo*. It is also possible to decrease expression of a gene by designing MOs that target splice junctions of pre-mRNA. For developmental biology, the translation-blocking MOs are especially useful for knocking down maternal mRNA, while splice-blocking MOs are more effective on actively transcribed zygotic RNA.

Two transcripts produced from the *mdm1* gene have been identified in zebrafish embryos and adults. The long *mdm1* transcript (VEGA *mdm1*-001) is 2193bp long and includes 14 exons. The short *mdm1* transcript (VEGA *mdm1*-002) is 2160bp long and is a splice variant that does not include exon 8. Additionally, there is a third transcript that exists, but does not code for protein, and therefore was not explored further.

Table 4.1: Morpholinos Used for the Gene Function Experiments

Target	Sequence	Comments
mdm1-ATG	5'-TGATTGCCTTGAAACGGACAGGCAT-3'	Translation Blocking MO – targets the maternal products
mdm1-Ex1	5'-TTTACAAAGCTTACCTTGAAACGGA-3'	Splice-blocker that targets Exon 1
mdm1-Ex2	5'-CGCTGATTCCCTATTAGGAATATAT-3'	Splice-blocker that targets Exon 2. Labeled with Biotin
mdm1-Ex8	5'-AGTAACAGGTGAAATGTTACCTCAT-3'	Splice-blocker that targets Exon 8/9 to knockdown the long transcript only
p53	5'-AGTAACAGGTGAAATGTTACCTCAT-3'	Standard supplied by Gene-Tools, LLC.
Negative Control	5'-CCTCTTACCTCAgTTACAATTTATA-3'	Standard supplied by Gene-Tools, LLC.

A translation-blocking MO was designed (*mdm1*-ATG) that would bind to maternal mRNA from both *mdm1* transcripts. Several MOs were also generated to target specific splice junctions. These MOs allowed for the knockdown of both zygotically active *mdm1* transcripts or the knockdown of a single transcript depending on the target (Table 4.1, Figure 4.4). For all injection experiments, not-injected embryos, dye-only injected embryos and embryos injected with the standard negative morpholino were also raised as controls.

Figure 4.4: Schematic of the *mdm1* Coding Sequence (Long Transcript from VEGA), showing the locations of exons, 5'-UTR, 3'UTR, Start and Stop Codons and approximate Morpholino Target Sites. The *mdm1*-Ex1 MO is not shown here since it was designed to target Exon 1 in the 5'UTR sequence that was originally not included in the gene sequence.

Effects of the mdm1 ATG-Blocking Morpholino in WT(AB) Embryos: To investigate the role of *mdm1* in zebrafish development, the processed maternal transcript was first knocked down by a translation blocking MO, *mdm1*-ATG, in 1- to 8-cell stage embryos. Since both *mdm1* protein-coding transcripts have identical 5'-coding sequence, using this MO allowed for the knockdown of both transcripts to occur simultaneously. This MO appeared to be most effective when 8-10nL of solution was injected at concentrations of 200-350μM. As described in Chapter Two, the *mdm1*-ATG MO was also supplemented with 50μM *p53* MO to reduce necrosis in the injected embryos. Following the mdm1-ATG MO injections, a range of phenotypes was observed in 24-hpi embryos (Figure 4.5). Headless embryos that died shortly after 24-hpi were the most extreme of the observed phenotypes, while most of the injected embryos appeared to have defects in head and eye development, typically resulting in an embryo with a smaller than average head and tiny, underdeveloped eyes. Defects in tail development were also noted in approximately 50% of the embryos.

Injected embryos that survived to 72-hpi were also photographed and any abnormal phenotypes were recorded. The most obvious and consistent phenotype was that of embryos with eye deformities that ranged from small underdeveloped retina to embryos with completely missing eyes (Figure 4.6). This was noted in a large percentage of the injected embryos, as well as tail and some head irregularities (Table 4.2). This information was critical, since it appeared to be consistent with the previous *in situ* data, suggesting that the

mdm1 gene is expressed during the development of the primordial eye and CNS, and specifically within those tissues in the 24- to 72-hpf embryo.

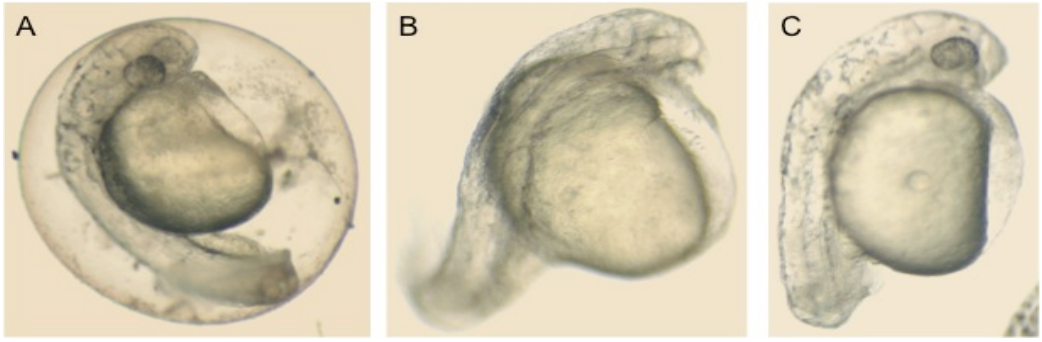

Figure 4.5: Photos of 48-hpi WT(AB) zebrafish embryos that were injected with the *mdm1*-ATG Morpholino supplemented with 50μM *p53* Standard Morpholino. (A) Embryo injected with 200μM *mdm1*-ATG MO exhibits a small head/small eyes phenotype following injection. (B) Embryo injected with 250μM *mdm1*-ATG MO displays an abnormal tail and small head, and does not appear to have any eye development. (C) Embryo injected with 300μM of *mdm1*-ATG MO appears to have a small head with only one developing eye; this embryo also displays defects in tail development.

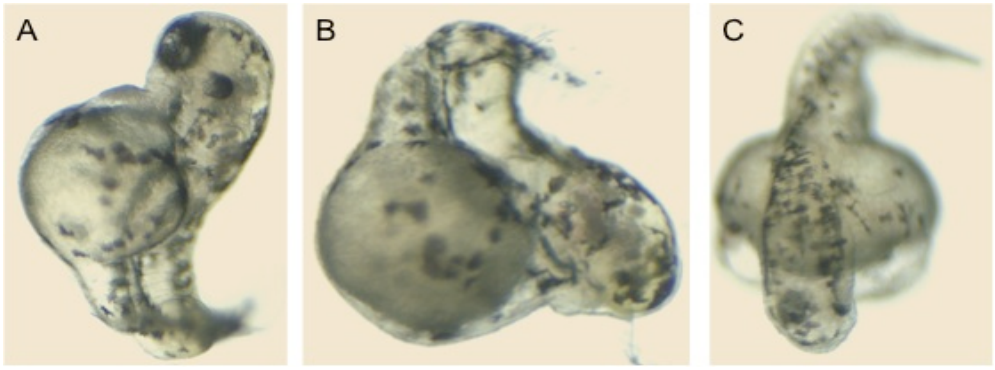

Figure 4.6: Results of 250μM *mdm1*-ATG Morpholino Injections supplemented with the *p53* Morpholino into WT(AB) Embryos shown at 72-hpi. (A) Embryo has obvious MO effects in eye and tail development causing an abnormally stubby appearing tail and underdeveloped eyes. (B) Embryo shown has no eye development in addition to a severe shortening of the tail. (C) Embryo has a small, abnormal sized head and severely underdeveloped eyes; tail is of normal length although it is slightly twisted.

Effects of the mdm1 Splice-Blocking Morpholinos in WT(AB) Embryos: Since the Mdm1 custom antibodies analyzed in Chapter Three did not properly detect the *in vitro* synthesized Mdm1 protein or Mdm1 in the embryo lysate,

verification of the knockdown by western blot analysis was not an available option. Fortunately, RT-PCR can be used to determine the effectiveness of splice-blocking MOs (Morcos 2007). Therefore, if the phenotypes observed following knockdown by a splice-blocking MO are identical to the results observed following the translation blocking MO, and the RT-PCR results suggest that the *mdm1* transcripts were knocked down, it can be concluded that the translation-blocking MO results are valid. Three different splice-blocking MOs (Table 1) were custom ordered from Gene-Tools to inhibit splicing at different intron-exon boundaries (mechanisms of MO action are explained in Chapter Two). Figure 4.4 shows the location of MO target sites within the *mdm1* gene.

Splice-blocking MOs were first designed to target both of the *mdm1* transcripts. The *mdm1*-Ex1 MO was injected into WT(AB) embryos at a range of concentrations from 200-550μM with and without *p53* MO supplementation. Regrettably, none of the injected embryos presented with any effects from the injections, implying that this particular MO did not work. Experiments continued by injecting the embryos with the *mdm1*-Ex2 MO that blocks splicing of Exon 2 of the *mdm1* mRNA. Eight-10nL of this MO at a concentration of 250-300μM was injected into embryos as described above (Figure 4.7). Knockdown of the *mdm1* mRNA was successful with the *mdm1*-Ex2 MO resulting in the same range of phenotypes in the morphants as observed from the translation-blocking MO experiments. These results not only confirmed the translation-blocking MO results, but also resulted in approximately 50% of the *mdm1*-Ex2 MO injected embryos exhibiting spontaneous rescue between 24- to 48-hpi. This result may

be due to the significant increase in *mdm1* transcripts after 24hpf that may titrate down the amount of the MO, resulting in a decrease the effectiveness of the splice-blocker after 24-hpi.

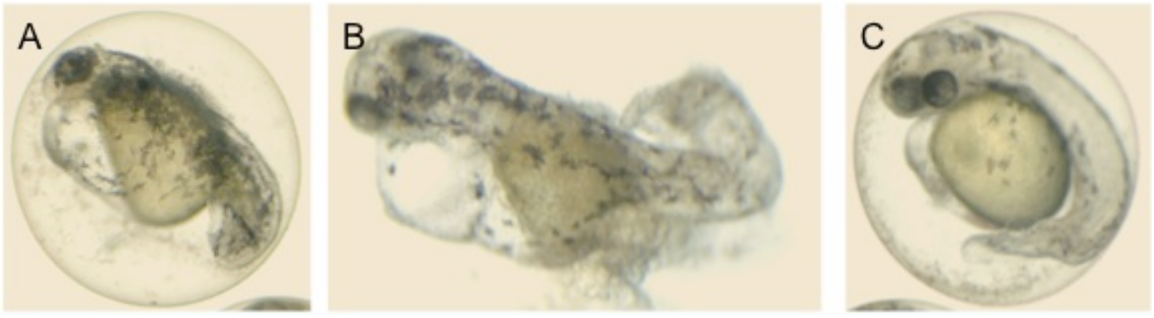

Figure 4.7: Results from Injection Experiments of the *mdm1*-Ex2 MO into Zebrafish Embryos. All embryos shown were injected with the *mdm1*-Ex2 MO, and are approximately 48-hpi. (A) Injected with 200μM MO and has obvious defects in eye and tail development. (B) Embryo injected with 250μM MO and also shows severe defects in eye and tail development. (C) Embryo injected with 300μM MO and appears to have a delay in development of the tail and eyes. All embryos shown also have pericardial edema, which is most likely a result of the injection process.

To determine whether there were any differences in resulting phenotypes when knocking down both *mdm1* transcripts as opposed to knocking down just the long transcript, the *mdm1*-Ex8 MO was specifically designed to target the *mdm1*-001 (VEGA) transcript and test this hypothesis. When injected into embryos, even at extremely low doses (50μM), this particular MO was completely lethal within a few hours following the injection. This was an unexpected result since none of the other *mdm1* MOs showed this level of lethality. Therefore the sequence of the *mdm1*-Ex8 MO was re-evaluated to determine if it may be targeting other sequences. BLAST analysis of the *mdm1*-Ex8 MO sequence revealed that it actually targeted multiple transcripts on a majority of the zebrafish chromosomes and was most likely knocking down multiple genes in the embryos.

The only difference between the two protein-coding *mdm1* transcripts is exon 8, which is very small, consisting of 11 amino acids. In an attempt to design another MO that would target just the longer transcript, it appeared that any MO designed around the 5' and 3' splice sites of exon 8 would result in a MO that targets multiple genes, based on BLAST analysis.

Since both *mdm1*-ATG MO and *mdm1*-Ex2 MO had similar results when injected into WT(AB) embryos, they were co-injected in combination with and without the *p53* MO (*mdm1*-ATG/*mdm1*-Ex2 combination). Interestingly, even at very low concentrations (50-100μM), the combination of these MOs was extremely lethal, and resulted in 0% survival after 24-hpi. A summary of the MO injection experiments is presented in Table 4.2. It is important to note that the total number of injected embryos does not include the embryos used for controls including the dye-only, buffer-only and standard negative control injected embryos. These embryos did not exhibit any developmental abnormalities following control injections. Additionally, several clutches of embryos injected with dye or buffer only were raised and bred, indicating that the injections did not interfere with development and fertility.

Table 4.2: Overview of Morpholino Injection Results.

	mdm1-ATG MO		*mdm1*-Ex1 MO		*mdm1*-Ex2 MO		*mdm1*-Ex8 MO	
	+ p53	***- p53***	***+ p53***	***- p53***	***+ p53***	***- p53***	***+ p53***	***- p53***
Survival at 24-hpi	78%	52%	20%	14%	62%	32%	0%	0%
Survival at 48-hpi	89%	80%	98%	96%	95%	88%	-	-
No Head Development	9%	13%	-	-	16%	16%	-	-
Small Heads Only	15%	21%	-	-	11%	28%	-	-
Small Heads/Small Eyes	62%	56%	-	-	64%	51%	-	-
Small Head/No Eyes	10%	7%	-	-	6%	4%	-	-
Tail Defects	43%	56%	2%	4%	43%	56%	-	-
No Abnormalities Observed	4%	3%	98%	96%	3%	1%	-	-
Total Injected	1926	882	305	298	2792	455	764	510

Results include all of the experimental injections for the above-mentioned *mdm1* MOs with and without the supplementation of the p53 Standard MO (the p53 supplementation was 50μM concentration of the p53 MO added to the experimental *mdm1* MO solution). The *mdm1*-ATG MO was injected into 1-2 cell zebrafish embryos at a range of concentrations between 200-350μM in a 0.1% Phenol Red solution. The *mdm1*-Ex1 MO was injected into 1-2 cell zebrafish embryos at a range of concentrations between 200-550μM in a 0.1% Phenol Red solution. Following these injections, it was apparent that the *mdm1*-Ex1 MO was not correctly targeting the *mdm1* mRNA, as determined by observing 96-98% of injected zebrafish embryos with no defects or abnormalities following the injections. The *mdm1*-Ex2 MO was injected into 1-2 cell zebrafish embryos at a range of concentrations between 250-300μM in a 0.1% Phenol Red solution. The *mdm1*-Ex8 MO was injected into 1-2 cell zebrafish embryos at 50μM (initial injections for this MO were concentrations between 200-400μM, but the concentration was reduced based on the lethality of this MO). Due to the lethality of this MO at low concentrations, the MO sequence was analyzed using BLAST, which revealed that it targets multiple transcripts on several chromosomes. Based on the data and observations noted above, it appeared that both the *mdm1*-ATG MO and the *mdm1*-Ex2 MO were causing similar defects during the development of zebrafish, which focused on the development of the head and eyes. Interestingly, approximately 50% of the injected embryos were observed to have defects in tail development.

Whole-mount Antibody Staining of mdm1-Ex2 Injected Embryos: In addition to confirming the morpholino injections by RT-PCR analysis, embryos injected with the *mdm1*-Ex2 MO were also subject to an *in situ* antibody staining

procedure that was used to detect the biotin label of that particular morpholino. This technique allowed for the visualization of morpholino target tissues within the whole injected embryo, and also enabled the verification of earlier whole-mount *in situ* hybridization data. The 3'- biotin label on the *mdm1*-Ex2 MO is a 394kDa affinity tag that can be detected with avidin or streptavidin conjugated with alkaline phosphatase.

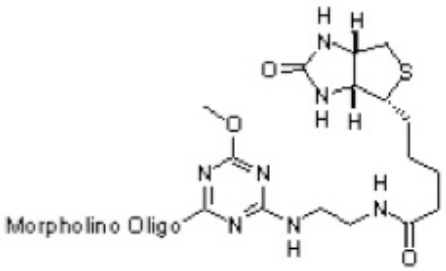

Figure 4.8: Structure of the Biotin label added to the *mdm1*-Ex2 MO (from Gene Tools, LLC.).

Embryos were injected with the *mdm1*-Ex2 MO with *p53* MO supplementation as previously described. Injected embryos were kept at 26-27^{o}C in petri dishes containing aquarium water with Methylene Blue, and collected at several developmental stages including 18-somite (18-hpi) through prim-6 (25-hpi). Following photodocumentation of the injected embryos, they were euthanized in Tricaine-S on ice and prepared accordingly for the antibody staining protocol described in Chapter Six. Colorimetric detection with Streptavidin-AP and NBT-BCIP was terminated after several minutes of treatment. The embryos were placed in glycerol to clear and were subsequently photographed.

Since the morpholino specifically targets *mdm1* RNA, it was expected that the results from the antibody staining procedure would be similar to the *in situ* hybridization data from previous experiments where the *mdm1* transcript expression within the embryo tissue was identified. As Figure 4.9 shows, there is a striking similarity between the antibody staining results and the initial *in situ* hybridization data. In both experiments *mdm1* RNA appeared to be expressed significantly in the anterior portion of the embryo, specifically in the CNS and primordial eye tissues. The morpholino injection and rescue results also suggested that *mdm1* may also be involved in the development of the tail, based on the observed phenotypes. In a 19-hpi embryo (Figure 4.9A), the morpholino appears to localize to regions of the CNS, specifically the diencephalon, midbrain, telencephalon and otic primordium. At approximately 22-hpi (Figure 4.9B), staining continues to appear robust within the diencephalon, midbrain and telecephalon. Additionally, the morpholino appears to localize within the optic cup, epiphysis and cerebellum. Similar staining was also observed in the 25-hpi embryos (Figure 4.9C and 4.9D), although the most intense staining occurred within the optic cup, lens, epiphysis and hindbrain. It is also important to note that all of the embryos had noticeable staining in the posterior portion of the tail, that may correspond to the tail defect phenotype that was observed during the injection experiments.

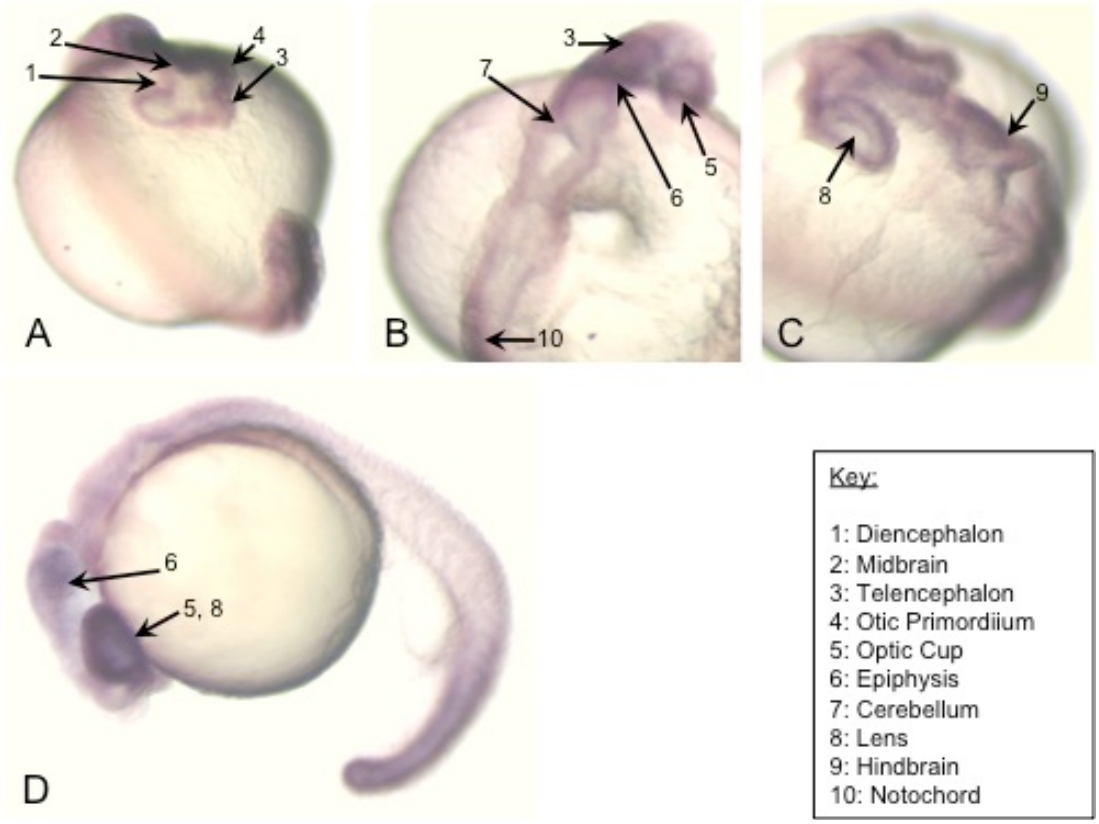

Figure 4.9: Whole-mount Antibody Staining of Morpholino Injected Zebrafish Embryos (A) 19-hpi injected embryo shows very distinct staining in the diencephalon, telencephalon and midbrain (B) Robust staining in the 22-hpi injected embryo indicates localization of the MO in the cerebellum, optic cup and epiphysis (C) Staining is also noted in the lens and hindbrain in the 25-hpi injected embryo (D) Lateral view of the 25-hpi injected embryo also shows staining in the optic cup and lens.

RNA Rescue of the Morphants: Although the results from the translation and splice blocking morpholinos were exciting, it was important to confirm that the phenotypes observed were due to the knockdown of the *mdm1* gene and not due to non-specific effects of the morpholino injections. One method to validate the results is to utilize RNA rescue experiments. The mMessage mMachine T7 kit (Ambion) was used to synthesize *in vitro* capped mRNA of the full-length *mdm1* gene with the Kozak sequence. A pCR4 clone containing the confirmed sequence was used for the transcription reaction (cloning and sequencing of the

gene is described in Chapter Three). Following the transcription reaction, the RNA was diluted 1:5 in 0.1M KCl and stored in 5µl aliquots at -80^{o}C. Prior to storage, the concentration of one aliquot was determined by spectrophotometry.

In order to control the RNA rescue experiments, the embryos were injected twice; first they were injected with the morpholino and then they were injected with the specific RNA (Ekker & Larson 2001; Nasevicius & Ekker 2000). Up to 100 embryos at a time were placed under the dissecting microscope and injected with the appropriate concentration of either the *mdm1*-ATG or *mdm1*-Ex2 MOs with *p53* MO supplementation. Once the embryos were injected with the morpholino solution, half of the embryos were removed and placed in a petri dish containing aquarium water with Methylene Blue and stored at approximately 27^{o}C in an incubator. The remaining embryos were then injected with 8-10nL of a 50-75pg dose of the capped mRNA. This procedure was repeated until all embryos were injected, and continued over a several week period. Additionally, not-injected embryos, dye-only injected embryos and embryos injected with the standard negative morpholino were also raised during each weekly injection session as controls. The embryos were then compared to each other to identify whether the morpholino effects were rescued.

Figure 4.10 shows a WT(AB) not-injected embryo, an *mdm1*-Ex2 morphant, and the RNA rescued embryo. Based on the observed phenotypes of the RNA rescued embryos, 98% of the RNA injected embryos appeared to have wildtype characteristics, including appropriate developing tails, heads and eyes, as compared to the morphants. Since the tail phenotype was also rescued in

these experiments, it can be concluded that the *mdm1* gene may be involved in the development of the tail as well as the eye in the early zebrafish embryo.

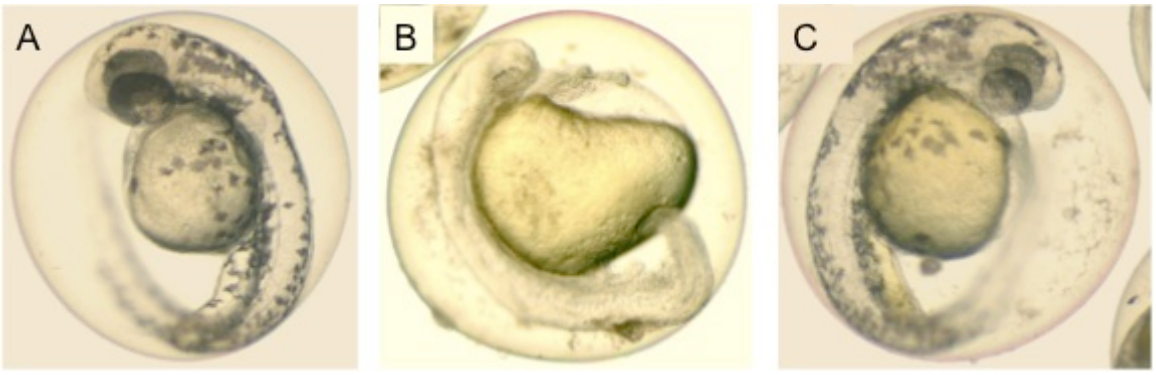

Figure 4.10: Zebrafish embryo morpholino rescue experiments (A) Not-injected 48-hpf *golden* heterozygous embryo control (B) *mdm1* MO knockdown in a *golden* heterozygous embryo (C) 48-hpi *golden* heterozygous embryo first injected with the *mdm1*-Ex2 MO, then injected with synthesized *mdm1* mRNA for a full rescue of the normal phenotype.

Confirming the Injection Experiments and Validating the *mdm1* Gene Analysis

It was important to verify that the *mdm1* MOs were actually targeting the *mdm1* mRNA within the zebrafish embryo. Two approaches were taken to explore the specificity of the knockdown experiments. First, embryos injected with the *mdm1*-Ex2 MO were collected and analyzed for *mdm1* transcript expression by RT-PCR. Second, an *in vitro* experiment was designed to test whether the *mdm1*-ATG MO successfully targeted the processed *mdm1* transcript. This allowed for the visualization of decreasing Mdm1 protein expression with the addition of morpholino to the reaction mix.

RT-PCR Analysis of Injected Embryos: All embryos from the knockdown, rescue, and overexpression experiments were collected into RNA Later (Qiagen), along with non-injected embryos, and used for analysis by RT-PCR. Total RNA was isolated from each set of embryos, and primers for *mdm1* were used to amplify the full-length coding sequence from each set of RNA. The prediction was that embryos injected with *mdm1* MOs will show decreased levels of mRNA from the gene. These experiments to confirm the specificity of the effect of the MO in the injected embryos were performed in triplicate, using embryo RNAs from 14 injection sets. Representative data from the RT-PCR experiments is shown in Figure 4.11.

The RT-PCR results suggest that the *mdm1*-Ex2 MO knockdowns were efficient in targeting the *mdm1* transcripts in the zebrafish embryos. The observed level of the *mdm1* transcripts in Lane 4 is significantly reduced from the normal expression shown in Lane 3 from the non-injected WT(AB) embryos. Although there is a weak band in Lane 4, which shows amplification from the morphant RNA, it is reasonable to conclude that the phenotypes observed following the MO injection was due to the *mdm1*-Ex2 MO. Additionally, the results in Lane 5 suggest that the RNA rescue phenotypic effects observed following the injections were also a result of successful knockdown and rescue of the *mdm1* gene in the zebrafish embryos, since the resultant cDNA band on the gel is consistent with the band in Lane 3. Interestingly, the embryos only injected with the *mdm1* synthesized capped mRNA, had approximately the same RT-

PCR expression results of *mdm1* as the non-injected and RNA rescued embryos. This result was observed numerous times.

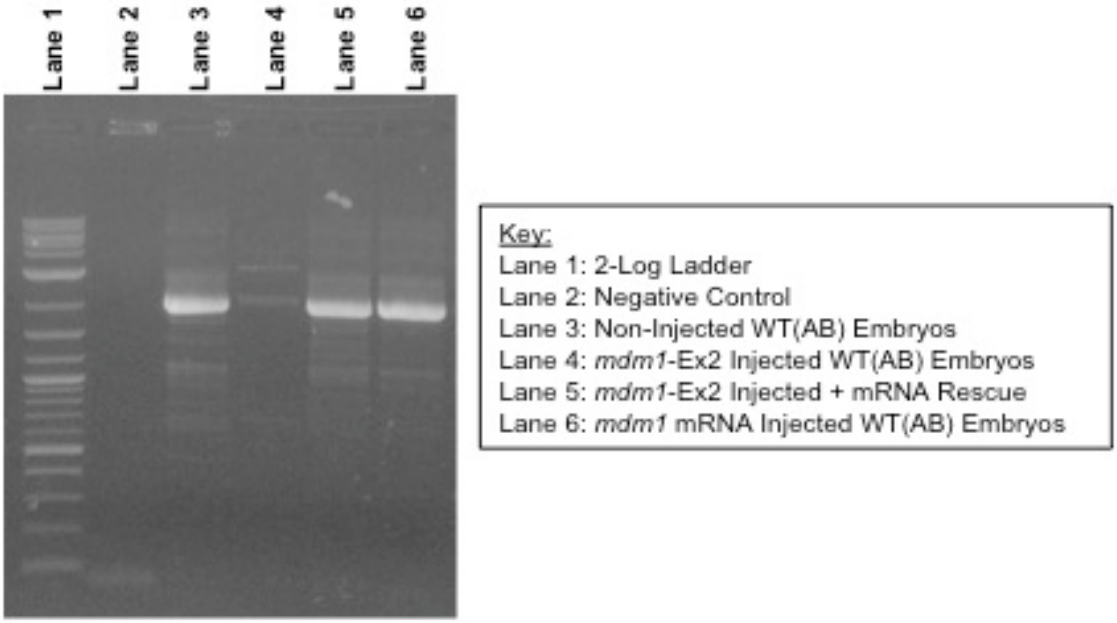

Figure 4.11: RT-PCR Confirmation of the Injection Experiments in Zebrafish Embryos.

Applying the in vitro Transcription and Translation System to Confirm the Translation-blocking Effects of the mdm1-ATG Morpholino: By knocking down *mdm1* mRNA, the MDM protein is presumed to also be depleted in the injected embryos, which would give the resulting phenotypes that were observed in the morphants (Figures 4.5 - 4.7). Without antibodies specific to the zebrafish Mdm1 protein, verifying MDM protein appeared to be a difficult undertaking *in vivo*. For this reason, the question was asked if it was possible to study the effect of the *mdm1*-ATG MO on protein levels *in vitro*. Previous experiments that utilized the Promega TnT kit resulted in the expression of the synthesized Mdm1 protein on

a western blot, which utilized biotinylated tRNA (lysine) and was then detected with Streptavidin-AP and stained with NBT-BCIP (Chapter Three). Using various dilutions of the *mdm1*-ATG MO in nuclease-free water, 0.5µl of each dilution was added to a 10µl reaction containing the TnT mastermix, amino acid mixture, biotinylated tRNA (lysine), and the full-length *mdm1* clone in the pCMVTnT Vector (Promega). The reaction products were then diluted 1:10 in Sample Buffer, run on an SDS-PAGE gel, and transferred to a nitrocellulose membrane. The TnT products were detected as previously described (Chapter Three) and the results are shown in Figure 4.12.

As Figure 4.12A indicates, the increased concentration of the *mdm1*-ATG MO added to the TnT reaction appears to decrease the expression of the synthesized Mdm1 protein on the western blot. These results were very exciting since they illustrate a novel way to confirm the MO targeting *in vitro* without a specific antibody. Importantly, the approximate concentrations of the *mdm1*-ATG MO injected into the live zebrafish embryos correspond with the total concentration of MO in lanes 10-12 in Figure 4.12A. Since the MO added to the TnT reaction significantly decreased the expression of the Mdm1 protein *in vitro*, it is likely that the resulting phenotypes from the *mdm1*-ATG MO injections are due to the decrease in maternal *mdm1*.

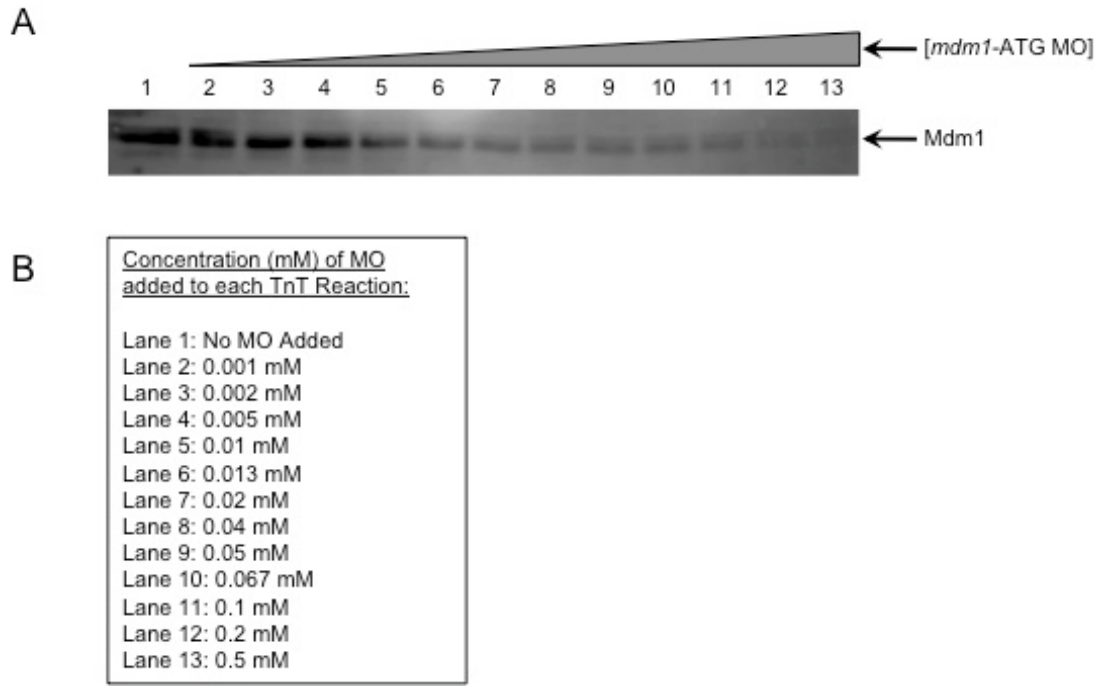

Figure 4.12: *In vitro* Synthesis of the Mdm1 Protein with Various Concentrations of the *mdm1*-ATG MO to Test for Specificity. (A) The western blot of the Mdm1 TnT products with an increasing amount of MO added to each reaction. (B) The concentration added to each TnT reaction.

Testing *mdm1* for Genomic Instability and Overexpression Experiments

Testing for Genomic Instability: Based on previous studies and mapping experiments, the *mdm1* gene is located within the *gin-12* candidate region on chromosome 4. While the interest of the experiments described throughout this chapter were designed to determine the developmental role of the *mdm1* gene, it was also important to continue investigating *mdm1* as a potential *gin-12* candidate by exploiting the knockdown coupled with the mosaic eye assay. For these experiments, *golden* heterozygous embryos were injected with various concentrations of the *mdm1*-ATG MO with and without the supplementation of the *p53* MO. Embryo survival at 24-hpi was maximized by the addition of the *p53*

MO, as described in Chapter Two, specifically when embryos were injected with 8-10nL of 250μM MO solution in Danieau Buffer with 0.1% Phenol Red. Unfortunately, mosaic eyes did not result in any of the *golden* heterozygous injections, suggesting that the *mdm1* gene was no longer a *gin-12* candidate.

Overexpression Analysis of the mdm1 Gene in Zebrafish Embryos: Since the *mdm1* gene was originally identified in transformed 3T3DM cells that expressed the gene, it was of interest to determine the effect of overexpression of *mdm1* mRNA in embryos. These experiments were carried out by injecting both WT(AB) and *golden* heterozygous embryos so that the mosaic eye assay could be used to observe potential genomic instability. The same *in vitro* synthesized capped full-length *mdm1* mRNA was utilized for this experiment that was used in the previous RNA rescue experiments. Approximately 100pg of *mdm1* mRNA was injected into 1-8 cell *golden* heterozygous and WT(AB) embryos, which were then kept in aquarium water at 26-27^{o}C in an incubator and monitored daily to remove any debris or decayed embryos and replenish the water. At 48-hpi, the *golden* heterozygous embryos were placed in 2X Tricaine solution (anesthetized) and screened for mosaicism. The injected WT(AB) embryos were screened for any abnormalities, then subsequently photographed and collected into RNA Later (Qiagen).

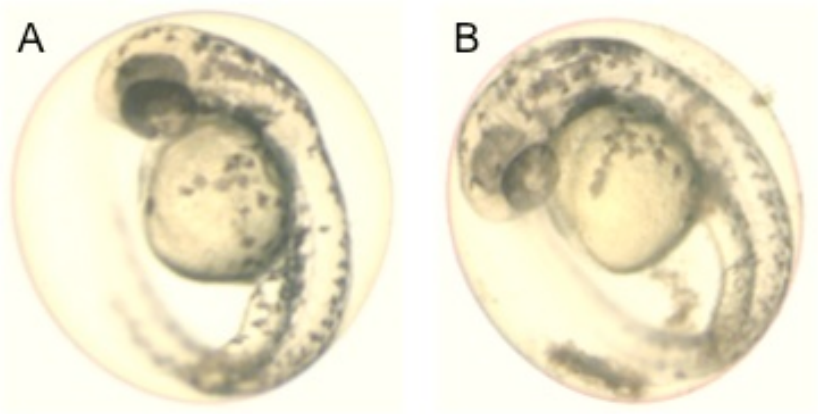

Figure 4.13: Injection of synthesized full-length *mdm1* mRNA into *golden* heterozygous zebrafish embryos. (A) 48-hpf Not-Injected embryo (B) Embryo injected with RNA.

Figure 4.13 shows that the embryos injected with an abundance of *mdm1* mRNA exhibit a fully wildtype phenotype. There appears to be a slight delay in pigment cell migration that is often a result from the injection itself and has been observed in all of the previous injection experiments. In the *golden* heterozygotes, some areas of the RPE appear lighter in color; however these are not the expected golden-colored patches observed in true mosaics, but rather layers of cells that have not developed pigment. By 72-hpi, these embryos had completely black-pigmented eyes, confirming that the *mdm1* gene did not have genomic instability activity in developing embryos by overexpression.

Summary of Experimental Results:

- The semi-quantitative RT-PCR results suggest that the expression of the *mdm1* gene in developing zebrafish embryos is quite varied. Interestingly, although this procedure was repeated several times using various embryo RNA samples, the RT-PCR results indicated that the expression of *mdm1*

transcripts is quite low in 18-hpf embryos. It has been shown with other experiments that there is in fact, *mdm1* expression in 18-hpf embryos and that it may potentially be involved in CNS and eye development at this stage.

- Whole-mount *in situ* hybridization was used to identify the spatial expression of the *mdm1* transcript within specific embryo tissues. These results suggested that the *mdm1* transcripts were initially expressed ubiquitously throughout the embryo, and then became confined to the anterior or cephalic region. This indicated that the *mdm1* gene may play a role in CNS development.
- Several morpholino oligonucleotides were designed to specifically target one or both *mdm1* transcripts within the zebrafish embryo. Unfortunately, two of the splice-blocking morpholinos did not appear to effectively target the *mdm1* gene as they either gave a “no effect” or “completely lethal” result. However, defects in eye, head and tail development were observed in embryos injected with either the *mdm1*-ATG MO or the *mdm1*-Ex2 MO, suggesting that these morpholinos are both correctly targeting the *mdm1* gene, and that it is in fact involved in the development of the CNS, particularly the eye.
- RNA rescue experiments were performed in order to confirm the observed morpholino phenotypes that occurred from the *mdm1* morpholino injections. Embryos that were co-injected with morpholino and the *in vitro* transcribed

capped *mdm1* mRNA displayed a full rescue phenotype of eye, head and tail development.

- Staining for the biotin label in whole embryos also confirmed much of the results from previous experiments that the *mdm1* gene is expressed significantly in the anterior portion of the embryo, particularly the CNS and eye. These results also verified the *in situ* data of RNA expression. Interestingly, it also suggested that the *mdm1* RNA is expressed in primordial eye and CNS at approximately 19-hpi, which is a slightly different result than the earlier semi-quantitative RT-PCR findings. Overall, these results confirm the expression of the *mdm1* RNA and the targeting ability of the morpholino within the embryo. Additionally, these results imply that the *mdm1* gene is a key component in the development of the eye in zebrafish embryos.
- The injection experiments were validated by RT-PCR analysis using total RNA from non-injected, *mdm1*-Ex2 injected, RNA Rescued, and RNA overexpressed embryos. The results confirmed that the *mdm1* gene is:
    - Expressed in non-injected embryos
    - Was knocked down in the morpholino injected embryos
    - Can be rescued in the morpholino-injected embryos with the *mdm1* RNA. Additionally, the *mdm1* transcript expression did not appear to change in the embryos injected with the *in vitro* transcribed mRNA.

- Novel use of the *in vitro* Transcription and Translation kit to detect the effectiveness of the *mdm1*-ATG MO targeting proved to be successful. This allowed for the verification of the translation-blocking MO without having a specific antibody reactive to zebrafish Mdm1. Since there are relatively few zebrafish antibodies available, this technique is extremely useful for rapid confirmation of decreased protein expression levels *in vitro*.
- Morpholinos were also used to test for genomic instability activity of *mdm1* in *golden* heterozygous embryos, as *mdm1* was currently a candidate gene on the *gin-12* list. In embryos with at least one developing eye, mosaics were not observed, resulting in *mdm1* no longer being considered a *gin-12* candidate gene. Overexpression of the mRNA was also performed in *golden* heterozygous embryos to determine if this caused genomic instability activity in the embryo. Again, mosaics were not observed in any of the injected embryos. Thus, it appears that *mdm1* has no potential genomic instability activity.

CHAPTER FIVE

CONCLUSIONS, IMPLICATIONS, AND FUTURE DIRECTIONS

Conclusions and Implications

The overall purpose of this research was to identify and characterize a unique set of genomic instability mutants in the freshwater zebrafish. These *gin* mutants exhibit increased incidence of somatic mutation during early embryogenesis. Identifying the genes responsible for these modifications in the zebrafish model will eventually lead to a better understanding of the development and disease in humans.

The data presented throughout this dissertation demonstrate an in depth investigation into the developmental expression and function of several genes, located within known regions of genomic instability activity in the zebrafish model organism. This project had three distinct objectives.

1. Chapter Two focused on the first objective, which was to explore candidate genes within the *gin-10* region of chromosome 18. Specifically, the RNA expression and developmental function of *synbl, rfx4,* and *sir2* genes were examined.

2. Chapter Three, dealt with the optimization of Mdm1 protein expression experiments and determining the specificity of custom zebrafish Mdm1 antibodies.
3. Chapter Four focused specifically on the expression and function of the *mdm1* gene, a candidate for the *gin-12* studies, during the early zebrafish developmental stages.

All of the gin-10 Candidate Genes showed both Maternal and Zygotic Gene Expression: Preliminary genetic studies determined that the *gin* mutants required both maternal and zygotic expression in developing zebrafish. Using RT-PCR, ten candidate genes were analyzed in WT(AB) embryos for maternal and zygotic gene expression using 4-hpf and 24-hpf embryo RNA. Interestingly, all of the candidate genes tested appeared to have both maternal and zygotic transcript expression (Table 2.1). Predicted Sanger and NCBI orthology information for the *gin-10* candidate genes was used to select the top three candidate genes, *synbl, rfx4,* and *sir2* for future experimental focus. Transcript expression analyses of these genes utilized the semi-quantitative RT-PCR and whole-mount *in situ* hybridization techniques (Figures 2.5, 2.7, and 2.8). The *rfx4* and *sir2* transcripts appeared to have very distinct patterns of expression throughout the zebrafish embryogenesis according to the semi-quantitative RT-PCR data.

While exploring the *synbl* candidate gene, a paralog, *ric8a*, was found during the database searches. Since it appeared that these paralogs were

involved in asymmetric cell division in other organisms, it was important to look for any variations in the temporal and spatial expression of these genes during development to determine whether they function cooperatively or have diverged in function during teleost evolution. There was a very interesting difference in the pattern of expression between the *synbl* paralogs during early zebrafish development. The maternal expression of *synbl* is robust at 4-hpf, then a distinct transitional period occurs when active zygotic transcription of the *synbl* gene appears around 12-hpf. Expression levels appear to peak at 24-hpf but are still detectable through 7-dpf. The *ric8a* gene does not appear to have maternal expression or be actively transcribed in the embryo until approximately 18-hpf and peaks at 72-hpf. It is clear that there is some divergence in the expression of these genes during zebrafish development.

The Developmental Functions of Several gin-10 Candidate Genes were Identified by Morpholino Injections: Translation-blocking MOs were designed to target each of the *gin-10* candidate genes and the *ric8a* gene (Table 2.2). Additionally, a splice-blocking MO was designed for the *synbl* gene, which was used alone and in combination with the *ric8a* MO and *synbl*-ATG MO. Injections were performed in both WT(AB) and *golden* heterozygous embryos, which allowed for the use of the mosaic eye assay to determine if the gene knockdown led to mosaic eyes. The results of the MO injections suggested that none of the targeted genes had genomic instability activity, since mosaic eyes were never observed at 48- through 72-hpi (Figure 2.11). However, these experiments were

important to understand the general role of each of these genes in zebrafish development. For example, based on the injection experiments and the resulting phenotypes of the morphants, it appears that the *sir2* gene is involved in metabolic activity and had a 90-100% lethality rate in the injected embryos by 48-hpi. These results further suggest that the zebrafish *sir2* gene is more closely related to the human *sirt3* gene, which has been implicated in the regulation of metabolic processes. Based on the morpholino and cloning data, it has been concluded that the zebrafish *sir2* gene is no longer a *gin-10* candidate, but may become useful for studying metabolic regulation and adaptive thermogenesis in zebrafish.

When using the MOs to determine differences in the function of the *synbl* and *ric8a* genes, it was determined that although some off-target effects occurred in the development of the tail, both MOs caused cerebral edema and the general abnormal development in the brain, as compared to the non-injected embryos. Some published data had suggested that the *synbl* gene is involved in the migration of pigment cells of the developing zebrafish. Interestingly, all of the *synbl*, *ric8a* and combination injected embryos had normal looking melanocytes that appeared to migrate properly. Based on these results, it is unclear whether the morpholinos used (*synbl*-ATG, *synbl*-splice, and *ric8a*-ATG) were correctly targeting the appropriate transcripts. However, it is important to note that similar phenotypes were observed from each of these MO injections and when injected in combination, which suggests the reported data is consistent with *synbl* and *ric8a* function in the developing embryo. When applying the mosaic eye assay to

all of the knockdowns performed, it appears that none of the genes tested had genomic instability activity.

Re-Mapping the Viral Insert of the ZIRC Transgenic Fish Line Led to an Unexpected Result: To continue the research on the *synbl* paralogs, zebrafish embryos containing a transgenic viral insert were purchased from the Zebrafish International Research Center in Oregon. Self-crosses of the Tg-*synbl* fish were performed and the resulting embryos were injected with *synbl*-ATG, *ric8a*-ATG or *synbl*-splice/*ric8a*-ATG MOs to determine the effect of these knockdowns in a *synbl* null background. The phenotypic results of these morphants did not vary from the initial *synbl* injection experiments, which was an unexpected result (Figure 2.12). Furthermore, the self-crosses did not result in a 25% dead-loss of homozygous mutants, and therefore the transgenic insert was remapped in order to determine the exact chromosomal location. Genomic PCR and cloning analyses repeatedly suggested that the transgenic insert was not affecting the *synbl* gene, but rather it was located within the second intron of the *cry1b* gene (Figure 2.15, Table 2.3). The *cry1b* gene is also on chromosome 18 and is located within the *gin-10* region; however, it is on the adjacent contig to the location of the *synbl* gene, and appears to be involved in circadian rhythms according to recent published reports. Without having the appropriate transgenic fish for these studies, moving forward to determine the developmental differences of these genes *in vivo* was not plausible at the time.

Protein Expression Studies were Optimized in the Zebrafish Model for Future Experiments to Study Mdm1 Protein Interactions: Studying protein expression by western blotting and other techniques is a trivial component in many research laboratories. However, it is highly underused in the zebrafish community due to the unavailability of zebrafish specific antibodies and protocols. For this reason, custom Mdm1 antibodies were designed and ordered to look at the expression of this protein during zebrafish development, and use it for protein-protein interaction studies to determine whether the Mdm1 protein is involved in the regulation of the p53 tumor suppressor or another component of its pathway. As Chapter Three describes, much of the initial effort was placed on optimizing the lysate preparation and western blotting techniques using various stage zebrafish embryos (Figure 3.1). Once a protocol was defined, it was imperative to ensure the quality and specificity of the custom antibodies. The use of the *in vitro* transcription and translation kit was utilized for this purpose, to synthesize the Mdm1 protein and several control proteins that were run on the western blots with embryo lysate to test for the specificity of the custom antibodies (Figure 3.5). Repeatedly, the results indicated that the custom Mdm1 antibodies did not detect the Mdm1 protein (74 kDa), but rather a protein at approximately 55 kDa; the custom antibodies also did not detect the synthesized Mdm1 protein on any of the blots (Figures 3.6 and 3.7).

To further study the Mdm1 protein interactions *in vivo* without an antibody, injecting embryos with FLAG or 6X-His tagged Mdm1 protein would potentially allow for the co-immunoprecipitation of the tagged Mdm1 and interacting proteins

for analysis. It was unfortunate that during the time spent on cloning these tags into the full-length *mdm1* sequence, none of the clones analyzed by restriction digests or sequencing contained the tags (Figures 3.11 and 3.15). Rather than struggle with the protein expression studies, analyzing the developmental function and expression of the gene was pursued. Since little was known about the *mdm1* in zebrafish or other organisms, using knockdown technologies and developing novel techniques for these studies was crucial in identifying it's biological role during development.

The mdm1 Gene is Involved in the Development of the Zebrafish Eye and CNS: Using many of the techniques described in Chapter Two, the developmental expression patterns (both temporal and spatial) of the *mdm1* gene were explored specifically in Chapter Four. Expression analysis results consistently showed that the transcript expression of *mdm1* was extremely varied during development, implying that the transcription of this gene was highly regulated during specific developmental time points (Figure 4.2). The *in situ* hybridization data also suggested that the gene expression of *mdm1* was localized to the head of the embryo from approximately 24-hpf through 72-hpf (Figure 4.3).

Morpholinos were also used for the targeted knockdown of the *mdm1* transcripts *in vivo* (Table 4.1). Two of the *mdm1* MOs, a translation-blocker and a biotin-labeled splice-blocker, reliably gave the same phenotypic results in the morphants. This data showed that the *mdm1* gene is involved in the

development of the eye and CNS, since the knockdowns caused abnormal development of the eyes and portions of the brain (Figures 4.5, 4.6, and 4.7). In higher concentrations of the MOs, embryos would develop without eyes; however, the survival of these was limited. To prove that the effects of these MOs were not due to off-target events, RNA rescue, biotin staining for the splice-blocking MO, and RT-PCR experiments were performed (Figures 4.9, 4.10, and 4.11). The combined results of these experiments were exciting in that they all appeared to confirm the appropriate targeting of the *mdm1* splice-blocking MO and even the earlier *in situ* expression analysis. Importantly, these results imply that the *mdm1* gene is a key component in zebrafish eye development.

It was also important to show that the *mdm1*-ATG MO was also correctly targeting the *mdm1* gene. However, the only known way to determine this is by using western blot analysis to look at the decrease of protein expression following the injection. Using the tools available to the lab, a novel approach was developed that allowed for the visualization of the MO effects on the synthesized Mdm1 protein. By adding different concentrations of the *mdm1*-ATG MO to TnT reaction samples, along with the biotin labeled tRNA (lysine), the final products were run on a gel and detected with streptavidin. The results demonstrated the successful targeting of the MO to the Mdm1 protein by decreasing protein expression, which corresponded to the addition of increasing concentrations of MO (Figure 4.12). The success of this technique to show direct targeting of the MO *in vitro* should prove to be a rapid and useful tool for the zebrafish research community. In addition to this *in vitro* approach to testing for morpholino

specificity, it may be possible to also show a rescue in this system by imitating an *in vivo* rescue experiment by adding synthesized mRNA to the reactions. Although this method has not yet been tested, it may prove to be an invaluable step in assessing the specificity and quality of morpholinos prior to embryo injections.

Finally, the underlying goal was to determine whether the *mdm1* gene had any genomic instability activity in the developing zebrafish embryo, as it was identified within the *gin-12* region of chromosome 4. Knockdown and RNA overexpression experiments of the *mdm1* gene in *golden* heterozygous embryos did not give rise to mosaics. Additionally, the phenotype of the *mdm1* RNA injected embryos was normal as compared to non-injected embryos (Figure 4.13). From these results, it can be concluded that the *mdm1* gene is no longer a *gin-12* candidate.

Future Directions

The gin-10 Project: Since the genes that were focused on in the current project did not lead to any genomic instability activity in the zebrafish embryos with the knockdowns, it is important to reevaluate the genes within the mapped *gin-10* region. The most recent annotated zebrafish chromosome 18 information had suggested that some of the candidates listed in Table 2.1 are actually located outside the *gin-10* region, while new genes have recently been identified. Some preliminary RT-PCR for those genes has been done (Appendix A) although much more work is needed for the continuation of this project. While

knocking down individual candidate genes is a necessary component of this project, it may not be an effective way to identify the cause of genomic instability activity since it can be expensive to design the MOs and is very time consuming. An alternative approach may be to use microarrays and comparative genomics with cDNA from the known *gin-10* carriers and either WT(AB) or *golden* fish to determine the location of the loss of expression on chromosome 18 that leads to the mosaic phenotype. It would also be interesting to look at the upstream and promoter regions of the genes within the mapped *gin-10* area, to identify important transcription factor binding sites and other regulatory elements that may be involved in the cause of genomic instability in these *gin* mutants. Another direction that can be taken, although difficult in the zebrafish, is to fluorescently label specific genes within the *gin-10* region for fluorescent *in situ* hybridization (FISH) analysis of chromosome spreads. It is possible that the genomic instability is caused by a loss of function of more than one gene in this region, which may not be found by individual gene knockdowns or even microarrays.

The Mdm1 Protein Expression and Interaction Studies: Given that the custom Mdm1 antibodies failed to detect the appropriate size protein in the embryo lysate and the TnT product, it is reasonable to continue by designing other peptides that target other regions of the Mdm1 protein. By looking at the Mdm1 peptide sequences, it may be possible to find better epitope sites for western blotting and co-IP techniques with zebrafish embryo lysates. While

having an effective antibody is important for these studies, it would be interesting to determine what protein the custom Mdm1 antibodies were detecting at 55 kDa protein on the western blots. Running an SDS-PAGE with zebrafish embryo lysate and cutting out the 55 kDa proteins for mass spectrometry analysis or using the antibody for an immunoprecipitation (IP) combined with mass spectrometry may allow for this determination.

Another experimental approach that was partly explored in these studies was adding a tag to the *mdm1* sequence for protein interaction studies. Since the 5'-region of the *mdm1* sequence was modified by the addition of the Kozak sequence and restriction sites, the research efforts focused on adding a FLAG or 6X-His tag to the 3' sequence before the stop codon. Unfortunately, the tags were not successfully added to the *mdm1* sequence, although it did not appear that there should be any sequence issues to complicate cloning based on the sequence information. Another method would be to clone the full-length *mdm1* gene without the stop codon (insert a restriction site immediately before the stop codon), and insert this sequence into a vector containing the tag of choice. Upon verification of the correct reading frame, this can be synthesized *in vitro* and the tagged protein can be injected into zebrafish embryos and used for co-IPs to look at potential Mdm1 protein interactions. Although this would not allow for exploring the endogenous Mdm1 protein interactions, it could give rise to pertinent preliminary protein data and lead to the identification of the pathways that Mdm1 is involved in. Additionally, other tags could be incorporated into the *mdm1* sequence for the same purposes.

Further Analysis of the Zebrafish mdm1 Gene Function: While the results described in Chapter Four have implicated the zebrafish *mdm1* gene as having a role in eye development, and recently published data have suggested its involvement in age-related retinal degeneration in mouse models, the next step should be to determine the mechanisms by which the *mdm1* gene functions within the development of the eye. One approach would be to evaluate the gene and protein expression of Mdm1 in various known zebrafish eye mutants, such as *cyclops, chokh* and *pax6*, which are used in studying eye development and diseases. It was clear from our studies that *mdm1* plays a role in the proper development of the eye during early zebrafish development. The *wnt11* and *shh* gene families are well studied and known to be involved in the development of the eye in zebrafish. It may be possible that the Mdm1 protein functions within these pathways or is part of a protein complex that gives way to some of the known zebrafish eye mutant phenotypes.

Another experimental approach would be to work across species using the *arrd* (retinal degeneration) mice and try to rescue the phenotype with the zebrafish Mdm1. By doing so, it would show that the zebrafish model is useful for evaluating human/mammalian diseases and would also provide insight into the cause of this age-related eye disorder. Evaluating the functional role of this gene in zebrafish and the mechanism underlying eye development may reveal critical biological pathways that operate in maintaining the normal functioning of the eye, or future therapeutic targets for those affected by retinal degenerative disorders.

CHAPTER SIX

MATERIALS AND METHODS

Materials:

Tricaine-S (Tricaine Methanesulfonate) was obtained from Western Chemicals Inc. (Ferndale, WA) and was reconstituted in deionized water (1.5g/L) to make the 10X stock. CSPD (chemiluminescence substrate) and NitroBlock II were obtained from Roche and prepared as directed from the manufacturer. 1-phenyl-2-thiourea (PTU) was obtained from Sigma and stored as a 10mM solution in deionized water.

Buffers and Solutions:

Embryo bleach solution is 65µl/100ml bleach in aquarium water. Methylene blue solution is 0.0015M Methylene Blue in aquarium water. 10X Tricaine is 1.5g of Tricaine powder dissolved in 1 liter of distilled water. 10X Loading dye is 0.41% Bromophenol Blue, 50% Glycerol. Semi-quantitative RT-PCR wash buffer is 0.1M Maleic Acid, 0.15M NaCl, 0.3% Tween-20 pH 7.5. Semi-quantitative RT-PCR Detection buffer is 1M Tris pH 9.5, 1M NaCl. Denaturing solution is 1.5M NaCl, 0.5M NaOH. Neutralizing solution is 1M Tris pH 8.0, 1.5M NaCl. Low-stringency buffer is 2X SSC, 0.1% SDS. High-

stringency buffer is 0.5X SSC, 0.1% SDS. *In situ* Full Hybridization mix is 50% Formamide, 5X SSC, 0.1% Tween-20, 50µg/ml Heparin, 500µg/ml tRNA, adjusted to pH 6.0 with citric acid. *In situ* 1X blocking buffer is 1X PBT, 2% Sheep Serum, 2 mg/ml BSA. AP buffer is 1M Tris pH 9.5, 1M $MgCl_2$, 5M NaCl, 0.1% Tween-20. Stop solution is 1X PBT pH 5.5, 1mM EDTA. 1X Danieau solution is 58mM NaCl, 0.7mM KCl, 0.4mM $MgSO_4$, 0.6mM $Ca(NO_3)_2$, 5.0mM HEPES pH 7.6. Embryo lysis buffer is 10mM Tris pH 8.1, 1mM EDTA, 0.3% Tween-20, 0.3% NP-40. Ringer's solution is 116mM NaCl, 2.9mM KCl, 1.8mM $CaCl_2$, 5mM HEPES pH 7.2. Deyolking buffer is 55mM NaCl, 1.8mM KCl, 1.25mM $NaHCO_2$ pH7.5. Wash buffer for embryo lysate preparation is 110mM NaCl, 35mM KCl, 27mM $CaCl_2$, 10mM Tris pH8.5. SDS Sample buffer is 63mM Tris pH 6.8, 10% Glycerol, 2% SDS, 5% β-ME. 2X sample buffer for western blots is 125mM Tris, 4mM EDTA, 0.005% Bromophenol Blue, 4% SDS, 25% Glycerol. Tobin buffer is 192mM Glycine, 25mM Tris, 0.038% SDS, 20% MeOH. 1X PBS is 137mM NaCl, 27mM KCl, 4.3mM Na_2HPO_4, 1.47mM KH_2PO_4. TBST is 50mM Tris pH 7.5, 150mM NaCl 0.2% Tween-20. 1X assay buffer is 20mM Tris, 1mM $MgCl_2$. CSPD detection solution is 0.1M Diethanolamine, 1mM $MgCl_2$, 0.25mM CSPD, 5% NitroBlock II.

Zebrafish Husbandry

Fish are raised in a modular system consisting of 1-, 3-, and 10-liter overflow style tanks. Water conditions are maintained by the addition of sodium bicarbonate and instant ocean solutions to pure reverse osmosis (RO) water.

System water is also run through a variety of filters including biofilters, carbon, and ultraviolet (UV) light. The general conditions of the fish system water are pH between 6.8-7.2, conductivity of approximately 350mS and a temperature of 25-27^{o}C. Weekly tests are also performed on the system water to check for ammonia, nitrite and nitrate levels, and alkalinity. The facility itself has a timed overhead lighting system that allows for a 14-hour light, 10-hour dark cycle. Maintenance of the fish system is relatively easy and inexpensive when compared to other facilities housing mice, rats, rabbits and other model organisms. Due to the modularity of the system, it is very easy to change and clean tanks and maintain consistent water conditions.

Figure 6.1: Modular Fish System

Typically, larvae will be raised in small dishes in a 27^{o}C incubator until approximately 7 days post fertilization (dpf), when they can be placed in a larger tank and fed an algae diet. Over several weeks, the fish diet is gradually changed over to adult food, which includes live brine shrimp, flake food, and bloodworms, and the fish will be at breeding age within approximately six months

Primers:

Numerous oligonucleotide primers were generated (IDT) in order to obtain the results described in this report. The primers that were used are listed below by primer name, grouped by gene of interest.

Table 6.1: List of Primers for *gin-10*, *synbl* and *mdm1* projects**.**

Primer Name	Sequence	Project
BTB F1	5'- ACAGGAACCAGCAGTGCTCAAGTA -3'	*gin-10*
BTB F2	5'- TCTTCACCGCCTCCAACAGGTTTA -3'	*gin-10*
BTB F3	5'- ACAACAGCCTAGACACCGTCAACA -3'	*gin-10*
BTB R1	5'- TGAGCATTCGGAAACCCAGATCCT -3'	*gin-10*
BTB R2	5'- AGTTCGGGTGCCTCCAG AATTTA -3'	*gin-10*
BTB R3	5'- TACTTGAGCACTGCTGGTTCCTGT -3'	*gin-10*
cirh1a F1	5'- AATGGCAGCTGCGAAGATGAATGG -3'	*gin-10*
cirh1a F2	5'- ATGATGTTCGAGCTGTGGCTGAGA -3'	*gin-10*
cirh1a R1	5'- ATCTCAGCCACAGCTCGAACATCA -3'	*gin-10*
cirh1a R2	5'- TACTATCAGGCAGTGGCTGGCTTT -3'	*gin-10*
cry1b F1	5'- TGGAGATGCCAGCAGAGACAATCA -3'	*gin-10*
cry1b F2	5'- ATGTGGCTTTCGTGCAGCTCATTC -3'	*gin-10*
cry1b F3	5'- TTGCTTCCATGTTGTTGACGTGCG -3'	*gin-10*
cry1b R1	5'- AATGAGCTGCACGAAAGCCACATC -3'	*gin-10*
cry1b R2	5'- ACCACATGACACTGCAAATGCTGG -3'	*gin-10*
cry1b R3	5'- TCTGGCGAAGCGTTTGATTTAGCC -3'	*gin-10*
Hi2039A F1	5'- CCATCATCGCAGGCTAACTAAG -3'	*synbl*
Hi2039A R1	5'- ACCCGTGTATCCAATAAACCC -3'	*synbl*

liprin F1	5'- TCAGTCCTGGAACACATGCAGTCA -3'	*gin-10*
liprin F2	5'- ATTGAGGAGTTGCGGCAGTCACTA -3'	*gin-10*
liprin F3	5'- TGGGACTGTATGTGACTTTGGCGA -3'	*gin-10*
liprin R1	5'- TCGCCAAAGTCACATACAGTCCCA -3'	*gin-10*
liprin R3	5'- TGATGCCCTCAGAGAAAGCTCCAA -3'	*gin-10*
mapk12 F1	5' - CAGGCTGCTCAAACACATGAAGCA - 3'	*gin-10*
mapk12 F2	5' - TAGACGATCAGCCTGTTGTGTGCT - 3'	*gin-10*
mapk12 R1	5' - TCCAGGTGGTCGTGTCCTTTGAAT - 3'	*gin-10*
mapk12 R2	5' - GAATGCCTGCTGTGCCAGCTTTAT - 3'	*gin-10*
mdm 1 R8	5'- CCTCAGACGCCATGGAGCATGAAG -3'	*mdm1*
mdm1 F1	5' - TGCGCTCTGACCAGTCAGGAATTA - 3'	*mdm1*
mdm1 F10	5'- ACGCCTCACCA GGTAACAG -3'	*mdm1*
mdm1 F2	5' - ACACATCACGATCGAACCACTCCA -3'	*mdm1*
mdm1 F3	5'- AGAAGAAGAAGGAGCGACCACACA -3'	*mdm1*
mdm1 F8	5'- CTTCATGCTCCATGGCGTCTGAGG -3'	*mdm1*
mdm1 F9	5'- CCCTAGTCACTACCGGCGTA -3'	*mdm1*
mdm1 koz F1	5'- CTCGAGCTGAAAGCCGCCATGCCTGTCCGTTTCAAG -3'	*mdm1*
mdm1 koz F2	5'- CTGAAAGCCGCCATGCCTGTCCGTTTCAAG -3'	*mdm1*
mdm1 R1	5' - AAGGGTGGGATGGCTCTGTTGTTA -3'	*mdm1*
mdm1 R10	5'- ACGTTTCCTCGTGAGATCAGGCTT -3'	*mdm1*
mdm1 R2	5'- AATTCCGCGTTTCTCATTGTGCCC -3'	*mdm1*
mdm1 R3	5'- AATATGGCTTGTGCTTCTGCAGGC -3'	*mdm1*
mdm1 R9	5'- TTGCATAGTTGAAGTGTGCTTTGACAGATTAGC -3'	*mdm1*
mdm1-rHis1	5'-TTAATGATGATGATGATGATGTTGAGGAAGCACAAACAGCTC-3'	*mdm1*
mdm1-rHis2	5'-TTAATGATGATGATGATGATGTGAGGAAGCACAAACAGCTC -3'	*mdm1*
mdm1a F4	5'- TCTCCTAATCTGTTGACAAACCAAAGCAAG -3'	*mdm1*
mdm1a F5	5'- GCCTGCAGAAGCACAAGCCATATT -3'	*mdm1*
mdm1a F6	5'- TGCGCTCTGACCAGTCAGGAATTA -3'	*mdm1*
mdm1a F7	5'- CGGAGCTGTTTGTGCTTCCTCAAT -3'	*mdm1*
mdm1a R4	5'- ACCAACCCAATCTCACGGCAATTC -3'	*mdm1*
mdm1a R5	5'- AATATGGCTTGTGCTTCTGCAGGC -3'	*mdm1*
mdm1a R6	5'- AAGGTGGATGTCTGAGCTGCTTCT -3'	*mdm1*
mdm1a R7	5'- ACGTTTCCTCGTGAGATCAGGCTT -3'	*mdm1*
mdm1a R8	5'- CCATTTGTTGTCTATGCACAATACTGGTC -3'	*mdm1*
mdm2 F1	5'- CAACGGTCACCAGCAGATAA -3'	*mdm1*
mdm2 F3	5'- GATTCGCGCAACGGTCACCAGCAGATAACTACCAA -3'	*mdm1*
mdm2 F4	5'- TCTCGGTGCTGTTCTTGGAGTGAA -3'	*mdm1*

mdm2 F5	5'- TCGCACGTGCTGGAAGTGAACAAT -3'	*mdm1*
mdm2 F6	5'- ACGGTCACCAGCAGATAACTACCA -3'	*mdm1*
mdm2 koz F7	5'- CTACCAAAGCCGCCATGGCAACAGAGA -3'	*mdm1*
mdm2 koz F8	5'- CTCGAGCTACCAAAGCCGCCATGGCAACAGAGA -3'	*mdm1*
mdm2 R1	5'- AGTTTGGGAGTTGCCTTGTG -3'	*mdm1*
mdm2 R2	5'- TCAGTGCCTCAGCTCATGTAAGTC -3'	*mdm1*
mdm2 R3	5'- ACAACCACAAGGCAACTCCCAAACTTC -3'	*mdm1*
mdm2 R4	5'- TCCCGGGACAGAATCCACATCATT -3'	*mdm1*
mdm2 R5	5'- AGACAGTCTTCGCAGCCGAAAT -3'	*mdm1*
mdm2 R6	5'- ATCAATACAGCACCTCACAAGC -3'	*mdm1*
mdm2 R7	5'- CAGTGCCTCAGCTCATGTAAGTCA -3'	*mdm1*
mdm2 R7b	5'- GGTATATTTCAGTGCCTCAGCTCATGTAAGTC -3'	*mdm1*
mdm4 F1	5'- CACACACACGTCTCCCTTTC -3'	*mdm1*
mdm4 F2	5'- ACGTGACGACATACACCACGTCAA -3'	*mdm1*
mdm4 F4	5'- CTTTCAGGGTTGCCTTGGTGGTTT -3'	*mdm1*
mdm4 koz F5	5'- GAGTGAAAAGCCGCCATGACCTCATTGGCA -3'	*mdm1*
mdm4 koz F6	5'- CTCGAGGAGTGAAAAGCCGCCATGACCTCATTGGCA -3'	*mdm1*
mdm4 R1	5'- CTAGCCTCGCATTGATGGTT -3'	*mdm1*
mdm4 R2	5'- TCTTCCCACTCAGGCAGTAGCAAA -3'	*mdm1*
mdm4 R4	5'- CTGGGCAAGGAGCGTGAAATTTGT -3'	*mdm1*
mdm4 R5	5'- GATTTGTTGCTCATGCAATGAAGGT -3'	*mdm1*
mdm4 R5b	5'- AGATTTGTTGCTCATGCAATGAAGGTTTTGATGA -3'	*mdm1*
p53 F1	5'- GGCAATCCGAAAGTCGATAA -3'	*mdm1*
p53 F1b	5'- TCCGGGCAATCCGAAAGTCGATAA -3'	*mdm1*
p53 koz F2	5'- GCAAAGCAGCCGCCATGGCGCAAAACGA -3'	*mdm1*
p53 R1	5'- GCTCTTTTTGGACTGCCTTTT -3'	*mdm1*
p53 R2	5'- GCACAGTTGTCCATTCAGCACCAA -3'	*mdm1*
p53 R3	5'- ATCGGCTTGCAACCAATTCCGATG -3'	*mdm1*
p53 R4	5'- ACAAAGGTCCCAGTGGAGTGAACA -3'	*mdm1*
p53 R5	5'- GCATCCCATCACCTTAATCAGAGTCGCT -3'	*mdm1*
p53 R5b	5'- TAGCATCCCATCACCTTAATCAGAGTCGCTTCTTCC -3'	*mdm1*
pME F1	5'- CATTGTGCTGGCGCGGATTCTTTA -3'	*mdm1*
pME F2	5'- TTGCAGCCGAATACAGTGATCCGT -3'	*mdm1*
pME F3	5'- GGATCCGGTGGTGCAAATCAAAGA -3'	*mdm1*
pME F4	5'- TGTTCTGCGCCGTTACAGATCCAA -3'	*mdm1*
pME R1	5'- AGCGAGGAAGCGGAAGAGGAATTA -3'	*mdm1*
pME R3	5'- TTATAGTCCTGTCGGGTTTCGCCA -3'	*mdm1*
PS20 F1	5'- AAGAAGGACGGTCAGGCTGAATGA -3'	*gin-10*
PS20 F2	5'- ACCGAGGACAGTGCATCAAACAGA -3'	*gin-10*

PS20 R1	5'- TGGGTTGATGATGTGGCACTCGTA -3'	*gin-10*
PS20 R2	5'- AATAGTTGGCGGTTCATTCCGCTG -3'	*gin-10*
PS20b F3	5'- TACGAGTGCCACATCATCAACCCA -3'	*gin-10*
PS20b R3	5'- AATGCGGTCACCAACAGAAACTGG -3'	*gin-10*
ptn F1	5'- TGCATTCAGTCTGTCGCTCTCACA -3'	*in situ* control
ptn F2	5'- ACCACAGGAATGAAGACTCGCACT -3'	*in situ* control
ptn R1	5'- AGTGCGAGTCTTCATTCCTGTGGT -3'	*in situ* control
ptn R2	5'- ACAGCAGCCTCTGGTGGATTTACA -3'	*in situ* control
rfx4 F5	5' - TGATGCTGATGAGCTCCACTCCAA - 3'	*gin-10*
rfx4 F6	5' - TGGCTCGTTTCATCTGATTCACCT - 3'	*gin-10*
rfx4 F7	5' - ACTGGATACTGTCATACGCGCCAA - 3'	*gin-10*
rfx4 R10	5'- AGGTGATGTCTGCACTGTGGATCA -3'	*gin-10*
rfx4 R11	5'- CAGCTGCTTGGCAAACTTCCTGAT -3'	*gin-10*
rfx4 R13	5'- TGCTCGTATTCAGAGTTCCTGCGT -3'	*gin-10*
rfx4 R5	5' - AGTTTACCCACATCGGGATGAGCA - 3'	*gin-10*
rfx4 R6	5' - TGATCCACAGTGCAGACATCACCT - 3'	*gin-10*
rfx4 R9	5'- TGCTCATCCCGATGTGGGTAAACT -3'	*gin-10*
ric8a F1	5'- GTTTGATTCCAACCGACGCCATGT -3'	*synbl*
ric8a F2	5'- ACAGAGAGGCCAAACCACACATCA -3'	*synbl*
ric8a F3	5'- TTCTGGATCGCCCAGATAAAGCCA -3'	*synbl*
ric8a R1	5'- TCTCCATGAACTCCACCAGCACTT -3'	*synbl*
ric8a R2	5'- ATTGGACTCTCCGAACTGTTGGCT -3'	*synbl*
ric8a R3	5'- TGATCAGGAACGTAAGGCGCAGAT -3'	*synbl*
Rp11 F2	5'- TCTGGACAGGCTGAAGGTGTTTGA -3'	*in situ control*
Rp11 F3	5'- TTTCCGCTATTGTGGCCAAGCAAG -3'	*in situ control*
Rp11 R2	5'- GTGGATGCAGCCTTTATGACGCAA -3'	*in situ control*
Rp11 R3	5'- ACAATCTTGAGAGCAGCTGGGACA -3'	*in situ control*
RPB5 F1	5'- ACGAGGCGACAAATTGAGTGCAAC -3'	*gin-10*
RPB5 F2	5'- ATGGTGGCAGTGATGTCCAGGTTA -3'	*gin-10*
RPB5 R1	5'- GGCATGAAAGCCAAGGGACCAAAT -3'	*gin-10*
RPB5 R2	5'- TTGGTTCTCCATTCACCAGGTCCA -3'	*gin-10*
rpc2 F1	5'- GCGCAAACTTCCGTTCTGAGTGTT -3'	*gin-10*
rpc2 F2	5'- TTACTTTAGCAGGACTTGCCCGGA -3'	*gin-10*
rpc2 F3	5'- TGATGCCGACCCAATGTGGTATCT -3'	*gin-10*
rpc2 F4	5'- TCGCTGTAATGGTTCGCAGAGTGA -3'	*gin-10*
rpc2 F5	5'- TGAATAAGTCCATGCCCACCGTCA -3'	*gin-10*
rpc2 R1	5'- TCACTCTGCGAACCATTACAGCGA -3'	*gin-10*

rpc2 R3	5'- ACTTCTCTGTATTGTGGCTGGCCT -3'	*gin-10*
rpc2 R4	5'- TCCTGAATATCCCAGCAAGCCACA -3'	*gin-10*
rpc2 R5	5'- GCTTCGCAGCATTATTGGCATCCT -3'	*gin-10*
rpc2 R6	5'- ACATCGGTCAGTCAGGTTGGTTGA -3'	*gin-10*
rpc2 R7	5'- CAGTTTGAGGCGAGGGATGATGTT -3'	*gin-10*
Zrpc2 F2	5'- TCAACCAACCTGACTGACCGATGT -3'	*gin-10*
Zrpc2 F6	5'- AGGCCAGCCACAATACAGAGAAGT -3'	*gin-10*
Zrpc2 R2	5'- TGATCTGGTCCTGCCTCATGTGTT -3'	*gin-10*
Sir2 F1	5'- TGTGGTAGTTGCTGGAGCAGGAAT -3'	*gin-10*
Sir2 F2	5'- TTTGACGGTCTTCCCTTCATCCCT -3'	*gin-10*
Sir2 F3	5'- CAGCAGTCCTCATTGGCTGTTGAT -3'	*gin-10*
sir2 F4	5'- GTGTCGTGATGAGCAAGGCGAGGTTGAGCAG -3'	*gin-10*
Sir2 R1	5'- CAAGCTGGCAAAGGGCTCAATCTT -3'	*gin-10*
Sir2 R2	5'- TGCTGATTCCTGCTCCAGCAACTA -3'	*gin-10*
Sir2 R3	5'- ATGGCTGTTCATCAGGGTCTGGAT -3'	*gin-10*
Sir2 R4	5'- AGTCTTCCTGCAGACAGCCTCAAT -3'	*gin-10*
sir2 R5	5'- TCTCCGCTGTTCTCACCACTGCTGCTGATGTATG -3'	*gin-10*
synbl F1	5'- AAGAATTTGGCCTCCGTCCAGGTA -3'	*synbl*
synbl F10	5'- AGCAGAGTCCCTTGCTGTCTTCAA -3'	*synbl*
synbl F11	5'- TCTCTGCCTGCCTGTCAGACATTT -3'	*synbl*
synbl F12	5'- CGGATGCAACTGCAAGAGGGTTTA -3'	*synbl*
synbl F13	5'- GAAGCGAGAAGCGAACTGATTGGT -3'	*synbl*
synbl F14	5'- AGCTGTTCCATCTGTTCCTGACCT -3'	*synbl*
synbl F2	5'- TTACTTTAGCAGGACTTGCCCGGA -3'	*synbl*
synbl F3	5'- CATTTGGTCAGCGCGTCACATCAT -3'	*synbl*
synbl F4	5'- TGACACCTGTGCTGAGTCTGTTGA -3'	*synbl*
synbl F5	5'- TGAAGCCCAGAGGCTTGTCAGTAT -3'	*synbl*
synbl F6	5'- GACAGTGTTTCTAAGTGGACGGCA -3'	*synbl*
synbl F7	5'- TGAAGCCCAGAGGCTTGTCAGTAT -3'	*synbl*
synbl F8	5'- GACAATTTCCCTCCATGCACCGTT -3'	*synbl*
synbl F9	5'- TTCCCGAACTCCCAAATCTTCCCA -3'	*synbl*
synbl R1	5'- GATGCCTGCAATCAGCCGAAGTTT -3'	*synbl*
synbl R12	5'- GTATGCACAGATTCCATGTGGACC -3'	*synbl*
synbl R13	5'- CTGTTCCTACAGGAATAACTTGGGT -3'	*synbl*
synbl R14	5'- GACTTTCCAAGGAACATGGTTTCA -3'	*synbl*
synbl R2	5'- CACAGAGTGCCACAAACACACGTT -3'	*synbl*
synbl R3	5'- ATGATGTGACGCGCTGACCAAATG -3'	*synbl*
synbl R4	5'- TAAAGGTGCCAGAGTCCCGTCTTT -3'	*synbl*
synbl R5	5'- TAGCCAACGGCTAACTCGCTAACA -3'	*synbl*
synbl R6	5'- ACCTGGACGGAGGCCAAATTCTTA -3'	*synbl*
synbl R7	5'- ACACTGTCAGTCCTTCTGCACACA -3'	*synbl*

synbl R8	5'- ATGGAACCCTGAGGCGACGTTTAT -3'	*synbl*
synbl R9	5'- TTGTAGCCGGTCAACCAGCAAATG -3'	*synbl*
synbl sh F1	5'- AGAGCGATTGTGTGTTCAGTTGAGTCAT -3'	*synbl*
synbl.sh R1	5'- AGGAGGAGGTGTCTGTTAGGTTGT -3'	*synbl*
zActin F1	5'- TTGGCATGGGACAGAAAGACTCCT -3'	*control*
zActin F2	5'- TCACACCTTCTACAACGAGCTGCG -3'	*control*
zActin F3	5'- CACCACGGCCGAAAGAGAAATTGT -3'	*control*
zActin F4	5'- TTGCGGTATCCATGAGACCACCTT -3'	*control*
zActin R1	5'- ACTCCTGCTTGCTGATCCACATCT -3'	*control*
zActin R2	5'- GAAGCTGTAGCCTCTCTCGGTCAG -3'	*control*
zActin R3	5'- AAATGCATGGCAAGGAACTCACCC -3'	*control*
zActin R4	5'- TACCTCCCTTTCCAGTTTCCGCAT -3'	*control*

Antibodies:

Polyclonal rabbit antibodies against zebrafish p53 and mdm2 were purchased from Anaspec (Freemont, CA). Polyclonal rabbit antibody against zebrafish β-actin was purchased from Cell Signaling Technologies. Polyclonal Goat Anti-Rabbit Alkaline Phosphatase Conjugated antibodies were purchased from both Anaspec and Southern Biotech (Birmingham, AL). Streptavidin Alkaline Phosphatase Conjugated antibody was purchased from Thermo Scientific as a ready-to-use solution. Digoxigenin Alkaline Phosphatase antibody was purchased from Roche.

Embryo Collection for RNA:

Embryos were collected from breeding tanks and brought over to the lab in system water. They were then transferred into a glass bowl and washed using embryo bleach solution, rinsed several times in aquarium water then stored in Methylene Blue solution. Developing embryos were sorted into new petri dishes

(100 embryos per dish) and allowed to develop at approximately 27^{o}C in an incubator until appropriate age was reached. Embryos were collected in aliquots of 50 per 1.5ml tube. Aquarium water was removed using a pulled glass pipette and 1ml of 10X Tricaine was added to each tube on ice and allowed to incubate 10-15 minutes. The tricaine was then removed using a pulled glass pipette and 300µl of RNA Later was added to each tube and the embryos were stored at -80^{o}C.

RT-PCR Recipe and PCR Machine Program:

After RNA was isolated from the frozen embryos, it was quantified using a spectrophotometer (A_{260}) and a 1µg/µl dilution was made. The RT-PCR recipe is based on the recommended recipe from Invitrogen, but modified for a 20µl reaction:

Table 6.2: Standard RT-PCR Recipe

Component	Volume µl
RNA (1µg)	1
PCR Water	7.24
2X Buffer	10
Forward Primer (20µM)	0.68
Reverse Primer (20µM)	0.68
Platinum Taq	0.4
Total	**20µl**

Table 6.3: RT-PCR Program

	Temperature	Time
Reverse Transcription	50	30 minutes
Pre-Denaturation	94	2 minutes
Denature	94	45 seconds
Anneal	55 (varied slightly based on primer T_m)	45 seconds
Extension	72	1 minute 30 seconds
Repeat 35 Cycles		
Final Extension	72	10 minutes
Hold	4	--

Once finished, 2.3µl of 10X loading dye was added to each PCR tube and the products were run on an agarose gel (0.7-2.5% depending on the expected size of the fragment). All gels were photographed and recorded by date and PCR number. Primers that gave a robust band on the initial gel were repeated with 24-hpf and 72-hpf RNA and run on a 0.7-1% low-melting temperature agarose gel for extraction. The bands were purified using Qiagen's MinElute PCR purification kit and stored at -20^{o}C for several days or used immediately.

TOPO TA Cloning with pCR4 and Top10 Cells:

Cloning fragments of candidate genes was done using RT-PCR and TOPO TA Cloning kit (Invitrogen). Purified PCR product was ligated into pCR4 (sequencing) vector at room temperature for 30 minutes. The ligated plasmid was then transformed into chemically competent Top 10 *E.coli* cells on ice for 30 minutes; the cells were heat shocked for 30 seconds at 42^{o}C and placed immediately on ice. SOC medium was added to the cells and they were shaken at 37^{o}C for 1 hour prior to plating on either ampicillin or carbenicillin plates, which

were then incubated at 37^{o}C overnight. The plates were removed from the incubator, checked for colony growth, sealed in parafilm, and stored at 4^{o}C.

Sequencing Preparation:

In order to sequence the candidate gene, plasmid DNA was isolated from the *E. coli* cells using Qiagen's miniprep kit and the insert was verified by an EcoRI digest. The EcoRI digest was performed because there are restriction sites flanking the insert region in the pCR4 vector. So far, there have not been any issues with digest sites within the inserts themselves, and this remains the best way to determine if there is an appropriate insert in the plasmid prior to sequencing. Once the digests were analyzed, the plasmid DNA was quantified by spectrophotometry and dilutions of 5ng/µl were made and sent to Macrogen Inc.

Sequencing Analysis:

Sequences were downloaded from the Macrogen website and analyzed using the Geneious software program (Biomatters, Ltd.). Primers used for sequencing and any internal primers were identified, sequences assembled, and consensus sequences verified by NIH BLAST analysis.

DNA Probe Synthesis for Semi-quantitative RT-PCR:

DNA probes for semi-quantitative expression analysis were made using the DIG High Prime Labeling Kit from Roche. Plasmid DNA was linearized using

a restriction enzyme that did not cut the insert itself, usually SpeI, NotI, or PstI based on the vector map. The digest was performed for 3-4 hours and the product was run on a 1% low-melting temperature agarose gel for 90 minutes, photographed, extracted, and purified using Qiagen's MinElute Kit. The plasmid DNA was quantified by spectrophotometry before DIG labeling.

Only 1µg of linearized plasmid (up to 16µl) was needed for the probe and was denatured in a boiling water bath for 10 minutes prior to labeling. DIG-High Prime was added to the denatured DNA mixed briefly and collected at the bottom of the tube by centrifugation and incubated overnight at 37^{o}C according to the Roche Protocol. The reaction was stopped the next day by adding 0.2M EDTA to the tube and heating to 65^{o}C for 10 minutes.

Labeling efficiency of the probe was determined before using in a semi-quantitative experiment. A series of probe dilutions was made from 1ng/µl to 0.01pg/µl in supplied dilution buffer. A 1µl spot of each dilution was placed on a positively charged nylon membrane and allowed to air dry. The membrane was UV cross-linked then placed into a small container of Maleic Acid Buffer and incubated for 2 minutes. The membrane was then placed in blocking solution for 30 minutes at room temperature. Once blocked, the membrane was placed in a 1:10,000 anti-DIG antibody solution for 30 minutes at room temperature. The membrane was then transferred to a dish containing wash buffer and incubated with agitation twice for 15 minutes. The Wash Buffer was poured off and Detection Buffer was added to the membrane for 5 minutes. The membrane was then placed on a piece of clear transparency film and covered with 1 ml of CSPD

for 5 minutes. A second piece of transparency film was placed on top of the membrane and it was exposed to x-ray film for several minutes. The probes that worked at the 0.1pg/µl dilution well were used for semi-quantitative analysis.

Semi-quantitative RT-PCR:

To further assess the expression of candidate genes in wildtype embryos, semi-quantitative RT-PCR analysis was performed. The number of PCR cycles varied between 15 and 21 for each of the candidate genes; this was tested by using two different time points of embryo RNA (usually 24-hpf and 72-hpf) in a normal 20µl RT-PCR reaction with primers specific to a particular candidate gene and varying the number of cycles for each set. Once all of the reactions were complete, the products were loaded onto an agarose gel and run for 90 minutes. If bands were present on the gel with Ethidium Bromide staining then the reactions were repeated and the number of PCR cycles were decreased until bands were faint and difficult to see on the gel. Once the appropriate number of cycles was determined for each candidate, an RT-PCR developmental profile was performed using primers for the candidate gene that only amplified a single band and was approximately 500-1000 base pairs.

Gels were run for 90 minutes at 80 Volts and placed on the transilluminator to verify faint or no bands and photographed. The wells were removed from the gel and the top left corner was notched for directionality. Gels were placed in Denaturing Solution on a rocker for 30 minutes, rinsed briefly with sterile deionized water, then washed in Denaturing Solution for another 30

minutes. The Denaturing Solution was discarded and the gel was placed in Neutralizing Solution for 30 minutes on a rocker, rinsed briefly with sterile deionized water and washed with Neutralizing Solution for another 30 minutes. While the gel was in the last wash, the blot transfer stack was prepared by soaking a positively charged nylon membrane (Roche) and two pieces of Whatman paper in 2X SSC, and a long piece of Whatman paper in 20X SSC. The transfer set-up was made by placing a large pipette tip box lid in a glass baking dish and placing a piece of glass on top of the lid to create a platform. The long piece of Whatman paper was laid across the glass creating a bridge; 20X SSC was then poured onto the platform and halfway up the baking so that both ends of the Whatman paper were submerged. The two smaller pieces of Whatman paper that had been soaking were placed onto the center of the platform and air bubbles were removed prior to the next step. Once the gel was ready, it was placed facedown onto the Whatman paper. The membrane was placed directly on top of the gel. A glass pipette was rolled across the membrane to remove any air bubbles between it and the gel at this point. Two more pieces of Whatman paper was placed on top of the membrane, and then approximately 3-4 inches of cut paper towels were stacked on top. The stack was finished by placing another piece of glass on top of the paper towels, covering with saran wrap to keep it in place and adding a weight (two heating block inserts). Another piece of saran wrap was added to keep the weight centered on the stack, and it was allowed to sit over night, approximately 20 hours.

Once the transfer was complete, the stack was carefully disassembled and the membrane was labeled with pencil and washed in 5X SSC with agitation for 5 minutes. The membrane was then air dried for several minutes and was UV cross-linked (1200J) and stored between two pieces of clean Whatman paper until hybridization. The hybridization temperature was determined by calculating the T_m and T_{opt} for the probe being used. The membrane was then soaked in 5X SSC and placed in a glass hybridization tube with 10ml of warm hybridization solution. The tube was tightly capped and placed in the pre-warmed hybridization oven for 1-2 hours. When pre-hybridization was almost complete, the probe was denatured by placing it in a 15ml conical tube and boiling the probe for 5 minutes then placing the probe on ice for 1-2 minutes. The pre-hybridization solution was removed from the glass tube and the denatured probe was added (approximately 10 ml). Blots were hybridized overnight and the total hybridization time was recorded.

$$T_m = 49.82 + 0.41(\%\ G + C) - (600/\text{Length of Probe})$$

$T_{opt.}$ = Range of Temperatures that the hybridization can occur:
$T_m - 25$ (Low-End Temp), $T_m - 20$ (High-End Temp)

Figure 6.2: Calculation of Hybridization Temperature for each Probe. Melting temperature of the probe was calculated then a range of hybridization temperatures was determined by the formulas above.

Following hybridization, the probe was poured back into a 15ml conical tube and stored at -20^{o}C for future use. The blot was briefly washed in a low-stringency buffer at 68^{o}C. The buffer was removed and replaced with fresh low-

stringency buffer and washed with agitation at 68°C for 5 minutes; this step was repeated twice. Once the low-stringency washes were complete, the membrane was washed twice in high-stringency buffer at 68°C with agitation. The membrane was then placed in a Wash Buffer at room temperature for 5 minutes with agitation.

The membrane was placed in a shallow dish containing 50ml of Roche 1X Blocking Buffer and allowed to incubate with agitation for 1 hour. Once the membrane was blocked, it was placed in a 1:10,000 anti-DIG antibody solution and incubated for 1 hour at room temperature. To remove the excess antibody, the membrane was rinsed with Wash Buffer briefly then incubated in fresh Wash Buffer at room temperature twice for 15 minutes. The Wash Buffer was removed and the membrane was soaked in detection buffer for 5 minutes. The membrane was placed on a clean piece of Whatman paper to remove excess Detection Buffer, then immediately transferred onto a piece of clear transparency film. Approximately 1-2ml of CSPD was pipetted onto the membrane then a second piece of clear transparency film was placed on top of the membrane spreading out the CSPD. The membrane was incubated at 37°C for 10-15 minutes to activate the CSPD and exposed to x-ray film.

Embryo Collection for *In Situ* Hybridization Experiments:

Embryos were collected from breeding tanks and brought over to the lab in system water. They were then transferred into a glass bowl and washed using an embryo bleach solution, rinsed several times in aquarium water then stored in

a 0.003% PTU solution, which inhibits pigment formation. Developing embryos were sorted into new petri dishes (100 embryos per dish) and allowed to develop at approximately 27^{o}C in an incubator until appropriate age was reached. Embryos were collected in aliquots of 50 per 1.5ml tube. Aquarium water was removed using a pulled glass pipette and 1ml of 10X Tricaine was added to each tube on ice and allowed to incubate 10-15 minutes. The tricaine was then removed using a pulled glass pipette and 300µl of 4% PFA in PBS was added to each tube and stored at 4^{o}C overnight.

The next day, the PFA was removed and the embryos were washed several times in 1X PBS with agitation (until all of the PFA was removed, usually 3-4 washes). Embryos were then manually dechorionated in 1X PBS on an agar-coated plate if needed and dehydrated by washing in increasing MeOH in PBS solution (25% MeOH, 50% MeOH, 75% MeOH and 100% MeOH). Embryos were stored in 100% MeOH at -20^{o}C.

RNA Probe Synthesis for *In Situ* Hybridization Experiments:

DIG-labeled RNA probes were used for *in situ* hybridization experiments in zebrafish embryos. Plasmids containing the appropriate gene fragment (approximately 600-800bp) were linearized by restriction digest, either NotI or SpeI depending on the orientation of the insert in the plasmid. The digest ran approximately 3-4 hours and the product was run on a 1% low-melting temperature agarose gel for 90 minutes, extracted, and purified using Qiagen's

MinElute kit. The linearized plasmid was quantified by spectrophotometry prior to the transcription reaction.

Ambion's MAXIScript Transcription reaction kit was used to prepare RNA Probes for *in situs* with 1µg of the linearized plasmid DNA. The transcription reaction using a DIG-labeled UTP and either T3 or T7 enzyme was prepared depending on the orientation of the fragment in the plasmid. The transcription reaction was incubated at 37^{o}C for 1 hour then Turbo DNase (from kit) was added to the reaction and incubated at 37^{o}C for an additional 15 minutes. The reaction was stopped by the addition of 0.5M EDTA followed by purification of the reaction using NucAway Spin Columns. Probes were stored at -20^{o}C.

Whole Mount *In Situ* Hybridization:

Since the purpose of this experiment was to see spatial expression of candidate gene transcripts in whole embryos, it was essential to properly and carefully handle the embryos that were extremely fragile at this point. Embryos were removed from the freezer, thawed on ice, placed in 6-well culture dishes according to age, and rehydrated in PBT with increasing MeOH solution (25% PBT, 50% PBT, 75% PBT and 100% PBT). The embryos were washed in 100% PBT several times with gentle swirling at room temperature then treated with Proteinase K diluted in PBT at room temperature.

Table 6.4: Proteinase K treatment of zebrafish embryos for *in situ hybridization* experiments (From Thisse & Thisse 2008).

Developmental Stage	Duration of Proteinase K Treatment
1 cell – 1 somite stage	30 seconds
1-8 somite stage	1 minute
9-18 somite stage	3 minutes
18 somite – 24hpf	10 minutes
24hpf – 7dpf	30 minutes

The Proteinase K was removed from the embryos and a second PFA fix at room temperature was done. The PFA was removed and the embryos were washed in 100% PBT several times with gentle swirling to prepare embryos for pre-hybridization. The PBT was removed and the embryos were incubated in Full hybridization mix at 65^{o}C for 5 hours without rocking. Prior to hybridization, the RNA probe was boiled for 10 minutes and placed on ice. The probe was added to each well of embryos, they were gently swirled for several seconds and incubated for 1-2 days in a 65^{o}C oven.

The probe was removed and stored at -80^{o}C for future use. Embryos were briefly washed in Full hybridization mix, then in a hybridization mix that did not contain tRNA or heparin. Embryos continued to be washed in an increasing 2X SSC solution (25% 2X SSC, 50% 2X SSC, 75% 2X SSC and 100% 2X SSC). The 2X SSC solution was removed from the embryos and they were washed twice in a 0.2X SSC with 0.01% Tween-20 solution for 30 minutes. The embryos were then washed in increasing PBT in 0.2X SSC solutions (25% PBT, 50% PBT, 75% PBT and 100% PBT) in preparation for blocking.

The PBT was removed from the wells and the embryos were incubated at room temperature in 1X blocking buffer for 4 hours. A 1:10,000 anti-DIG

antibody solution was made in 1X blocking buffer; the blocking buffer was removed from the embryos and the antibody was added and incubated at 4^{o}C with gentle rocking overnight.

The following day, the antibody solution was removed and the embryos were washed several times with PBT at room temperature. The PBT was removed and the embryos were allowed to briefly dry in the wells to reduce the formation of precipitate in the wells. Embryos were washed several times in AP buffer at room temperature. BM Purple was used to stain the embryos; the AP buffer was removed and fresh AP buffer added to each well. The BM Purple was briefly centrifuged and added to each well, the entire dish was covered in foil and placed in a drawer until color developed. The color development was stopped by removing the BM Purple solution and adding fresh Stop Solution, incubating for 15 minutes at room temperature, and repeating this process. Embryos were stored in Stop solution at 4^{o}C or cleared in glycerol and photographed.

Fish Breeding for Injections:

Adult fish (1-2 females with 1 male) were placed in a breeding tank containing a divider the evening prior to injections. The next morning, the dividers were pulled out of the tanks and the fish were allowed to breed. As soon as the females laid eggs, the divider was replaced and the eggs were collected into a small plastic container and transported to the microinjection room. Dividers were subsequently re-pulled and replaced until the fish stopped

breeding for that day. Females were given a minimum of two weeks rest between injection experiments while the males were bred every 1-2 weeks.

Morpholino Injections:

Custom MOs were designed to the 5' UTR and early coding sequence of the specific candidate genes in order to block translation. The morpholino powder was first resuspended in 1X Danieau solution to a concentration of 1mM stock MO. Once the stock solution was prepared, MOs were diluted in 1% phenol red and 1X Danieau at various concentrations. Prior to injections, the MOs were heated to 65^{o}C for 10 minutes, vortexed, and briefly centrifuged so that any precipitate that may have formed was at the bottom of the tube. Approximately 10µl of MO was loaded into a 1.2mm pulled glass capillary tube containing filament using a gel-loading tip. The needle was placed in a vertical mount (beaker with a mound of clay along the edge) until the MO solution migrated to the tip of the needle. It was then placed in the micromanipulator and the tip was broken using forceps in aquarium water.

Embryos were brought over from the fishroom and were immediately transferred into glass bowls containing 0.0015M MeBlue in aquarium water. Embryos were briefly observed under dissecting microscope to make sure that they were all less than 8-cell stage and approximately all the same age for consistency. 100 embryos were transferred to an area of a large petri dish lid containing MeBlue water placed on the dissecting scope with a black background. Embryos were held with a pair of forceps while the needle was

carefully extended through the chorion and into the yolk just below the developing cell(s). The MO solution was released using a remote foot pedal (pressure and volume settings were adjusted based on the needle) and a red spot was seen in the yolk once the solution was injected. Embryos were transferred to a new petri dish containing MeBlue water and allowed to develop in a 27^{o}C incubator.

Figure 6.3: Morpholino Injection set up.

Screening Morphants:

Although mosaicism can be seen at 48-72hpf, the morphant embryos were screened daily for any obvious phenotypic changes. Any dead or decayed embryo (which is often seen since it is difficult to differentiate 1-cell embryos from water-activated eggs at the time of injection) were removed from the dishes and recorded. The MeBlue water was also changed daily to keep the embryos as clean as possible.

At 48-72hpf, embryos were placed in 2X Tricaine and viewed under the dissecting scope. Embryos were scored for mosaicism and any developmental

abnormalities observed; the embryos were then grouped together by phenotype and placed into a 6-well culture dish. Groups and/or single embryos were photographed then collected into either 4% PFA in PBS or RNA Later for future use.

Fin Clipping Adult Zebrafish:

Adult fish were placed in a 1X Tricaine solution until anesthetized. Each fish was then removed from the solution, briefly blotted on a paper towel and placed on a small cutting board. Using a scalpel, a small portion of the lower tail fin was cut and placed in a 0.5ml thin-walled tube containing 50µl of embryo lysis buffer on ice. The fish was promptly placed in a 1L tank and swirled around until it began swimming on its own.

Genomic DNA Preps from Fin Clips:

After the fin clips were obtained, the 0.5ml tubes were incubated at 98^{o}C for 10 minutes. Then 5µl of Proteinase K (10mg/ml) was added to each tube; they were briefly vortexed, centrifuged, and then placed in a 55^{o}C incubator overnight. The next day, the tubes were vortexed and re-centrifuged, and an additional 45µl of lysis buffer and 5µl of Proteinase K were added to each tube. Tubes were spun down and incubated at 55^{o}C overnight. The DNA was then stored at -20^{o}C.

Genomic DNA PCR:

Before PCR was performed on the genomic samples, they were diluted 1:20 with Nuclease-free water and incubated at 98^{o}C to inactivate the Proteinase K. The PCR recipe is based on the recommended usage from Takara, but modified for a 20µl reaction.

Table 6.5: Genomic DNA PCR recipe used to amplify a portion of the transgenic insert and flanking genomic DNA in ZIRC fish**.**

Component	Volume (µl)
Diluted DNA	2.4
PCR Water	11.8
Takara 10X Buffer	2
Takara dNTPs	1.6
Forward Primer	1
Reverse Primer	1
Takara Taq	0.2
Total	**20µl**

A standard 35-cycle PCR program was used to amplify fragments from genomic DNA. Once finished, 2.3µl of 10X loading dye was added to each sample, and the products were run on an agarose gel.

Embryo Collection and Lysate Preparation for Western Blot Analysis:

Embryos were collected from breeding tanks and brought over to the lab in system water. They were then transferred into a glass bowl and washed using an embryo bleach solution, rinsed several times in aquarium water then stored in Methylene Blue solution. Developing embryos were sorted into new petri dishes (100 embryos per dish) and allowed to develop at approximately 27^{o} C in an incubator until appropriate age was reached. Embryos were dechorionated manually using #5 Forceps in a 10X Tricaine solution. Embryos remained in the

10X Tricaine on ice for 10-15 minutes, and then were transferred to a 1.5ml tube. While on ice, the Tricaine was removed using a pulled glass pipette and 1ml of cold Ringer's Solution was added to the tube. The embryos were gently rocked for 2 minutes to wash and the Ringer's Solution was removed with the glass pipette. 1ml of Deyolking Buffer was then added to the tube and the embryos were shaken for 5 minutes at 1100rpm. The embryos were centrifuged at 300 x g for 30 seconds and the supernatant was discarded. A wash buffer was then added to the embryos, shaken for 2 minutes at 1100rpm, and centrifuged to pellet the embryos. The supernatant was discarded and embryos were centrifuged again in order to remove any excess liquid that remained in the tube. Once the excess liquid was removed, 200µl of SDS Sample Buffer was added to the tube. The embryos were homogenized with a pestle and power homogenizer. The sample was then boiled for 5 minutes then centrifuged at high speed for 2 minutes. The supernatant was transferred to a new tube and stored at -20^{o}C (Link *et al.* 2006, O'Shea 1993).

Western Blot Analysis of Zebrafish Embryo Lysate:

Embryo lysates were diluted in 2X Cracking Buffer for a total volume of 15µl and incubated at 95^{o}C for 5 minutes. The samples were then loaded onto a 10% SDS-Polyacrylamide gel and run at 180 Volts for approximately 45-50 minutes. Once the gel was finished, the blocking stack was assembled in a shallow dish containing Tobin Buffer by placing two pieces of thick Whatman paper on the bottom of the dish then the gel was carefully placed on top of the

blotting paper. The nitrocellulose membrane was hydrated in a shallow dish containing deionized water then placed on top of the gel. Finally two more pieces of thick blotting paper was placed on top of the membrane to complete the stack. The stack was then removed from the dish and flipped over (membrane side down) and placed in a Hoefer Scientific Blotter; the blotter was run at 110mAmps for 1 hour. Once the gel transfer was complete, the membrane was stained with 0.1% Ponceau S to verify the protein transfer. Stained membranes were also scanned or photographed for documentation. The membrane was then rinsed several times in 1X PBS then blocked in 5% Nonfat Milk in TBST overnight at 4^{o}C. The membrane was then brought up to room temperature in the blocking solution prior to the addition of antibody. The primary antibody was diluted in blocking solution (1:500 – 1:4000 depending on the antibody), and the membrane was incubated in primary antibody for 1-2 hours at room temperature. The membrane was then washed several times in TBST then incubated for 1 hour at room temperature in AP-Conjugated secondary antibody (1:3000 dilution) in blocking solution. Prior to detection with CSPD, the blot was washed several times in TBST then in 1X Assay buffer. The membrane was placed on a piece of transparency film on a flat surface, and 1-2ml of CSPD detection solution was pipetted on and allowed to incubate for 5 minutes. A second piece of transparency film was then placed on top of the membrane and exposed to x-ray film.

***In Vitro* Expression of Protein:**

Recombinant protein was produced from full-length clones in the pCMVTnT expression vector (Promega) using the TnT Coupled Reticulocyte Lysate System as detailed by the manufacturer (Promega). Upon completion of the 90-minute TnT reaction, a portion of the sample was combined with an equal volume of 2X cracking buffer and boiled for 5 minutes for western blotting; the remaining sample was stored at -80^{o}C for future use.

Whole-mount Antibody Staining of Morpholino Injected Embryos

Following the morpholino injections, embryos were placed in cold 2X Tricaine-S solution in petri dishes and dechorionated with forceps. The embryos were then rinsed four times in cold 1X PBS for 15 minutes, then fixed overnight in 4% PFA in PBS at 4^{o}C. The following day, the fixed embryos were washed several times in 1X PBT for 5 minutes. Embryos were then blocked in 10% Normal Goat Serum (NGS) in 1X PBT for 1 hour at room temperature with gentle rocking. The NGS block was then removed and the embryos were incubated overnight at 4^{o}C with the primary antibody (Streptavidin-AP) in 10% NGS in 1X PBT. The primary antibody solution was removed the next day, and the embryos were washed 4 times in 1X PBT for 5 minutes each. Secondary antibody (AP-Conjugate) in 10% NGS/1X PBT (1:1000 dilution) was then added to the embryos and incubated at room temperature for 2 hours. The antibody solution was removed and the embryos were rinsed several times in 1X PBS for 10

minutes. The antibody was detected using NBT-BCIP and the reaction was stopped after successful color development with several washes of 1X PBS.

LITERATURE CITED

Aguilera, A., and Gómez-González, B. (2008). Genome instability: a mechanistic view of its causes and consequences. Nat Rev Genet *3*, 204-217.

Amatruda, J., Shepard, JL., Stern, HM., and Zon, LI (2002). Zebrafish as a cancer model system. Cancer Cell *1*, 229-231.

Amsterdam, A., Nissen, RM., Sun, Z., Swindell, EC., Farrington, S. and Hopkins, N. (2004). Identification of 315 genes essential for early zebrafish development. Proc Natl Acad Sci U S A *101*, 12792-12797.

Beckman, R.A., and Loeb, L.A. (2005). Genetic Instability in Cancer: Theory and Experiment. Seminars in Cancer Biology *15*, 423-435.

Beckwith, L.G., Moore, J.L., Tsao-Wu, G.S., Harshbarger, J.C., and Cheng, K.C. (2000). Ethylnitrosurea induces neoplasia in zebrafish (Danio rerio). Laboratory Investigation *80*, 379-385.

Bilotta, J., Barnett, J.A., Hancock, L. and Saszik, S. (2004). Ethanol Exposure alters zebrafish development: A novel model of fetal alcohol syndrome. Neurotoxicology and Teratology *26*, 737-743.

Blackshear, P., Graves, JP., Stumpo, DJ., Cobos, I., Rubenstein, JL. and Zeldin, DC. (2003). Graded phenotypic response to partial and complete deficiency of a brain-specific transcript variant of the winged helix transcription factor RFX4. Development *130*, 4539-4552.

Blander, G., and Guarente, L. (2004). The Sir2 Family of Protein Deacetylases. Annu Rev Biochem *73*, 417-435.

Brockerhoff, S.E., Dowling, J.E., and Hurley, J.B. (1998). Zebrafish retinal mutants. Vision Research *38*, 1335-1339.

Buck, S., Gallo, CM., and Smith, JS. (2004). Diversity in the Sir2 family of protein deacetylases. J Leukoc Biol *75*, 939-950.

Carroll, S., Grenier JK., Weatherbee, SD. (2000). From DNA to Diversity: Molecular genetics and the evolution of animal design, 2nd edn (Oxford, Blackwell Publishing).

Cavenee, W.K., Dryja, T.P., Phillips, R.A., Benedict, W.F., Godbout, R., Gallie, B.L., Murphee, A.L., Strong, L.C., and White, R.L. (1983). Expression of recessive alleles by chromosomal mechanisms in retinoblastoma. Nature *305*, 779-784.

Chakrabarti, S., Streisinger, G., Singer, F. and Walker, C. (1983). Frequency of gamma-ray induced specific locus and recessive lethal mutations in mature germ cells of the zebrafish, Brachydanio rerio. Genetics *103*, 109-123.

Chang, B., Mandal, Md. N. A., Chavali, V. R. M., Hawes, N. L., Khan, N. W., Hurd, R. E., Smith, R. S., Davisson, M. L., Kopplin, L., Klein, B. E. K., Klein, R., Iyengar, S. K., Heckenlively, J. R. and Ayyagari, R. (2008). Age-Related retinal degeneration (arrd2) in a novel mouse model due to a nonsense mutation in the mdm1 gene. Hum Mol Genet *17*, 3929-3941.

Chen, L., Gilkes, D.M., Pan, Y., Lane, W.S., and Chen, J. (2005). ATM and Chk2-dependent phosphorylation of MDMX contribute to p53 activation after DNA damage. EMBO *24*, 3411-3422.

Cheng, K., and Moore, JL. (1997). Genetic dissection of vertebrate processes in the zebrafish: a comparison of uniparental and two-generation screens. Biochem Cell Biol *75*, 525-533.

Couwenbergs, C., Spilker, AC. and Gotta, M. (2004). Control of embryonic spindle positioning and Galpha activity by C. elegans RIC-8. Curr Biol *14*, 1871-1876.

Currie, P.D. (1996). Zebrafish genetics: Mutant cornucopia. Current Biology *6*, 1548-1552.

David, N., Martin, CA., Segalen, M., Rosenfeld, F., Schweisguth, F. and Bellaïche, Y. (2005). Drosophila Ric-8 regulates Galphai cortical localization to promote Galphai-dependent planar orientation of the mitotic spindle during asymmetric cell division. Nat Cell Biol *7*, 1083-1090.

Detrich, H.W., III,, Westerfield, M., and Zon, L.I. (1999). The Zebrafish: Genetics and Genomics, Vol 60 (San Diego, Academic Press).

Dooley, K., and Zon, L.I. (2000). Zebrafish: a model system for the study of human disease. Current Opinion in Genetics & Development *10*, 252-256.

Driever, W., Solnica-Krezel, L., Schier, A.F., Neuhauss, S.C.F., Malicki, J., Stemple, D.L., Stainer, D.Y.R., Zwartkruis, F., Abdelilah, S., Rangini, Z., Belak, J. and Boggs, C. (1996). A Genetic Screen for Mutations Affecting Embryogenesis in Zebrafish. Development *123*, 37-46.

Drummond AJ, A.B., Buxton S, Cheung M, Cooper A, Duran C, Field M, Heled J, Kearse M, Markowitz S, Moir R, Stones-Havas S, Sturrock S, Thierer T, Wilson A (2011). www.geneious.com

Einhauer, A., and Jungbaur, A. (2001). The FLAG peptide, a versitile fusion tag for the purification of recombinant proteins. J Biochem Biophys Methods *49*, 455-465.

Eisen, J. (1996). Zebrafish make a big splash. Cell *87*, 969-977.

Eisen, J.S., and Smith, J.C. (2008). Controlling morpholino experiments: don't stop making antisense. Development *135*, 1735-1743.

Ekker, S.C., and Larson, J.D. (2001). Morphant technology in model developmental systems. Genesis *30*, 89-93.

Emery, P., Durand, B., Mach, B. and Reith, W. (1996). RFX proteins, a novel family of DNA binding proteins conserved in the eukaryotic kingdom. Nucleic Acids Res *24*, 803-807.

Feitsma, H., and Cuppen, E. (2008). Zebrafish as a Cancer Model. Mol Cancer Res *6*, 685-694.

Fornzler, D., Her, H., Knapik, E.W., Clark, M., Lehrach, H., Postlethwait, J.H., Zon, L.I., and Beier, D.R. (1998). Gene Mapping in Zebrafish Using Single-Strand Conformation Polymorphism Analysis. Genomics *51*, 216-222.

Fox, E.J., and Loeb, L.A. (2010). Lethal Mutagenesis: Targeting the Mutator Phenotype in Cancer. Seminars in Cancer Biology *20*, 353-359.

Freedman, D., Wu, L. and Levine, AJ. (1999). Functions of the MDM2 oncoprotein. CMLS, Cell Mol Life Sci *55*, 96-107.

Gasteiger, E., Gattiker, A., Hoogland, C., Ivanyi, I., Appel, R.D., Bairoch, A. (2003) ExPASy: the proteomics server for in-depth protein knowledge and analysis. Nuc Acids Res. *31*, 3784-3788.

Gerhard, G. (2003). Comparitive aspects of zebrafish (Danio rerio) as a model for aging research. Experimental Gerontology *38*, 1333-1341.

Gerlai, R. (2003). Zebra fish: An uncharted Behavior Genetic Model. Behavior Genetics *33*, 461-468.

Gerlai, R., Lahav, M., Guo, S. and Rosenthal, A (2000). Drinks like a fish: zebra fish (Danio rerio) as a behavior genetic model to study alcohol effects. Pharmacology, Biochemistry and Behavior *67*, 773-782.

Gestl, E.E., Kauffman, E.J., Moore, J.L., and Cheng, K.C. (1996). New conditions for generation of gynogenetic half-tetrad embryos in zebrafish. J Hered *88*, 76-79.

Gonzalez, C. (2007). Spindle orientation, asymmetric division and tumour suppression in Drosophila stem cells. Nat Rev Genet *8*, 462-472.

Greene, J. (1999). A little fish makes a big splash. In NCRR Reporter.

Grunwald, D.J., and Eisen, J.S. (2002). Headwaters of the zebrafish -- emergence of a new model vertebrate. Nat Rev Genet *3*, 717-724.

Grunwald, D.J., and Streisinger, G. (1992). Induction of recessive lethal and specific locus mutations in the zebrafish with ethyl nitrosurea. Genet Res Camb *59*, 103-116.

Guo, S. (2008). Animal Models for Anxiety Disorders. In Biomarkers for Psychiatric Disorders, C.W. Turk, ed. (San Francisco, Springer Science), pp. 203-216.

Haffter, P., Granato, M., Brand, M., Mullins, M.C., Hammerschmidt, M., Kane, D.A., Odenthal, J., van Eeden, F. J. M., Jiang, Y-J., Heisenberg, C-P., Kelsh, R. N., Furutani-Seiki, M., Vogelsang, E., Beuchle, D., Schach, U., Fabian, C. and Nusslein-Volhard, C. (1996). The Identification of Genes with Unique and Essential Functions in the Development of the Zebrafish, Danio rerio. Development *123*, 1-36.

Haffter, P., Odenthal, J., Mullins, M.C., Lin, S., Farrell, M.J., Vogelsang, E., Haas, F., Brand, M., van Eeden, F.J.M., Furutani-Seiki, M.*, et al.* (1996). Mutations affecting pigmentation and shape of the adult zebrafish. Developmental genes in evolution *206*, 260-276.

Hampoelz, B., Hoeller, O., Bowman, SK., Dunican, D., and Knoblich, JA. (2005). Drosophila Ric-8 is essential for plasma-membrane localization of heterotrimeric G proteins. Nat Cell Biol *7*, 1099-1105.

Hansen, C., Bartek, J., and Jensen, S. (2008). A functional link between the human cell cycle-regulatory phosphatase Cdc14A and the atypical mitogen-activated kinase Erk3. Cell Cycle *7*, 325-334.

Hendricks, J.C., Sehgal, A. and Pack, A.I. (2000). The need for simple animal model to understand sleep. Progress in Neurobiology *61*, 339-351.

Hengen, P. (1995). Purification of His-Tag fusion proteins from Escherichia coli. Trends Biochem Sci *20*, 285-286.

Hochuli, E., Bannwarth, W., Döbeli, H., Gentz, R., and Stüber, D. (1988). Genetic Approach to Facilitate Purification of Recombinant Proteins with a Novel Metal Chelate Adsorbent. Nat Biotech *6*, 1321-1325.

Hopp, T.P., Gallis, B., and Prickett, K.S. (1988). A short polypeptide marker sequence useful for recombinant protein identification and purification. Bio/Technology *6*, 1204-1210.

Ingham, P. (2009). The power of the zebrafish for disease analysis. Hum Mol Genet *18*, R107-112.

Ito, A., Kawaguchi, Y., Lai, C-H., Kovacs, JJ., Higashimoto, Y., Appella, E., and Yao, T-P. (2002). MDM2±HDAC1-mediated deacetylation of p53 is required for its degradation. EMBO *21*, 6236-6245.

Iwakuma, T., and Lozano, G. (2003). MDM2, an introduction. Molecular cancer research : MCR *1*, 993-1000.

Johnston, C., Afshar, K., Snyder, JT., Tall, GG., Gonczy, P., Siderovski, DP and Willard, FS. (2008). Structural Determinants Underlying the Temperature-sensitive Nature of a G Mutant in Asymmetric Cell Division of Caenorhabditis elegans. J Biol Chem *283*, 21550-21558.

Kari, G., Rodeck, U., and Dicker, AP. (2007). Zebrafish: an emerging model system for human disease and drug discovery. Clin Pharmacol Ther *82*, 70-80.

Karlovich, C., John, RM., Ramirez, L., Stainier, DYR., and Myers, RM. (1998). Characterization of the Huntington's disease (HD) gene homolog in the zebrafish Danio rerio. Gene *217*, 117-125.

Kawakami, K. (2005). Transposon Tools and Methods in Zebrafish. Developmental dynamics : an official publication of the American Association of Anatomists *234*, 244-254.

Kelsh, R.N., Schmid, B., and Eisen, J.S. (2000). Genetic analysis of melanophore development in zebrafish embryos. Developmental biology *225*, 277-293.

Kimmel CB, B.W., Kimmel SR, Ullmann B and Schilling TF. (1995). Stages of embryonoc development of the zebrafish. Developmental Dynamics *203*, 253-310.

Knudson, A.G. (1971). Mutation and cancer: statistical study of retinoblastoma. Proceedings of the National Academy of Sciences of the United States of America *68*, 820-823.

Knudson, A.G. (1985). Hereditary cancer, oncogenes, and antioncogenes. Cancer Research *45*, 1437-1443.

Krens, S., Spaink, HP., Snaar-Jagalska, BE. (2006). Functions of the MAPK family in vertebrate-development. FEBS Lett *580*, 4984-4990.

Langenau, D.M., Feng, H., Berghmans, S., Kanki, J.P., Kutok, J.L., and Look, A.T. (2005). Cre/lox-regulated transgenic zebrafish model with conditional myc-induced T cell acute lymphoblastic leukemia. Proceedings of the National Academy of Sciences of the United States of America *102*, 6068-6073.

Langheinrich U, H.E., Stott G, Vacun G. (2002). Zebrafish as a model organism for the identification and characterization of drugs and genes affecting p53 signaling. Curr Biol *12*, 2023-2028.

Lele, Z., and Krone, P.H. (1996). The zebrafish as a model system in developmental, toxicological and transgenic research. Biotechnology Advances *14*, 57-72.

Lieschke, G.J., and Currie, P.D. (2007). Animal models of human disease: zebrafish swim into view. Nat Rev Genet *8*, 353-367.

Link, V., Shevchenko, A., and Heisenberg, C-P. (2006). Proteomics of early zebrafish embryos. BMC Developmental Biology *6*.

Livingston, B.T. (2008), K. Griffett, ed. (Tampa).

Mach, B., Steimle, V., Martinez-Soria, E., and Reith, W. (1996). Regulation of MHC class II genes: lessons from a disease. Annu Rev Immunol *14*, 301-331.

Marone, M., Mozzetti, S., De Ritis, D., Pierelli, L., and Scambia, G. (2001). Semiquantitative RT-PCR analysis to assess the expression levels of multiple transcripts from the same sample. Biol Proced Online *3*, 19-25.

Maslow, T. (2010). Preparation of Zebrafish Embryo Protein Lysates, K. Griffett, ed.

Matsushita, H., Uenaka, A., Ono, T., Hasegawa, K., Sato, S., Koizumi, F., Nakagawa, K., Toda, M., Shingo, T., Ichikawa, T., Noguchi, Y., Tamiya, T., Furuta, T., Kawase, T., Date, I., and Nakayama, E. (2005). Identification of glioma-specific RFX4-E and -F isoforms and humoral immune response in patients. Cancer Sci *96*, 801-809.

Matsuzaki, F. (2005). Drosophila G-protein signalling: intricate roles for Ric-8? Nat Cell Biol *7*, 1047-1049.

Matthews, M., Trevarrow, B., and Matthews, J. (2002). A virtual tour of the Guide for zebrafish users. Lab animal *31*, 34-40.

Miller, K., and Rand, JB. (2000a). A Role for RIC-8 (Synembryn) and GOA-1 (Goa) in Regulating a Subset of Centrosome Movements During Early Embryogenesis in Caenorhabditis elegans. Genetics *156*, 1649-1660.

Miller, K.G., Emerson, M.D., McManus, J.R., and Rand, J.B. (2000b). RIC-8 (Synembryn): A Novel Conserved Protein that Is Required for Gqa Signaling in the C. elegans Nervous System. Neuron *27*, 289-299.

Mizgireuv, I.V., and Revskoy, S.Y. (2006). Transplantable tumor lines generated in clonal zebrafish. Cancer research *66*, 3120-3125.

Moore, J., Gestl, EE., and Cheng, KC. (2004). Mosaic eyes, genomic instability mutants, and cancer susceptibility. Methods Cell Biol *76*, 555-568.

Moore, J., Rush, LM., Breneman, C., Mohideen, MA., and Cheng, KC. (2006). Zebrafish genomic instability mutants and cancer susceptibility. Genetics *174*, 585-600.

Morcos, P.A. (2007). Achieving targeted and quantifiable alteration of mRNA splicing with Morpholino oligos. Biochem and Biophys Res Commun *358*, 521-527.

Moreira, J., and Deutsch, A. (2005). Pigment pattern formation in zebrafish during late larval stages: a model based on local interactions. Developmental dynamics : an official publication of the American Association of Anatomists *232*, 33-42.

Morotomi-Yano, K., Yano, K., Saito, H., Sun, Z., Iwama, A., and Miki, Y. (2002). Human regulatory factor X 4 (RFX4) is a testis-specific dimeric DNA-binding protein that cooperates with other human RFX members. J Biol Chem *277*, 836-842.

Moulton, J.D. (2007). Using morpholinos to control gene expression. In Curr Protoc Nucleic Acid Chem.

Muggerud, A., Edgren, H., Wolf, M., Kleivi, K., Dejeux, E., Tost, J., Sørlie, T., and Kallioniemi, O. (2009). Data integration from two microarray platforms identifies bi-allelic genetic inactivation of RIC8A in a breast cancer cell line. BMC Med Genomics *11*.

Mullins, M., Hammerschmidt, M., Haffter, P., and Nüsslein-Volhard, C. (1994). Large-scale mutagenesis in the zebrafish: in search of genes controlling development in a vertebrate. Curr Biol *4*, 189-202.

Nagayoshi, S., Hayashi, E., Abe, G., Osato, N., Asakawa, K., Urasaki, A., Horikawa, K., Ikeo, K., Takeda, H., and Kawakami, K. (2008). Insertional mutagenesis by the Tol2 transposon-mediated enhancer trap approach generated mutations in two developmental genes: tcf7 and synembryn-like. Development *135*, 159-169.

Nasevicius, A., and Ekker, S.C. (2000). Effective Targeted Gene "Knockdown" in Zebrafish. Nat Genet *26*, 216-220.

Nawrocki, L., BreMiller, R., Streisinger, G. and Kaplan, M. (1985). Larval and Adult Visual Pigments of the Zebrafish, Brachydanio rerio. Vision Res *25*, 1569-1576.

North, B., and Verdin, E. (2004). Sirtuins: Sir2-related NAD-dependent protein deacetylases. Genome Biology *5*, 224.

Norton, W., and Bally-Cuif, L. (2010). Adult zebrafish as a model organism for behavioural genetics. BMC Neuroscience *11*.

O'Shea, S., and Westerfield, M. (1993). Western Blots of Zebrafish Embryos. In The Zebrafish Book, M. Westerfield, ed. (Eugene, University of Oregon Press).

Oren, M., and Rotter, V. (1999). Introduction: p53 – the first twenty years. CMLS, Cell Mol Life Sci *55*, 9-11.

Perdiguero, E., Pillaire, MJ., Bodart, JF., Hennersdorf, F., Frödin, M., Duesbery, NS., Alonso, G., and Nebreda, AR. (2003). Xp38gamma/SAPK3 promotes meiotic G(2)/M transition in Xenopus oocytes and activates Cdc25C. EMBO *22*, 5746-5756.

Postlethwait, J., Amores, A., Force, A., and Yan, Y-L. (1999). The Zebrafish Genome. In Methods in Cell Biology (Academic Press), pp. 149-163.

Postlethwait, J., Johnson, SL., Midson, CN., Talbot, WS., Gates, M., Ballinger, EW., Africa, D., Andrews, R., Carl, T., and Eisen, JS. (1994). A genetic linkage map for the zebrafish. Science *264*, 699-703.

Postlethwait, J.H., and Talbot, W.S. (1997). Zebrafish genomics: from mutants to genes. Trends in Genetics *13*, 183-190.

Postlethwait JH, Y.Y., Gates MA, Horne S, Amores A, Brownlie A, Donovan A, Egan ES, Force A, Gong Z, Goutel C, Fritz A, Kelsh R, Knapik E, Liao E, Paw B, Ransom D, Singer A, Thomson M, Abduljabbar TS, Yelick P, Beier D, Joly JS, Larhammar D, Rosa F, Westerfield M, Zon LI, Johnson SL, Talbot WS. (1998). Vertebrate genome evolution and the zebrafish gene map. Nat Genet *18*, 345-349.

Qi, X., Pohl, NM., Loesch, M., Hou, S., Li, R., Qin, JZ., Cuenda, A., and Chen, G. (2007). p38alpha antagonizes p38gamma activity through c-Jun-dependent ubiquitin-proteasome pathways in regulating Ras transformation and stress response. J Biol Chem *282*, 31398-31408.

Rawls, J.F., Mellgren, E.M., and Johnson, S.L. (2001). How the Zebrafish Gets Its Stripes. Developmental Biology *204*, 301-314.

Reynolds, N., Schade, MA., and Miller, KG. (2005). Convergent, RIC-8-Dependent G Signaling Pathways in the Caenorhabditis elegans Synaptic Signaling Network. Genetics *169*, 651-670.

Robu, M., Larson, JD., Nasevicius, A., Beiraghi, S., Brenner, C., Farber, SA., and Ekker, SC (2007). p53 activation by knockdown technologies. PLoS Genet *3*.

Rubinstein, A. (2003). Zebrafish: From disease modeling to drug discovery. Current Opinion in Genetics & Development *6*, 218-223.

Sakaguchi, K., Herrera, JE., Saito, S., Miki, T., Bustin, M., Vassilev, A., Anderson, CW., and Appella, E. (1998). DNA damage activates p53 through a phosphorylation-acetylation cascade. Genes Dev *12*, 2831-2841.

Shin, J.T., and Fishman, M.C. (2002). From Zebrafish to Human: Modular Medical Models. Annu Rev Genomics Hum Genet *3*, 311-340.

Snyder, L., Trusko, SP., Freeman, N., Eshleman, JR., Fakharzadeh, SS., and George, DL. (1988). A gene amplified in a transformed mouse cell line undergoes complex transcriptional processing and encodes a nuclear protein. J Biol Chem *263*, 17150-17158.

Solnica-Krezel, L., Schier, AF., and Driever, W. (1994). Efficient recovery of ENU-induced mutations from the zebrafish germline. Genetics *136*, 1401-1420.

Streisinger, G. (1984). Attainment of Minimal Biological Variability and Measurements of Genotoxicity: Production of Homozygous Diploid Zebra Fish. National Cancer Institute Monograph *65*, 53-58.

Streisinger, G., Coale, F., Taggart, C., Walker, C., and Grunwald, D.J. (1989). Clonal origins of cells in the pigmented retina of the zebrafish eye. Developmental Biology *131*, 60-69.

Streisinger, G., Singer, F., Walker, C., Knauber, D., and Dower, N. (1986). Segregation analyses and gene-centromere distances in zebrafish. Genetics *112*, 311-319.

Streisinger, G., Walker, C., Dower, N., Knauber, D., and Singer, F. (1981). Production of clones of homozygous diploid zebra fish (Brachydanio rerio). Nature *291*, 293-296.

Summerton, J.E. (1989). Uncharged nucleic acid analogs for therapeutic and diagnostic applications: Oligomers assembled from ribose-derived subunits. In Discoveries in Antisense Nucleic Acids (Portfolio Publishing Company), p. 71.

Summerton, J.E., and Weller, D. (1997). Antisense properties of morpholino oligomers. Nucleosides Nucleotides *16*, 889-898.

Talbot, W.S., and Hopkins, N. (2000). Zebrafish mutations and functional analysis of the vertebrate genome. Genes & development *14*, 755-762.

Tall, G., and Gilman, AG. (2005). Resistance to inhibitors of cholinesterase 8A catalyzes release of Galphai-GTP and nuclear mitotic apparatus protein (NuMA) from NuMA/LGN/Galphai-GDP complexes. Proc Natl Acad Sci U S A *102*, 16584-16589.

Tang, J., Qi, X., Mercola, D., Han, J., and Chen, G. (2005). Essential role of p38gamma in K-Ras transformation independent of phosphorylation. J Biol Chem *280*, 23910-23917.

Thisse, C., and Thisse, B. (2008). High-resolution in situ hybridization to whole-mount zebrafish embryos. Nat Protoc *3*, 59-69.

Thisse, C., Neel, H., Thisse, B., Daujat, S. and Piette, J. (2000). The mdm2 gene of zebrafish (Danio rerio): preferential expression during development of neural and muscular tissues, and absence of tumor formation after overexpression of its cDNA during early embryogenesis. Differentiation *66*, 61-70.

Thomas, C., Tall, GG., Adhikari, A., and Sprang, SR. (2008). Ric-8A catalyzes guanine nucleotide exchange on G alphai1 bound to the GPR/GoLoco exchange inhibitor AGS3. J Biol Chem *283*, 23150-23160.

Thut, C., Goodrich, JA. and Tijan, R. (1997). Repression of p53-mediated transcription by MDM2: a dual mechanism. Genes Dev *11*, 1974-1986.

Tsugita, A., Inouye, M., Terzaghi, E., and Streisinger, G. (1968). Purification of Bacteriophage T4 Lysozyme. JOURNAL OF BIOLOGICAL CHEMISTRY *243*, 391-397.

Volff, J. (2005). Genome evolution and biodiversity in teleost fish. Heredity *94*, 280-294.

Walker, C., and Streisinger, G. (1983). Induction of of Mutations by gamma-rays in Pregonial Germ Cells of Zebrafish Embryos. Genetics *103*, 125-136.

Wang, X., McGowan, CH., Zhao, M., He, L., Downey, JS., Fearns, C., Wang, Y., Huang, S., Han, J. (2000). Involvement of the MKK6-p38gamma cascade in gamma-radiation-induced cell cycle arrest. Mol Cell Biol *20*, 4543-4552.

West, R. (1996). Tiny Fish Big Splash. Oregon Quarterly, 22-25.

White, R. (2005). RNA polymerases I and III, growth control and cancer. Nat Rev Mol Cell Biol *6*, 69-78.

Wilkie, T., and Kinch, L. (2005). New roles for Galpha and RGS proteins: communication continues despite pulling sisters apart. Curr Biol *15*, R843-854.

Yee, N., Gong, W., Huang, Y., Lorent, K., Dolan, AC., Maraia, RJ., and Pack, M. (2007). Mutation of RNA Pol III subunit rpc2/polr3b Leads to Deficiency of Subunit Rpc11 and disrupts zebrafish digestive development. PLoS Biol *5*.

Yoshikawa, K., and Touhara, K. (2009). Myr-Ric-8A Enhances Ga15-Mediated Ca21 Response of Vertebrate Olfactory Receptors. Chem Senses *34*, 15-23.

Zhang, D., Stumpo, DJ., Graves, JP., DeGraff, LM., Grissom, SF., Collins, JB., Li, L., Zeldin, DC., and Blackshear, PJ. (2006). Identification of potential target genes for RFX4_v3, a transcription factor critical for brain development. J Neurochem *98*, 860-875.

Zhang, D., Zeldin, DC., and Blackshear, PJ. (2007). Regulatory factor X4 variant 3: a transcription factor involved in brain development and disease. J Neurosci Res *85*, 3515-3522.

Zon, L., and Peterson, RT. (2005). In vivo drug discovery in the zebrafish. Nat Reviews Drug Discovery *4*, 35-44.

APPENDICES

Appendix A: Additional PCR Results and Updated Candidate List for the *gin-10* Studies

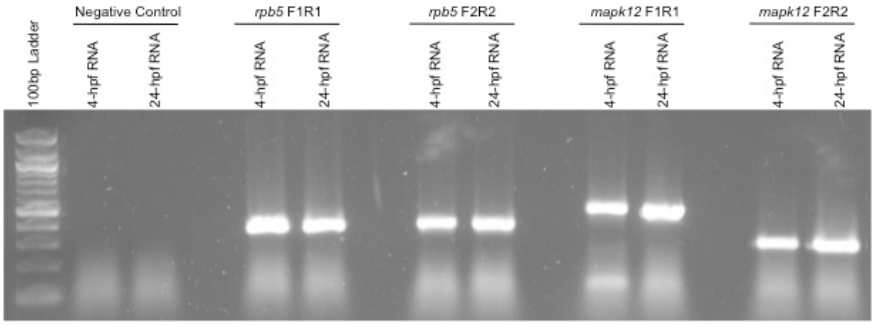

Figure A1: Maternal and Zygotic RT-PCR Results for the *rpb5* and *mapk12 gin-10* candidate genes. These results suggest that both genes are expressed maternally (4-hpf) and zygotically (24-hpf) during zebrafish development. The *rpb5* gene was removed from the candidate list based on homology and orthology information from Sanger. The *mapk12* gene is still a *gin-10* candidate and has not been pursued further at this time.

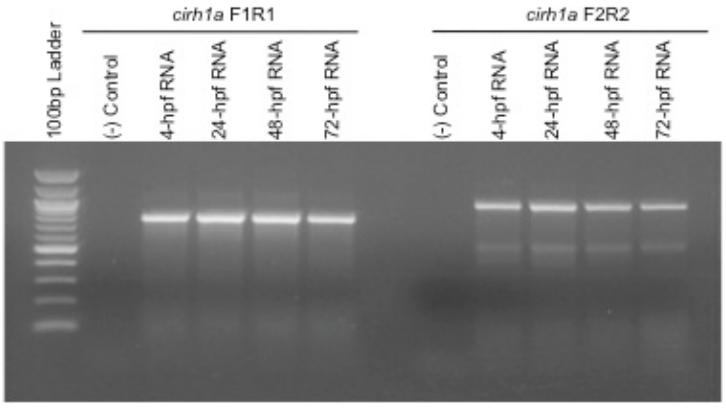

Figure A2: Developmental RT-PCR Results for two different primer sets of the *cirh1a gin-10* candidate gene. Although it appears that this gene has both maternal and zygotic expression in the developing zebrafish embryo, published data indicates that it is actually involved specifically in the development of the liver, and was therefore removed from the *gin-10* candidate list.

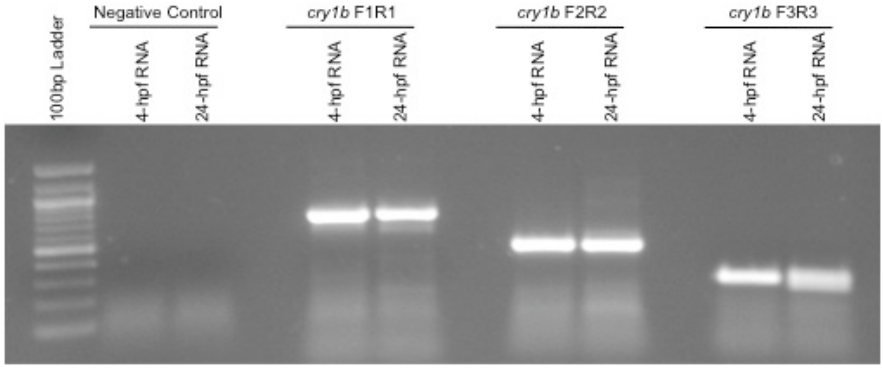

Figure A3: Maternal and Zygotic RT-PCR Results of three different primer sets for the *cry1b gin-10* candidate gene. Prior to the analysis of the transgenic fish, the *cry1b* gene was a candidate for the *gin-10* mutant based on its location on chromosome 18. Following an in-depth literature and sequence database search, it appeared that the *cry1b* gene functioned within the CLOCK and circadian rhythm pathways, and was no longer a candidate for this project.

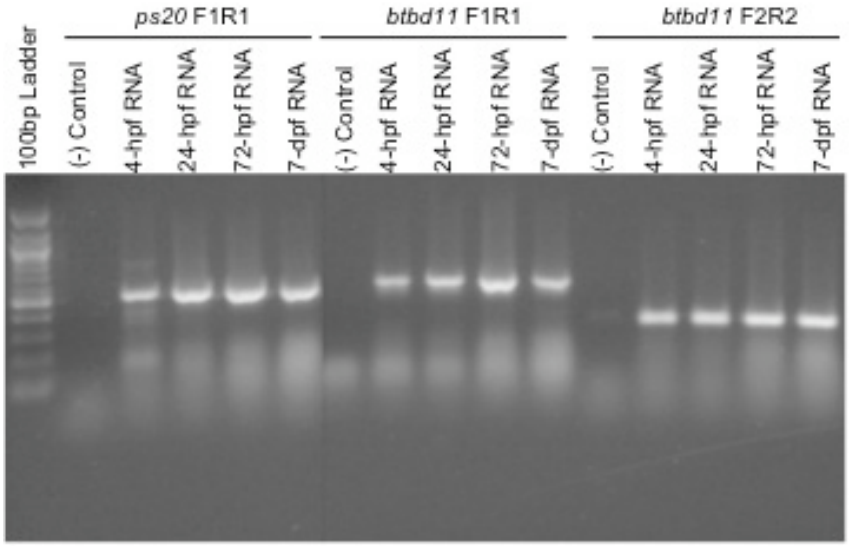

Figure A4: Developmental RT-PCR Results from the *ps20* and *btbd11 gin-10* candidate genes. The *ps20* gene was originally on the *gin-10* candidate list based on its location on chromosome 18. When the Sanger/Ensemble zv8 update was published, it appeared that this gene was actually located outside the mapped *gin-10* region, and therefore this gene was not pursued further. The *btbd11* gene has been suggested to interact with histones and may mediate transcriptional repression. This gene remains on the *gin-10* candidate list.

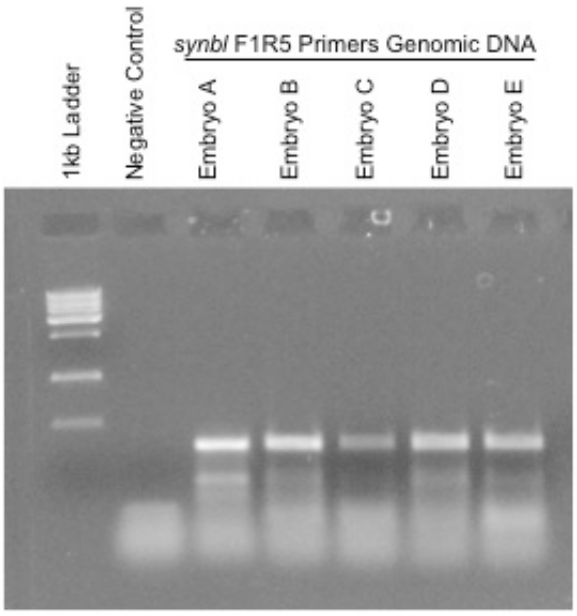

Figure A5: Genomic DNA PCR Results from individual WT(AB) Embryos using *synbl* primers for the 5'UTR. The 5' coding region of the *synbl* gene was difficult to clone from cDNA, so genomic DNA from individual embryos were used to clone the 5'UTR and part of the first exon of the *synbl* gene. The PCR products were sequenced and confirmed against the known Sanger sequence, and was then used to design the *synbl*-ATG MO.

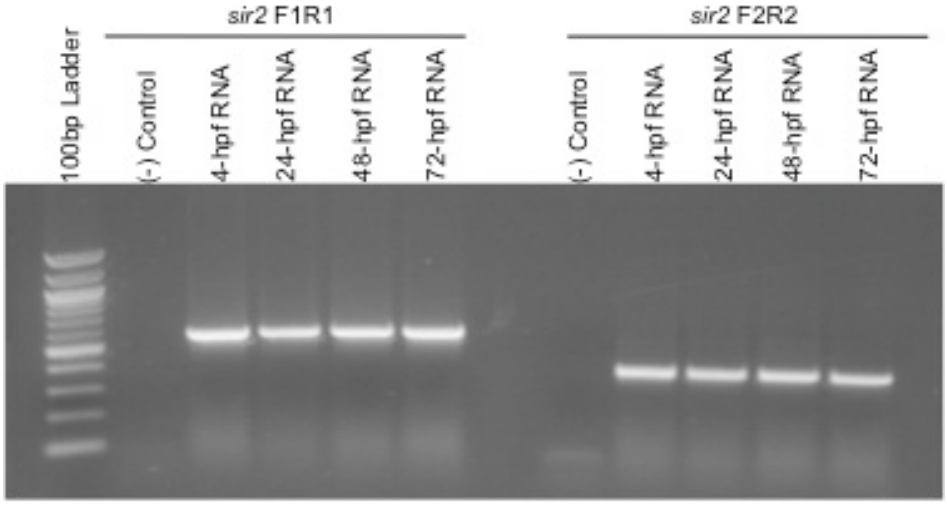

Figure A6: Developmental RT-PCR Results for two different primer sets for the *sir2 gin-10* candidate gene. These results suggested that the *sir2* gene was expressed both maternally and zygotically during zebrafish embryogenesis. The *sir2* candidate gene was studied in-depth until the MO experiments revealed that this particular sirtuin was involved in metabolic processes of the zebrafish embryo. Based on those results, the *sir2* gene was removed from the *gin-10* candidate list but is otherwise a very interesting gene in vertebrate studies.

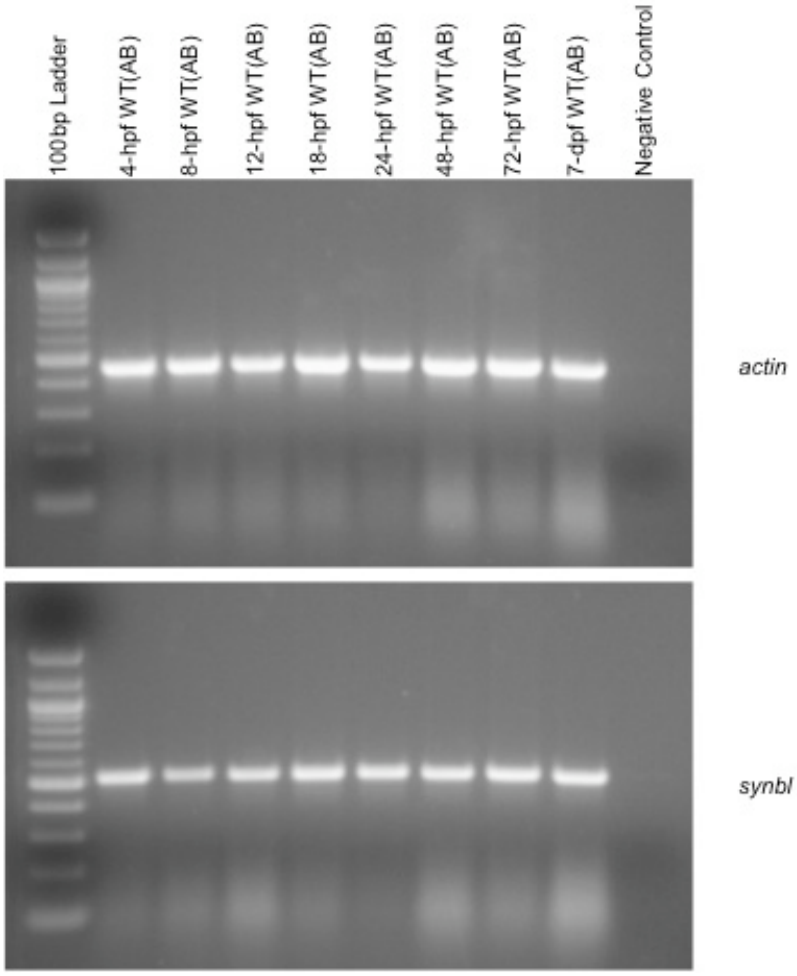

Figure A7: Developmental RT-PCR Profile of the *actin* and *synbl* genes from WT(AB) zebrafish using 30 cycles of amplification.

Table A1: Updated *gin-10* Candidate List

Gene Identification	Gene Name/Function	Additional Information
si:dkey103i16.2	placental protein 11	Function Not Identified
si:dkey103i16.1	PTPRF interacting protein (liprin beta 1)	➢ May be a scaffold protein that recruits and/or anchors transmembrane tyrosine phosphatases ➢ Interacts with S100A4 (calcium-binding protein involved in metastasis and tumorigenesis) ➢ may be involved in Chk2 pathway Has DNA binding domain
cry1b	cryptochrome 1b	➢ DNA repair (zebrafish) ➢ DNA photolyase activity (zebrafish) ➢ transcription repressor activity
polr3b	RNA pol III subunit B	➢ DNA-dependant RNA polymerase ➢ Synthesizes 5S rRNA and tRNAs ➢ Contributes to the polymerase catalytic activity (zinc finger) ➢ Nuclear
rfx4	winged-helix transcription factor	➢ HLA class II genes ➢ Histocompatibility, Immune system ➢ Testes development/cancer? (humans) ➢ Brain development ➢ Nuclear
synbl	guanine exchange factor (melanocytes)	➢ Can activate some G-alpha proteins ➢ Does not interact with G-alpha proteins when they are in a complex with beta and gamma subunits ➢ Cytoplasmic
si:dkey103i16.6	sir2 homolog	➢ mitochondrial NAD-dependant deacetylase (regulates acetyl-CoA synthetase) **VEGA** ➢ Nuclear Histone deacetylase activity (Ku-70 in cardiomyocytes) **VEGA/Not confirmed** ➢ Orthologue of HST2? (**Ensemble**) **Not Confirmed** o involved in cell cycle and tumorigenesis o deacetylase
zgc:64098	Unknown	➢ UPF0444 transmembrane protein C12orf23
ch73-62b13.1	carbohydrate sulfotransferase (CHST1)	➢ Catalyzes the transfer of sulfate to position 6 of galactose (Gal) residues of keratan. ➢ Has a preference for sulfating keratan sulfate, but it also transfers sulfate to the unsulfated polymer. ➢ May function in the sulfation of sialyl N-acetyllactosamine oligosaccharide chains attached to glycoproteins. Participates in biosynthesis of selectin ligands. o Selectin ligands are present in high endothelial cells (HEVs) and play a central role in lymphocyte homing at sites of inflammation (human/mouse)
si:ch211-	Unknown	Function Not Identified

170d11.1		
btbd11b	btb (POZ) domain containing 11b	➢ DNA binding ➢ H2A-H2B dimerization interface ➢ Ankyrin repeats ➢ May mediate transcriptional repression and interact with histone deacetylase co-repressor complexes (N-CoR and SMRT)
mlc1	megalencephalic leukoencephalopathy	Function Not Identified
panx2	gap junctions	➢ Forms panx1/panx2 heteromeric intercellular channels ➢ Variant found in breast cancer (somatic mutation)
trabd	Unknown	Function Not Identified
mapk12 (ERK6 or p38)	phosphorylates ATF-2, Mac and Mef2	➢ Responds to environmental stress and pro-inflammatory cytokines ➢ Plays a role in myoblast differentiation (human) ➢ Down-regulation of cyclin-D1 in response to hypoxia in adrenal cells (human) ➢ May inhibit proliferation and promote differentiation ➢ May use magnesium as a co-factor (zebrafish)
si:ch211-15i6.4	MTSS1 (vertebrate metastasis suppressor 1) “missing in metastasis protein 1”	➢ Inhibits the nucleation of actin filaments in vitro (mouse) ➢ binds actin monomers ➢ binds cytoplasmic domain of tyrosine-phosphatase delta receptor ➢ may be related to cancer progression and metastasis in a variety of organs (human)

Appendix B: Primer Maps and Supplementary Sequencing Results from the *gin-10* Candidate Genes

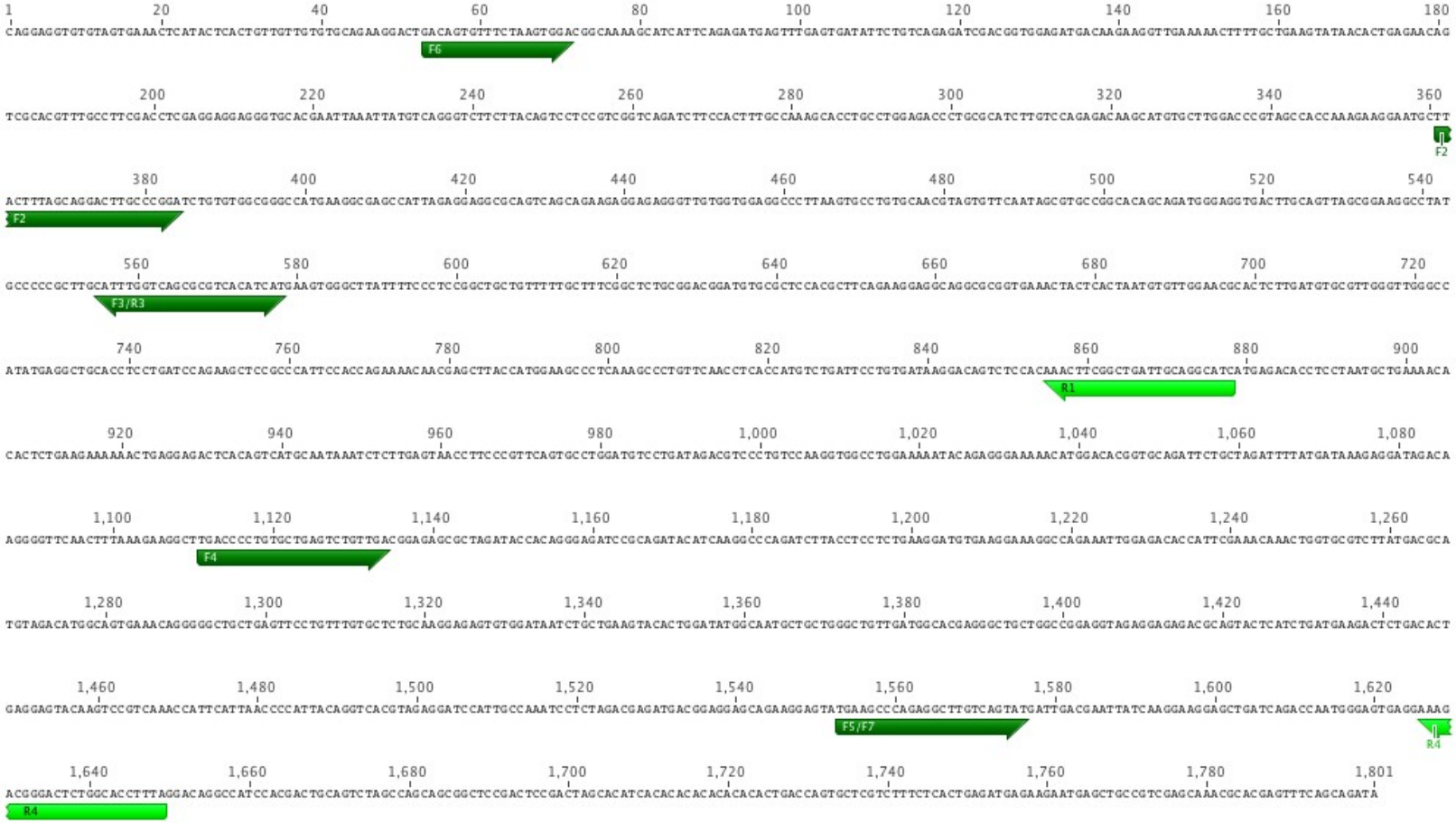

Figure A8: Known Sanger cDNA sequence for the *gin-10* candidate gene *synbl*. Forward primers used for RT-PCR, cloning and probes are shown in the dark green, and the reverse primers are shown in light green.

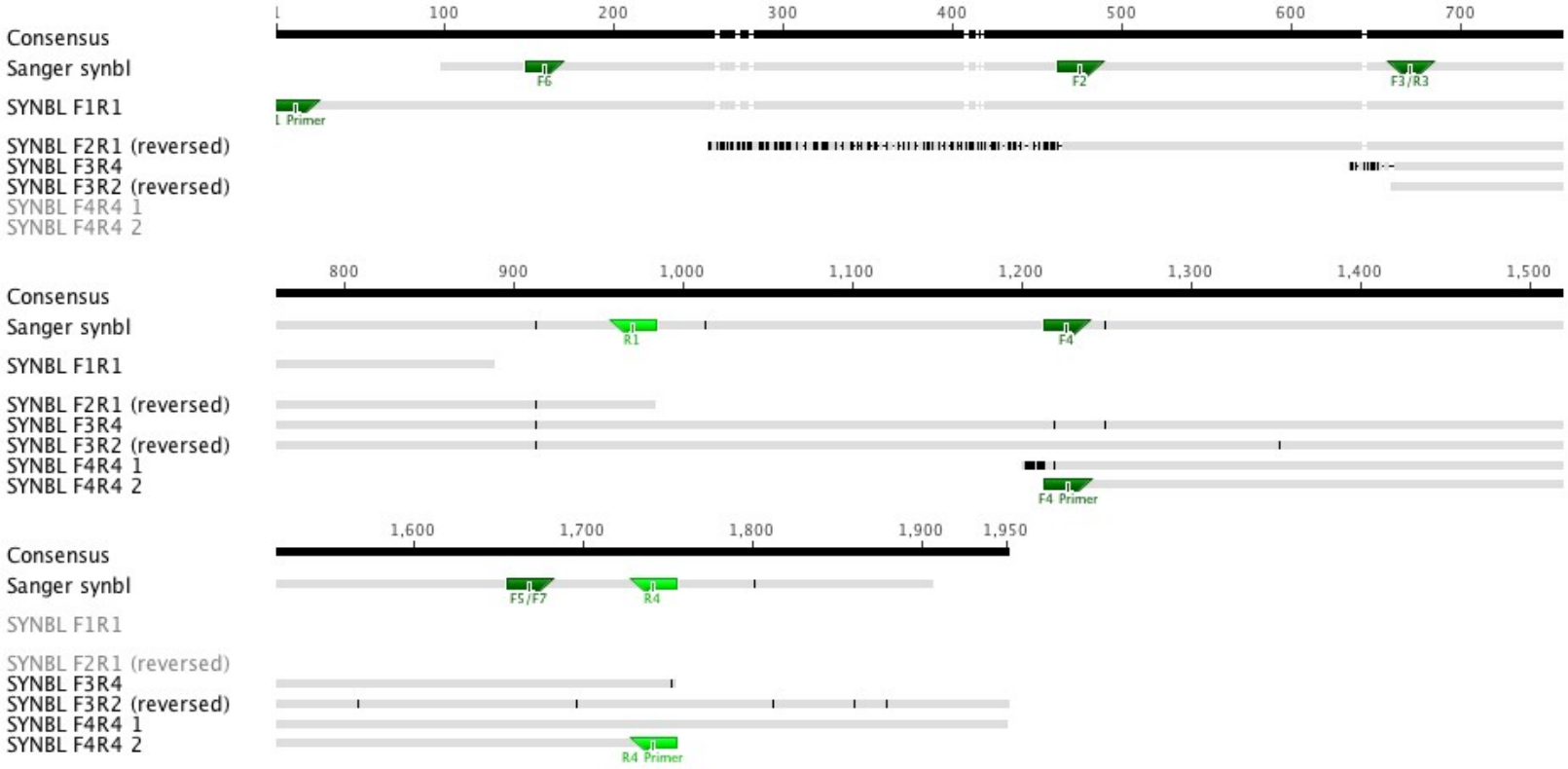

Figure A9: Alignment of several *synbl* clones against the Sanger database cDNA sequence. Primers used for the cloning are also shown. Black marks in the clone sequences highlight discrepancies from the Sanger sequence.

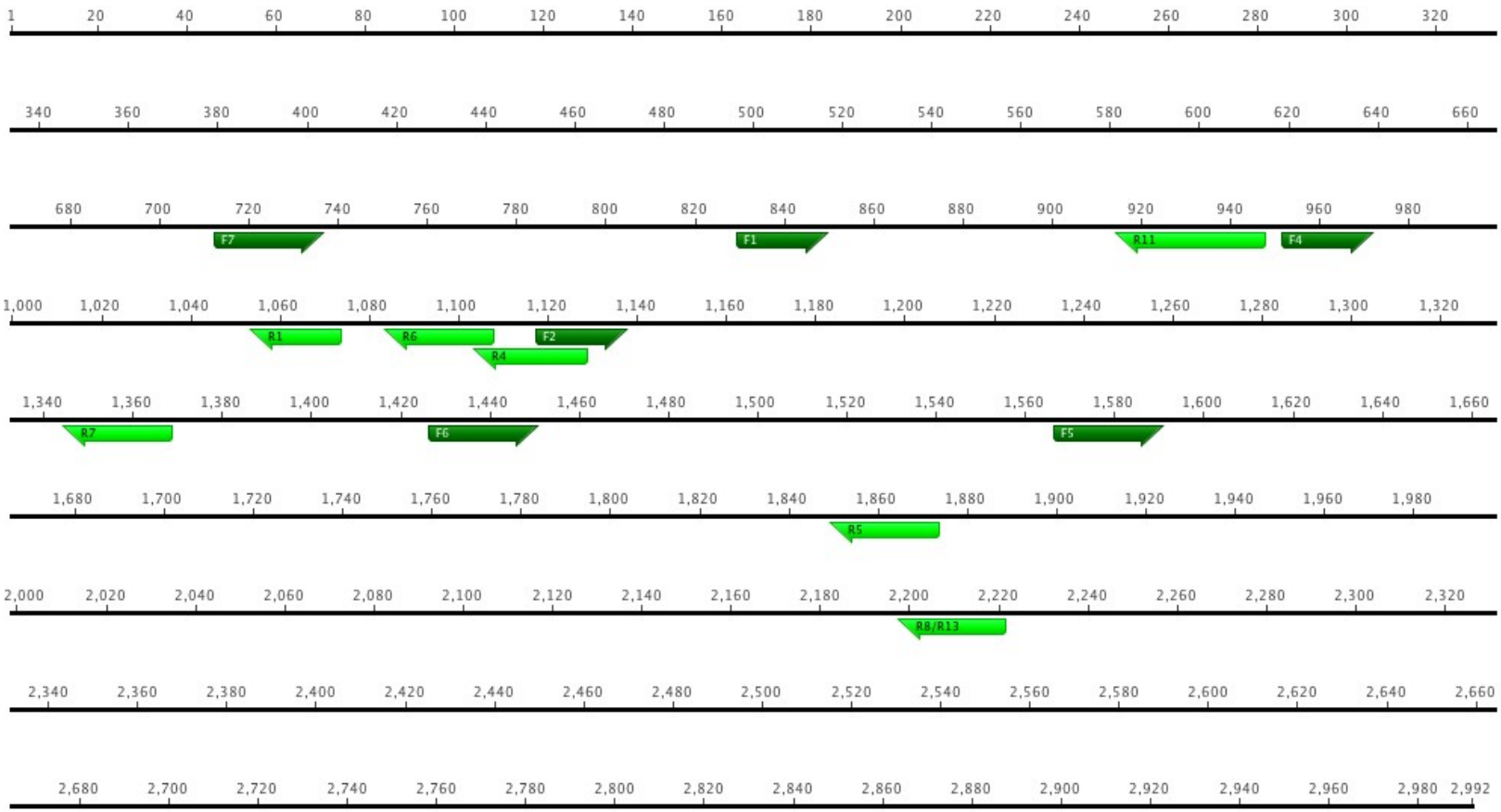

Figure A10: Known Sanger cDNA sequence for the *gin-10* candidate gene *rfx4*. Forward primers used for RT-PCR, cloning and probes are shown in the dark green, and the reverse primers are shown in light green.

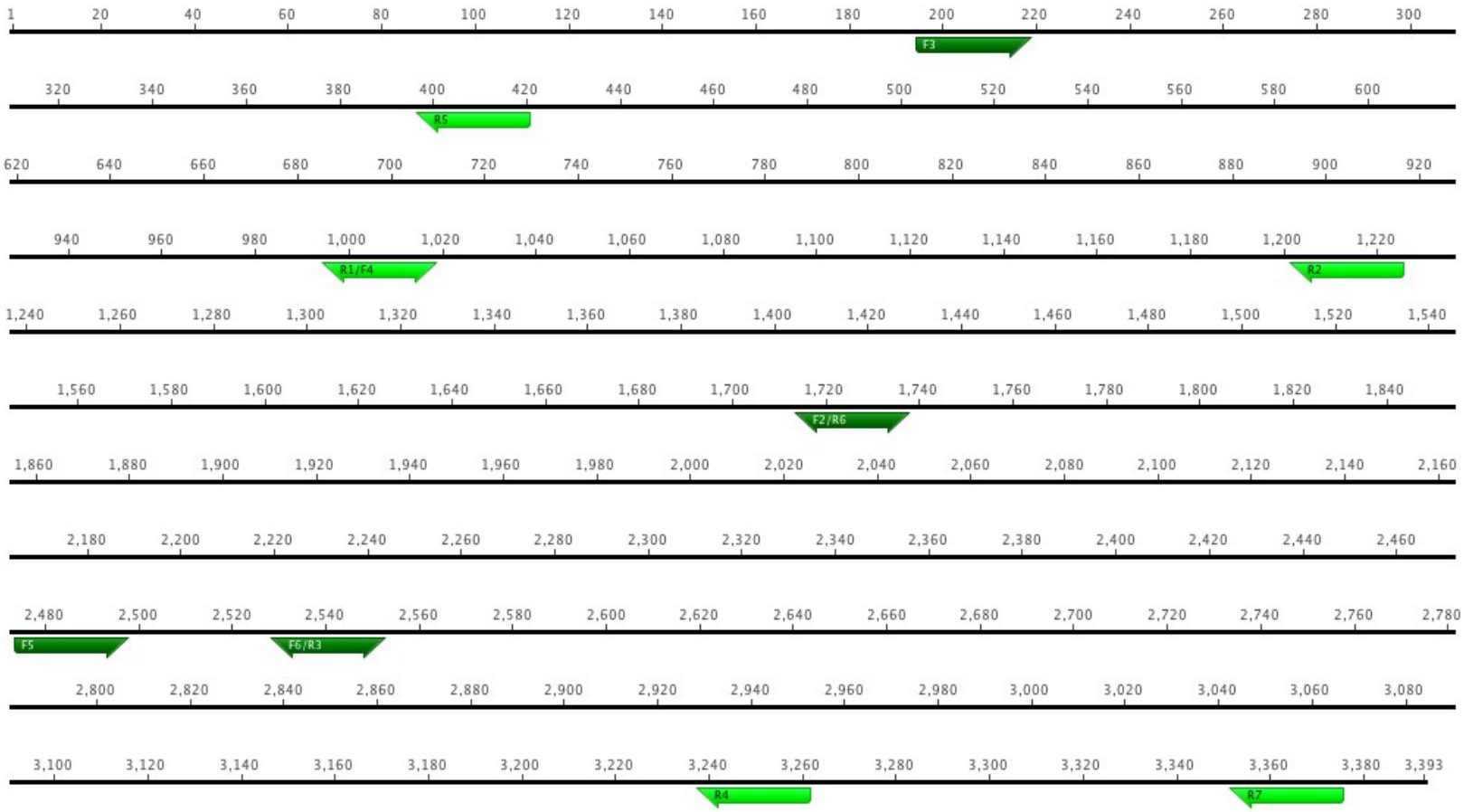

Figure A11: Known Sanger cDNA sequence for the *gin-10* candidate gene *rpc2*. Forward primers used for RT-PCR, cloning and probes are shown in the dark green, and the reverse primers are shown in light green.

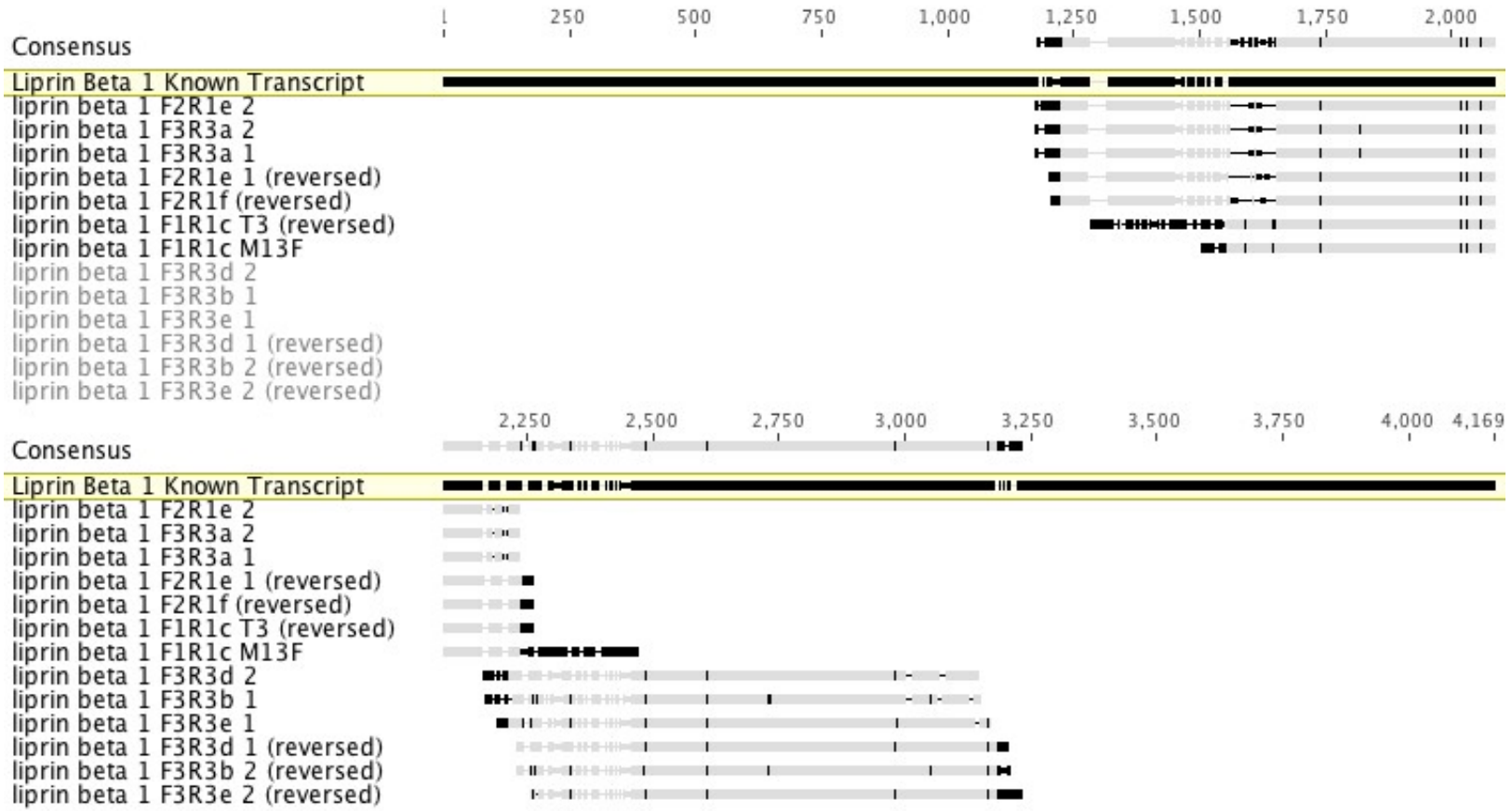

Figure A12: Alignment of the *liprin beta 1* clones to the known Sanger database cDNA sequence. Black marks in the sequenced clones indicate discrepancies from the known Sanger sequence.

Appendix C: Additional Figures from the Mdm1 Expression Studies

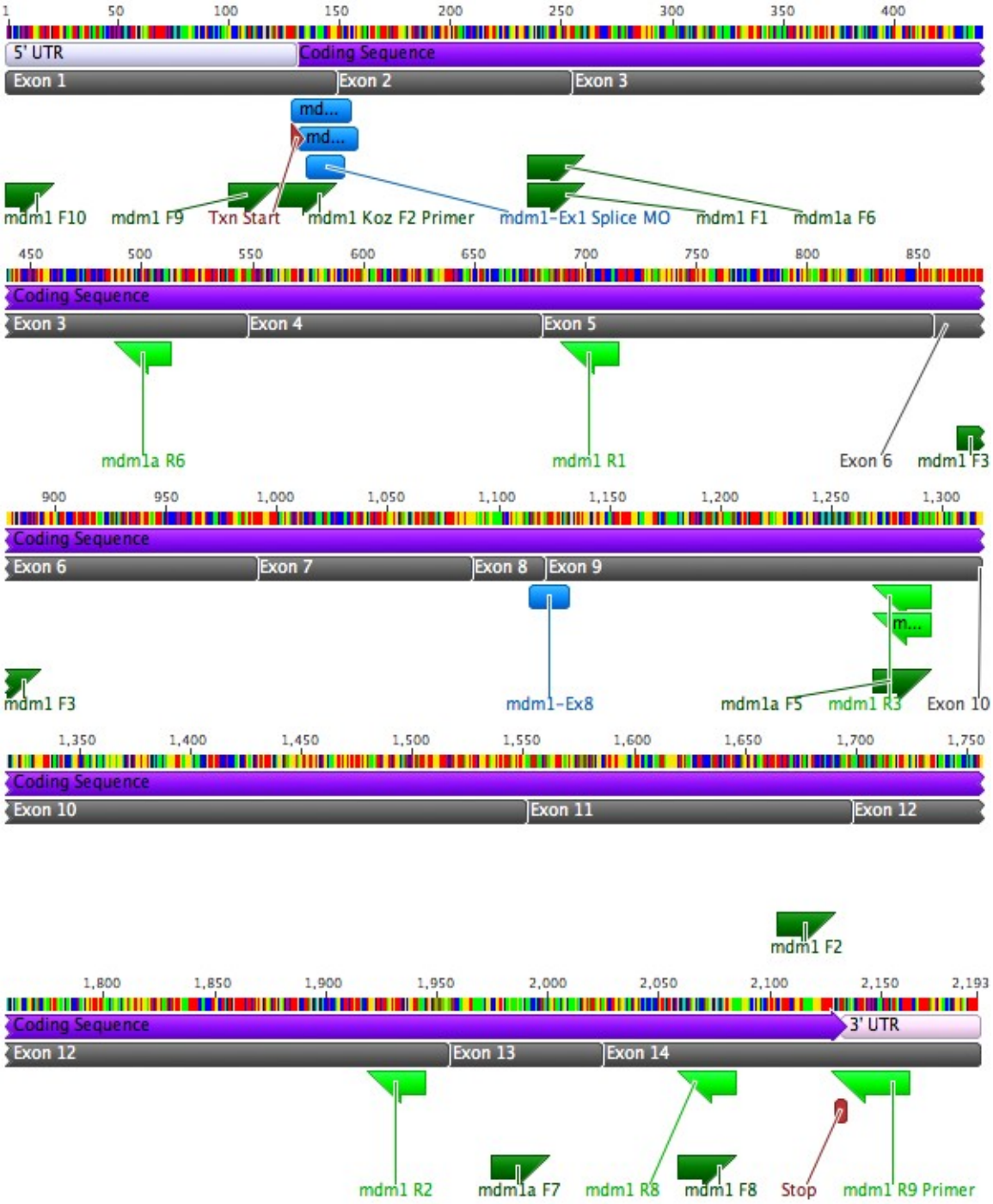

Figure A13: Coding sequence of the zebrafish long *mdm1* transcript showing the locations of the primers used for RT-PCR, cloning and probes for the *mdm1* projects. Also shows individual exons, 5'UTR, 3'UTR, Morpholino targets and start/stop codon locations.

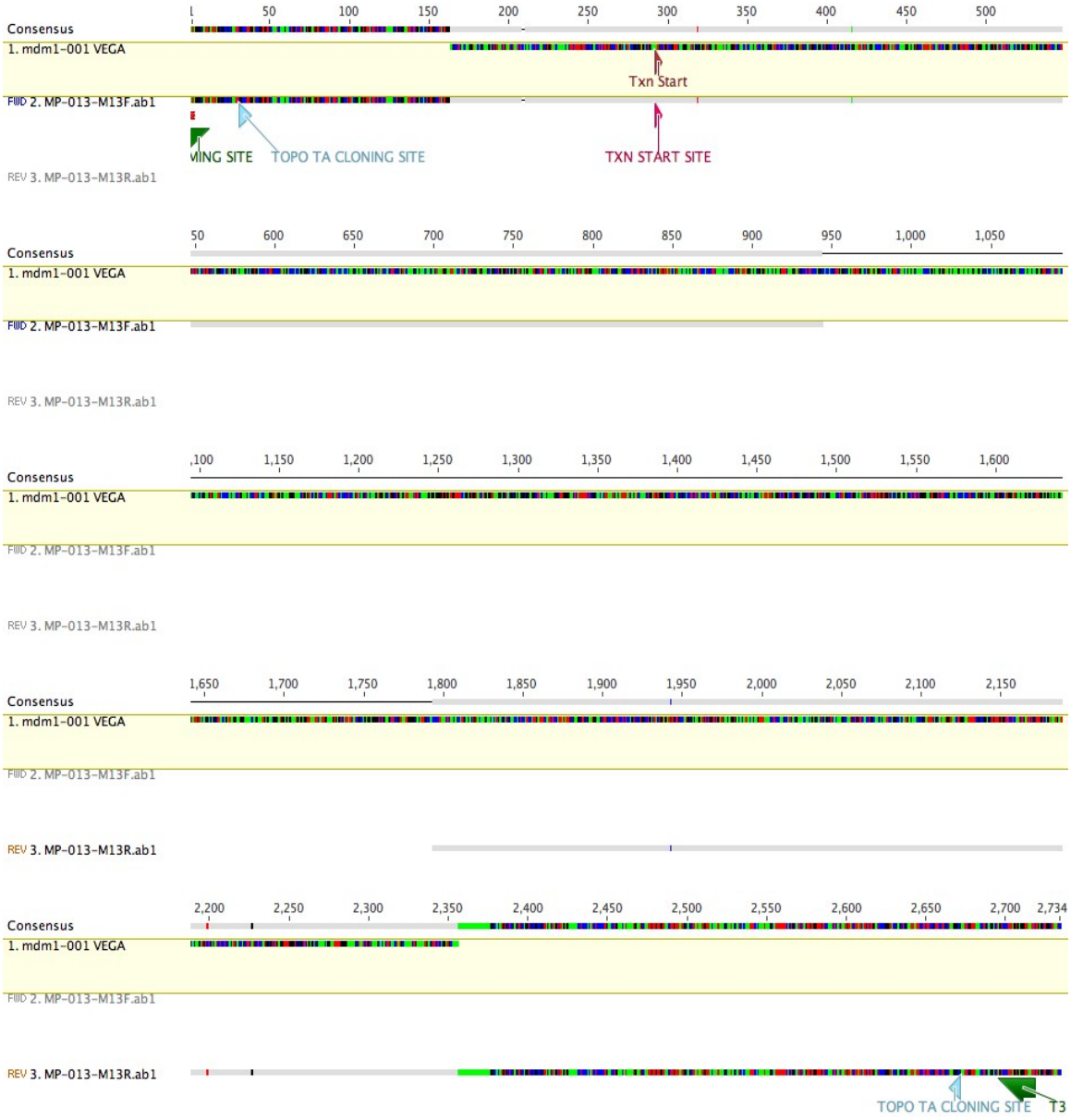

Figure A14: Sequence alignment between and *mdm1* Kozak F2R9 clone and the Vega *mdm1*-001 (long) sequence. The purpose of this cloning was to add the Kozak sequence just upstream of the transcriptional start site for use with the *in vitro* transcription and translation kit. The full-length *mdm1* sequence containing the Kozak is shown in the pCR4 vector, prior to subcloning into the pCMVTnT vector. Both T3 and T7 sequencing primers were used for this confirmation.

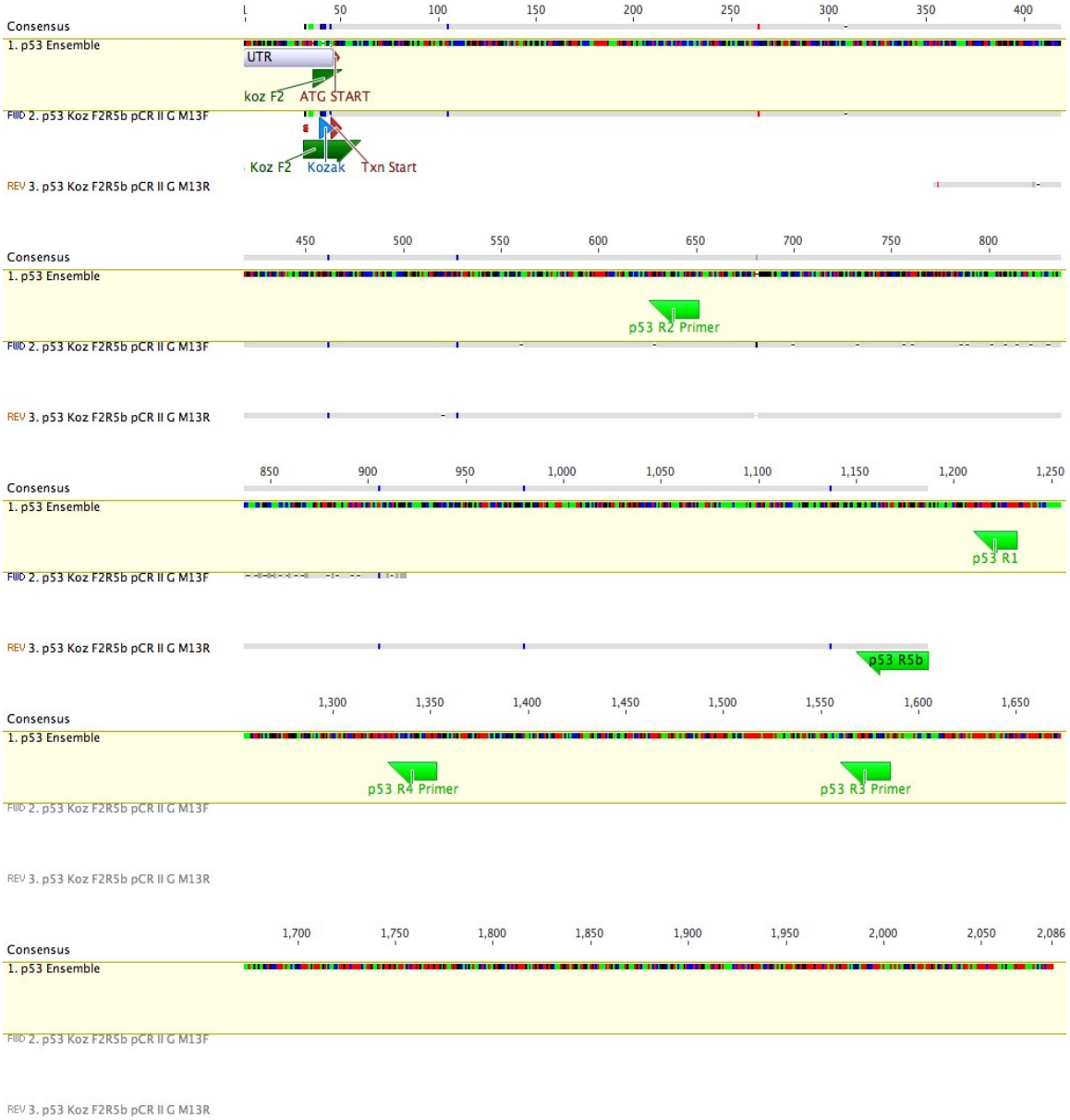

Figure A15: Sequence alignment of the known Ensemble *p53* sequence and the full-length cloned sequence including the Kozak. This clone was used as a control for western blotting and TnT experiments. Primers used for RT-PCR and probe making are also shown.

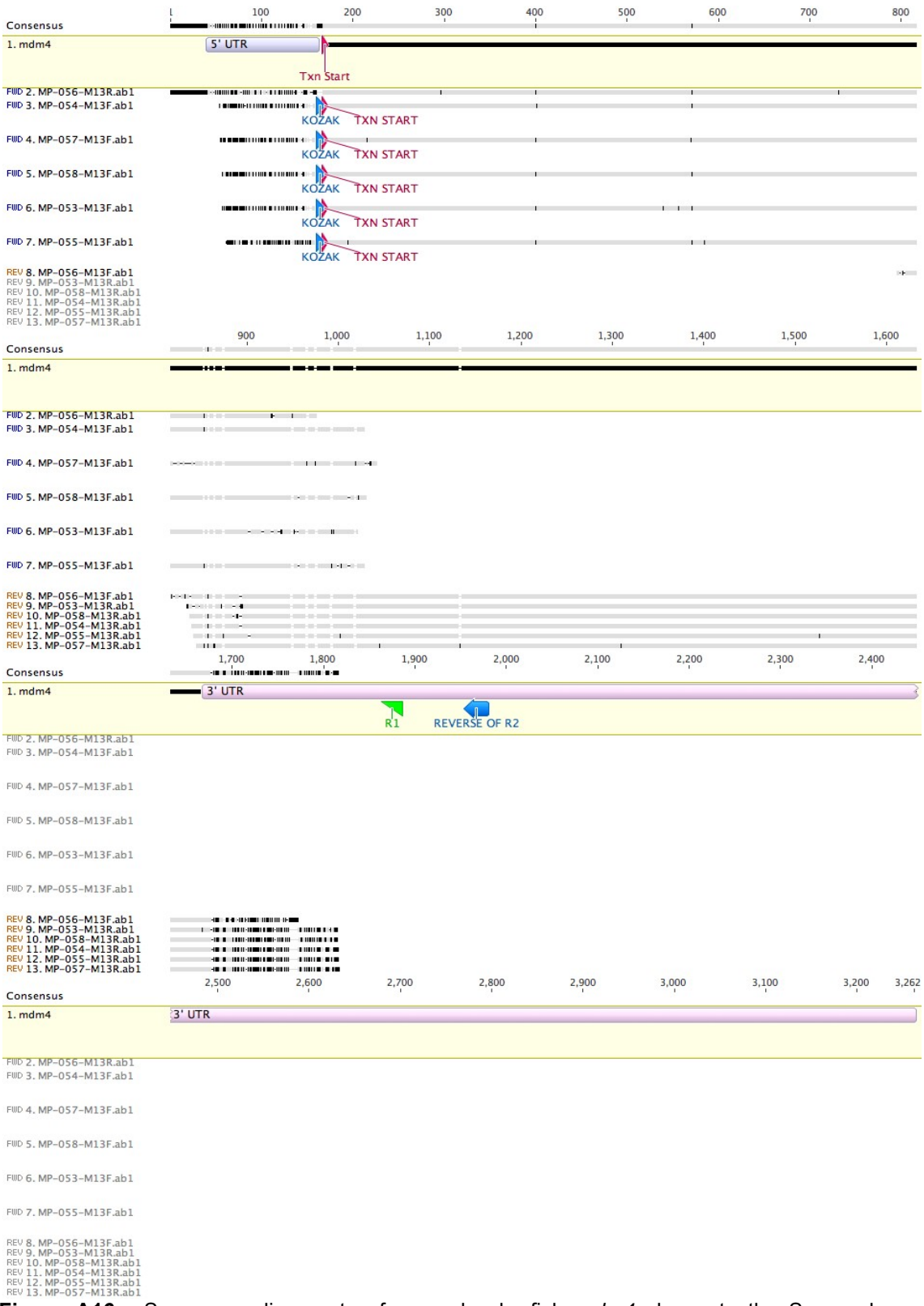

Figure A16: Sequence alignments of several zebrafish *mdm4* clones to the Sanger known sequence. This was also used as a control for western blotting and TnT experiments.

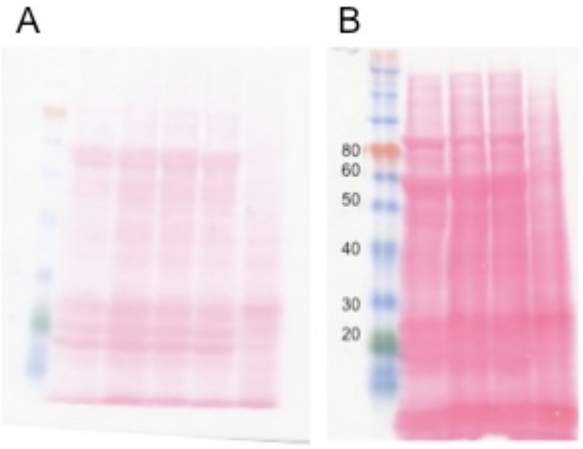

Figure A17: Samples of ponceau staining of initial embryo lysate western blots. (A) Embryo lysates prepared by using RIPA buffer with a protease inhibitor cocktail. (B) Embryo lysates prepared by the method described in the Zebrafish book, using an SDS sample buffer.

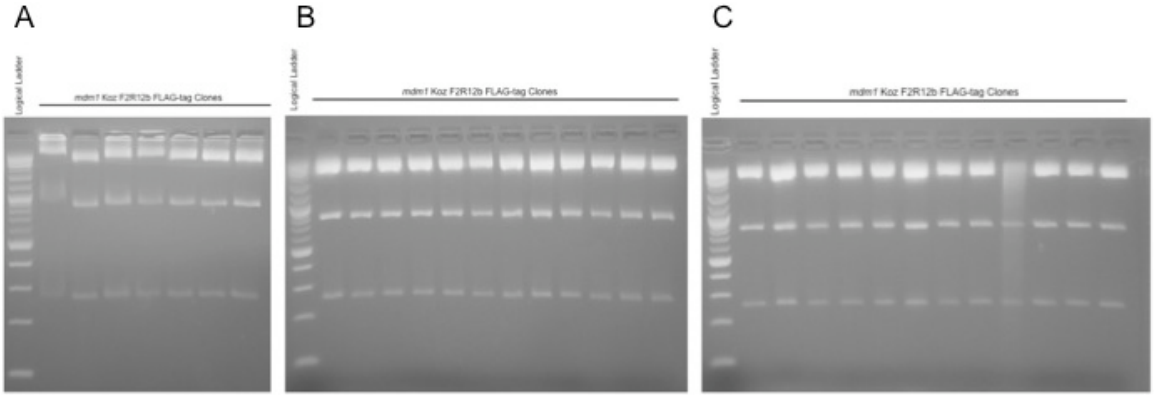

Figure A18: Restriction digests of the *mdm1* FLAG tag clones using the *hpy99i* enzyme. Based on the restriction map information, the results of these gels indicate that none of the clones contain the FLAG tag insert. (A) *mdm1* FLAG clones #1-7 in the pCMVTnT vector. (B) *mdm1* FLAG clones #8-19 in the pCR4 vector. (C) *mdm1* FLAG clones #20-31 in the pCR4 vector.

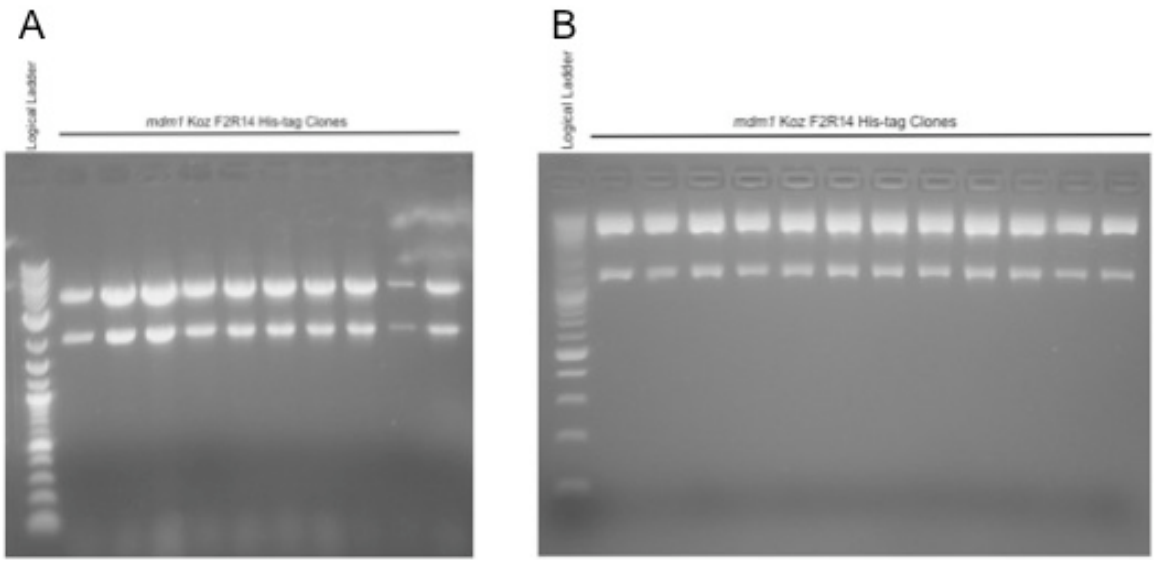

Figure A19: Restriction digests of the *mdm1* His tag clones using the *ase1* enzyme. Based on the restriction map information, the results of these gels indicate that none of the clones contain the His tag insert. (A) *mdm1* His clones #1-10 in the pCR4 vector. (B) *mdm1* His clones #11-22 in the pCR4 vector.

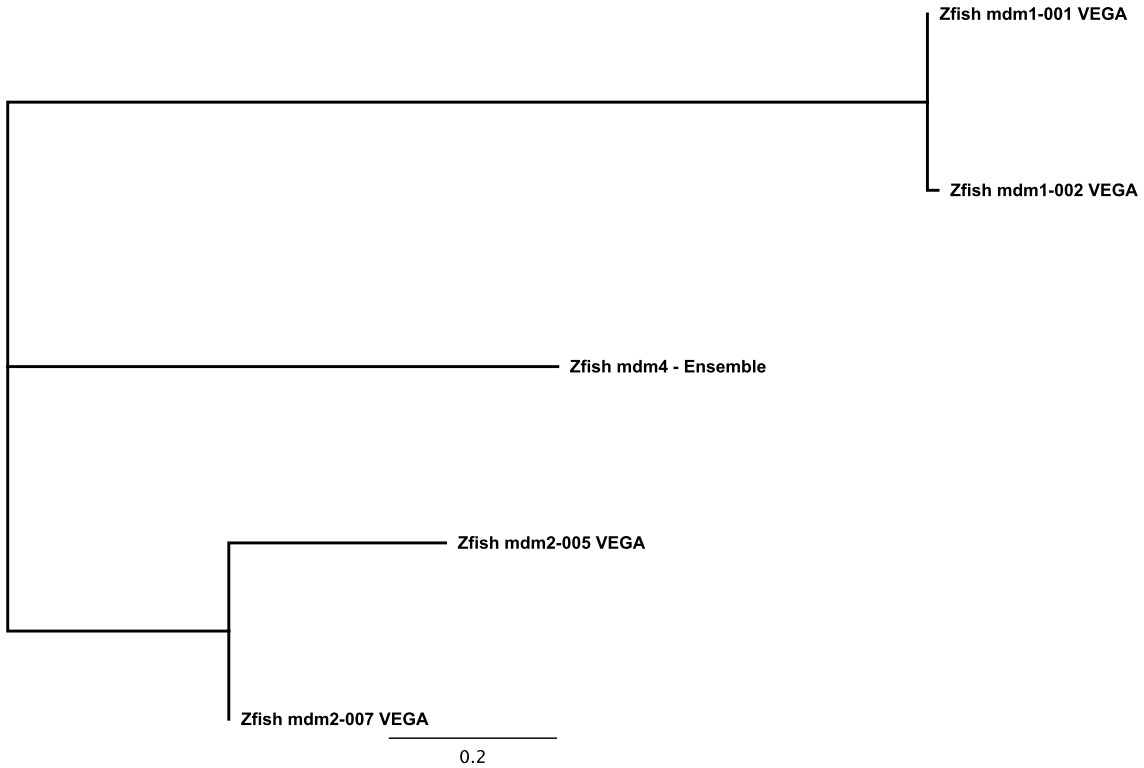

Figure A20: Mdm protein family tree based on amino acid sequence homology. Shown are the zebrafish Mdm1 long and short proteins, zebrafish Mdm4, and the long and short Mdm2 proteins.

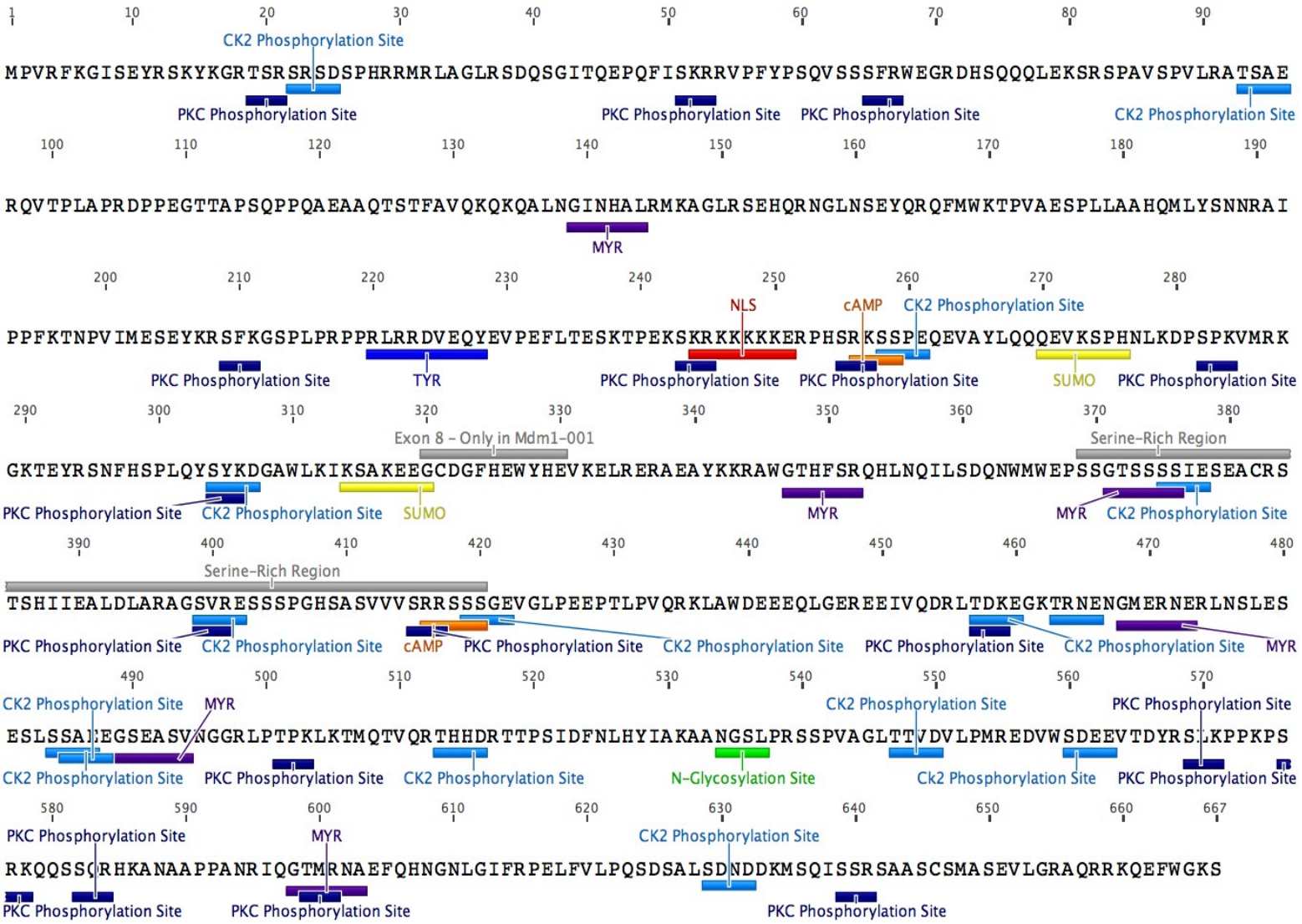

Figure A21: Zebrafish Mdm1 peptide sequence with predicted modification sites. It appears that Protein Kinase C (PKC), Casein Kinase II (CK2), cAMP/ cGMP, and Tyrosine Kinase (TYR) can phosphorylate the Mdm1 protein. This protein is also predicted to have two SUMO sites, a serine-rich region and a Nuclear Localization Signal (NLS).

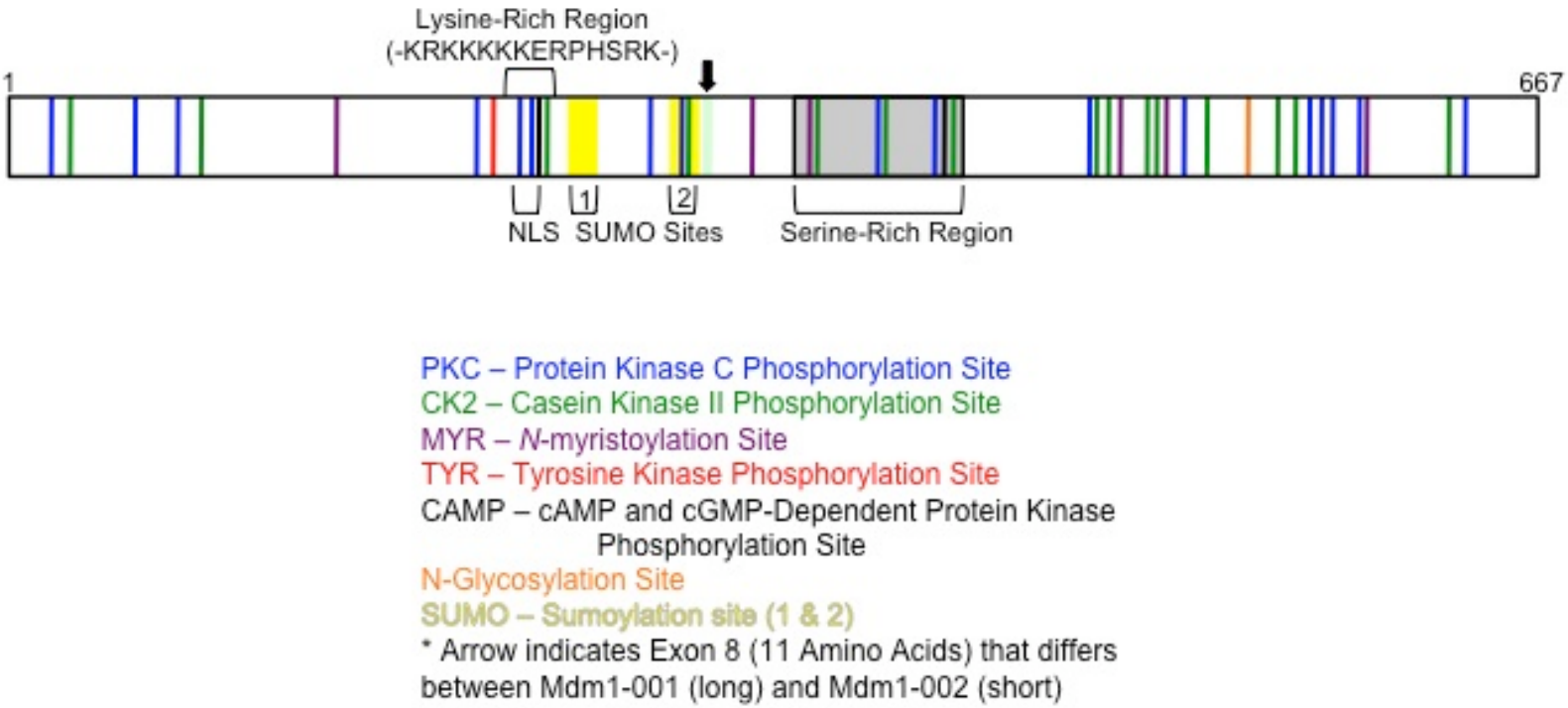

Figure A22: Schematic of the proposed structure of the zebrafish Mdm1 protein.

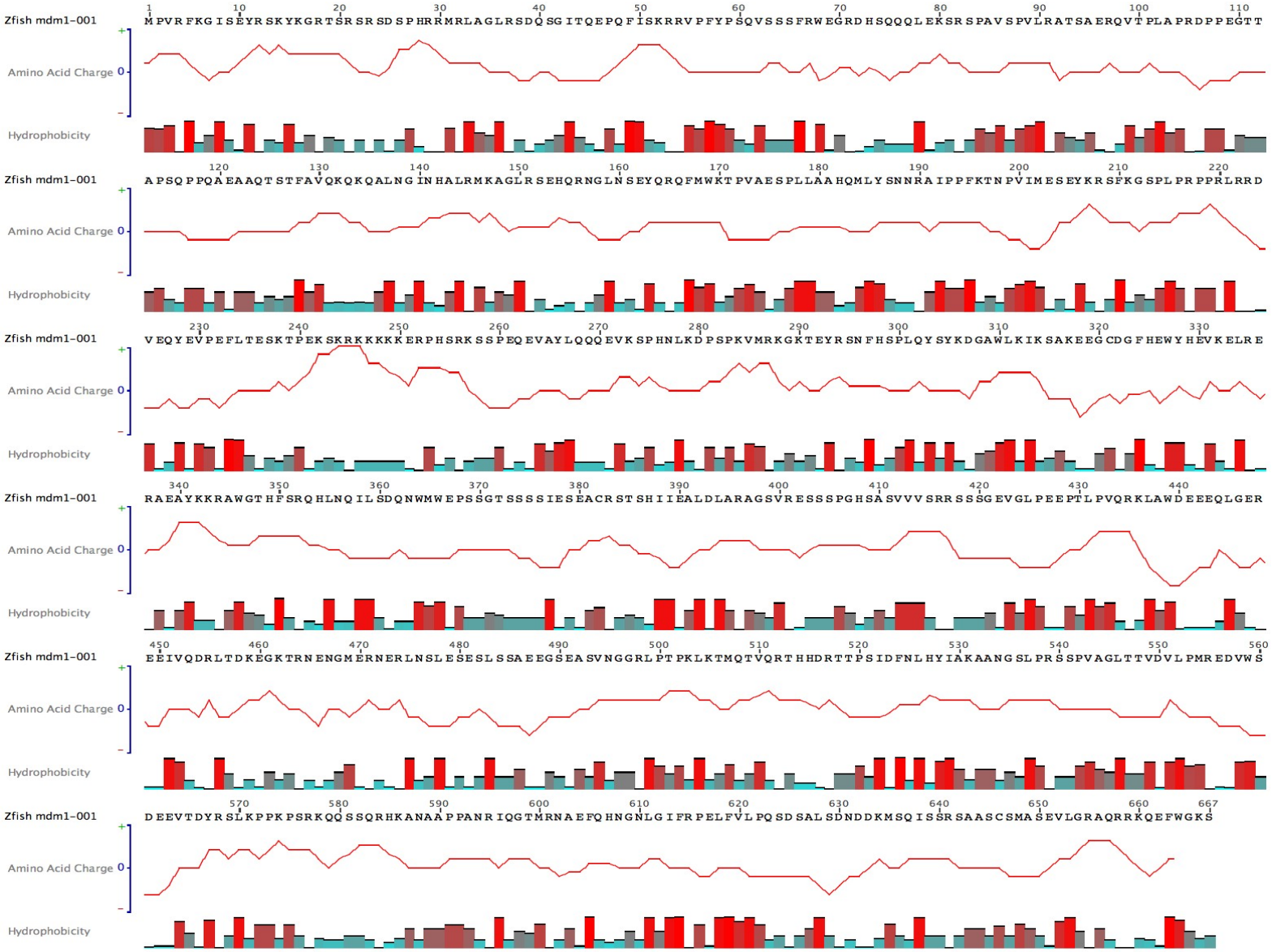

Figure A23: Hydrophobicity plot and amino acid charge of the zebrafish Mdm1 protein.

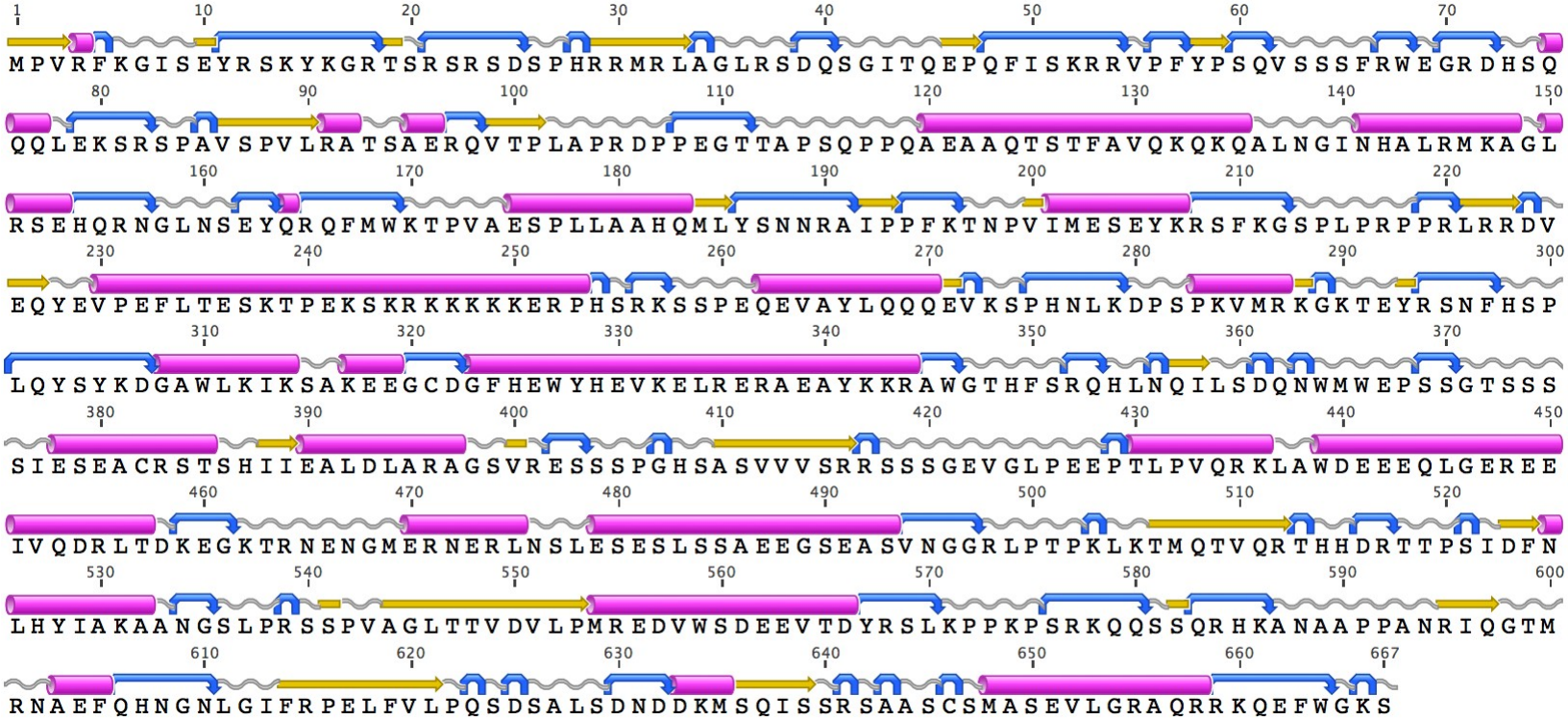

Figure A24: Predicted secondary structure of the zebrafish Mdm1 protein. Yellow arrows indicate β-sheets; Magenta cylinders indicate α-helices; Blue arrows indicate turns; Gray lines indicate coiled regions.